

STANDARDIZING MEASURES OF QUADRICEPS MUSCLE ARCHITECTURE

STANDARDIZATION OF MUSCLE ARCHITECTURE MEASUREMENTS OF THE
VASTUS LATERALIS AND RECTUS FEMORIS FROM IN VIVO ULTRASOUND
IMAGES IN HEALTHY ADULTS

BY

BRITTANY D. BULBROOK, BHSc KINESIOLOGY (HONS)

A Thesis Submitted to the Department of Kinesiology and the School of Graduate Studies
in Fulfilment of the Requirements for the Degree Master of Science

McMaster University © Copyright by Brittany D. Bulbrook, January 2019

Masters of Science (2019)
Department of Kinesiology

McMaster University
Hamilton, Ontario, Canada

TITLE: STANDARDIZATION OF MUSCLE ARCHITECTURE
MEASUREMENTS OF THE VASTUS LATERALIS AND RECTUS FEMORIS FROM
IN VIVO ULTRASOUND IMAGES IN HEALTHY ADULTS

AUTHOR: Brittany D. Bulbrook, BHSc
Department of Kinesiology

SUPERVISOR: Monica Maly, PhD & Peter Keir, PhD

NUMBER OF PAGES: viii, 140

Lay Abstract

The arrangement of small muscle components, known as fascicles, can be observed in humans using ultrasound imaging. These fascicle arrangements can be measured to improve understanding of muscle function and disease processes. A potential problem of viewing muscle with ultrasound is that the angle of the probe head against the skin can alter the appearance of the muscle fascicles. The goal of this research was to improve current methods of ultrasound imaging of two thigh muscles. We have created a novel 3D-printed device to attach to the existing ultrasound probe. This 3D-printed device stabilizes the ultrasound probe head; and accurately determines the angles between the ultrasound probe head and the surface of the skin. In this study, the use of this device improved reliability of our ultrasound images by >20%. Future use of this device may improve measurements of muscle fascicles acquired with ultrasound imaging.

Abstract

Background: Muscle thickness, pennation angle, and fascicle length describe the architecture of a muscle. These properties can be observed alongside subcutaneous fat thickness using ultrasonography; however, measurement is sensitive to the angle of the transducer against the skin. Typically, the transducer is held perpendicular to skin for imaging. Nonetheless, a convenient, reliable method to ensure transducer angle consistency has not been reported.

Objectives: The purpose of this study was to determine the influence of transducer angle on muscle architecture and subcutaneous fat measurements of quadriceps muscles (vastus lateralis and rectus femoris) in healthy young adults. A secondary objective was to determine intra- and inter-rater reliability.

Methods: Thirty men and women were recruited (25 ± 2.5 years; BMI: 22.6 ± 3.0 kg/m²). Ultrasound images were acquired from two muscles. An image was taken at an estimated perpendicular angle to the skin. Then, using a 3D-printed device with a protractor that attached to the ultrasound transducer, images were taken at measured angles 5-10° medial and lateral to perpendicular. Agreement and error were determined using intraclass correlation coefficients (ICCs) and standard error measurements (SEMs).

Results: Good to excellent agreement was demonstrated for muscle and fat thicknesses regardless of transducer angle (ICC >0.66). Intra-rater reliability was excellent for all outcomes within both muscles (ICC >0.89). Inter-rater reliability for the rectus femoris was good to excellent for all transducer angles except for measurements of fascicle

lengths at 85° (ICC: 0.33–0.99). Inter-rater reliability improved >20% for the vastus lateralis with the device.

Conclusion: Measurements of muscle pennation angle and fascicle lengths, but not muscle or subcutaneous fat thicknesses, were sensitive to transducer angle. Reliability of pennation angle and fascicle lengths improved with the use of our device. Using our device, reliable muscle architecture measures can be made for the rectus femoris and the vastus lateralis in healthy young adults.

Acknowledgements

Of course, I could not have done this alone. I am so fortunate to have so many people in my corner, supporting me and encouraging me as I pursue my goals. I am so grateful to each one of you as you've all helped me in different and significant ways over these past two plus years. First and foremost, I need to express sincere gratitude towards my supervisor, Dr. Monica Maly. You've mentored me throughout the (big and small) challenges in academia, and with your help I came out on the other side. To my committee members, Dr. Peter Keir, Dr. Janet Pritchard, and Dr. Audrey Hicks, your guidance and support was always beneficial, and I thank you for taking the time to provide me with valuable feedback, especially with presenting! I also need to express my sincere thanks to Dr. Karen Beattie, my independent study advisor. Thank you for helping me to reach out and network with other graduate students for assistance in writing my review. Thank you to Dr. Maureen MacDonald and Dr. Peter Keir for the use of your equipment and your lab spaces. Finally, to Marisa Kohut and Dr. Cheryl Quenneville, thank you for allowing me to use your equipment and helping me to scan my transducer!

I was also extremely lucky to have Jackie and Emily to assist with this project. Thank you for all of the parts you played along the way and for all the times you made me question my protocol. My project wouldn't be what it is without your critical thinking and genuine love of science. Thank you for always bringing your baked goods to group meeting. But most of all, thank you for always being in charge of tape. To the rest of my lab members, Tony, Dan, Amanda, Kumar, Elora, and Nick: Thank you for being there to

make me laugh, and (on the very rare occasion) listening to me complain! With your encouragement, I now consider myself a master of telling really terrible jokes!

On a more personal note, I absolutely could not have made it through this thesis without the consistent love and support of my Mom and Dad. Thank you for always being one phone call away. Not just during this degree, but throughout my life. You both mean everything to me, and I am so grateful for everything you do. Chase and Kristie, thank you for making me laugh on the worst days. To Kevin, you're always there to support me, calm me down, and challenge me. Thank you for understanding me and knowing exactly when to make a big bowl of popcorn (which is always). Deanna, you have stuck by me since we met. Thank you for driving all the way to Hamilton on multiple occasions just to hang out, thank you for always making time, and thank you for telling me when I'm wrong. You have been a source of unconditional support and a voice of reason. I am so glad you keep me around. To the rest of my friends, family, and colleagues, thank you. You, perhaps unknowingly, helped me so much the past 2 years. That dinner on the weekends or those texts to catch up were often exactly what I needed to pull me out of my own head and remind me that there are people who care about me. I love you all more than I could ever say.

Table of Contents

Lay Abstract.....	iv
Abstract.....	v
Acknowledgements.....	vii
List of Figures.....	xiii
List of Tables.....	xxii
List of Abbreviations and Symbols.....	xxviii
Chapter 1: Introduction.....	1
1.1 Muscle Anatomy	2
1.1.1 Sarcomere	3
1.1.2 Muscle Fibre	3
1.1.3 Muscle Fascicle	3
1.1.4 Aponeurosis	4
1.2 Muscle Architecture	5
1.2.1 Muscle Thickness	6
1.2.2 Pennation Angle	7
1.2.3 Fascicle Length	8
1.2.4 Subcutaneous Fat Thickness	8
1.3 Influence of Muscle Architecture on Muscle Function	10
1.4 Factors Affecting Muscle Architecture	10

1.4.1 Aging	10
1.4.2 Disease	11
1.4.3 Effect of Training on Muscle Architecture	12
1.5 Why Muscle Architecture is Important	14
1.5.1 Research Applications	14
1.5.2 Clinical Uses	14
1.6 Ultrasound to Measure Muscle Architecture In Vivo	14
1.7 Limitations of Ultrasound	16
1.8 Purpose and Hypothesis	20
1.8.1 Primary Hypothesis	21
1.8.2 Secondary Aim (A) Hypothesis	21
1.8.3 Secondary Aim (B) Hypothesis	21
1.9 Contributions to Literature	22
References	23
Chapter 2: Reliability of Muscle Architecture Measurements of the Vastus Lateralis and the Rectus Femoris Acquired Using a Novel 3D-Printed Device.....	31
2.1 Introduction	31
2.1.1 Purpose	34
2.1.2 Hypotheses	35
2.2 Methods	35

2.2.1 Study Design	35
2.2.2 Participants	36
2.2.3 Protocol	36
2.2.4 Positioning	37
2.2.5 Imaging Land-Marking	38
2.2.6 Image Acquisition	39
2.2.7 Muscle Architecture Measurements	44
2.2.8 Statistical Analyses	48
2.2.9 Data Quality	49
2.3 Results	51
2.3.1 Participants	51
2.3.2 Sex Differences	57
2.3.3 Assessment of Image Quality and Unusable Images	59
2.3.4 Effect of Transducer Angle on Muscle Architecture	62
2.3.5 Secondary Purposes	70
2.4 Discussion	79
2.4.1 Intra-rater reliability	83
2.4.2 Inter-rater reliability	84
2.4.3 Limitations	85
2.4.4 Future directions	86
2.5 Conclusions	87

References	88
Chapter 3: Discussion	92
3.1 Transducer Tilt	93
3.2 Transducer Attachment	96
3.3 Intra-Rater Reliability	97
3.4 Inter-Rater Reliability	99
3.5 Limitations	100
3.6 Future directions	101
3.7 Conclusions	102
References	104
APPENDIX A – 3D-Printed Attachment	107
APPENDIX B – Online Screening Questionnaire	111
APPENDIX C – Consent Form	116
APPENDIX E – Basic Collection Sheet	125
APPENDIX F – Six Minute Walk Test	126
APPENDIX G – Raw Data: Analyses Including All Images	127

List of Figures

- Figure 1:** Anatomy of a muscle. Muscle fascicles, muscle fibres, myofibrils and sarcomeres are shown (a, b, c, d, respectively). Image was taken with permission from Schuenke et al. (2014) and revised. 5
- Figure 2:** Representative ultrasound image of the vastus lateralis with an example of a muscle thickness, pennation angle (α), and fat thickness measurement. The dermis layer, as well as the aponeuroses are also shown using the orange lines..... 9
- Figure 3:** A 12L ultrasound transducer with the x, y, and z axis of the transducer labeled in red, green, and blue respectively..... 32
- Figure 4:** An image of the thigh showing the relative positioning of the transducer (the grey block) to the muscle fascicles (the black lines). 33
- Figure 5:** Image land-marking for the rectus femoris and vastus lateralis. A marking was drawn to identify the superior border of the patella and the lateral femoral condyle. A mark was made at the half point between the anterior superior iliac spine and the superior border of the patella and another mark halfway between the greater trochanter and the lateral femoral condyle..... 39
- Figure 6:** Figure 6A shows the 3D-printed transducer attachment device with a protractor marked with blue lines at 80°, 85°, 90°, 95°, and 100°. A black wedge attaches to the protractor using magnets. The bottom of the wedge fits along the thigh to limit movement of the protractor and to distribute pressure. Figures 6B, C, and D show the transducer with the attachment in use imaging the vastus lateralis. 41

Figure 7: Muscle architecture measurements made with a custom Python program. (A) Red lines represent the muscle thickness measurements. Green lines represent fat thickness measurements. Blue lines are traces of fascicles. (B) From muscle thickness measurements, a boundary for the superficial and deep aponeurosis were drawn (light blue and orange lines respectively). From the traces, the angle between the fascicles and the deep aponeurosis (shown in yellow) was recorded as the pennation angles. Finally, to define the fascicle length, an extrapolation line was created from the fascicle traces that continued until the superficial aponeurosis border (light blue line) was met. 47

Figure 8: Panel A presents an example of a vastus lateralis image that is not usable compared to a usable image shown in Panel B. *In Panel A, the deep aponeurosis is not visible, and the fascicles are unclear. 50

Figure 9: Mean muscle architecture measurements (and standard error bars) for the rectus femoris with unusable images removed and fascicle lengths exceeding the muscle lengths removed: muscle thickness (A, B), fat thickness (C, D), pennation angle (E, F), and fascicle length (G, H). Data from rater 1's images are displayed in the left column (A, C, E, G) and data from rater 2's images are shown in the right column (B, D, F, H). The lone markers represent the average value of the measurement from the images taken with the transducer at an estimated (EST) perpendicular angle..... 55

Figure 10: Mean muscle architecture measurements with unusable images and fascicle lengths exceeding the vastus lateralis removed: muscle thickness (A, B), fat thickness (C, D), pennation angle (E, F), and fascicle length (G, H). Data from rater 1's images are displayed in the left column (A, C, E, G) and data from rater 2's images are shown in the

right column (B, D, F, H). The lone markers represent the average value of the measurement from the images taken with the transducer at an estimated (EST) perpendicular angle. 56

Figure 11: Means (with standard error bars) for muscle thickness, fat thickness, pennation angle, and fascicle length separated by sex. Muscle architecture data from men participants are displayed with circle markers and solid lines; data from women are displayed with triangle markers and dashed lines. Rectus femoris data is shown in panels 10A, 10C, 10E, and 10G, respectively. Vastus lateralis data is shown in panels 10B, 10D, 10F, and 10H..... 58

Figure 12: The number of unusable images because the aponeurosis was not visible, per muscle and transducer angle. “Est” stands for the images taken at an angle that was estimated to be perpendicular. Only 60 images were taken in this condition per muscle, whereas 180 images were taken per muscle at all other measured transducer angles. These unusable images could not be used to calculate muscle thickness, fat thickness, pennation angle, and fascicle length. The bars with the black and white lines refer to images of the rectus femoris (RF) and bars with the solid black lines refer to images of the vastus lateralis (VL). The percentage of total images are displayed above the bars. 60

Figure 13: Number of unusable images because the fascicles were not clear, per muscle and transducer angle. “Est” stands for the images taken at an angle that was estimated to be perpendicular. Only 60 images were taken in this condition per muscle, whereas 180 images were taken per muscle at all other measured transducer angles. These unusable images could not be used to calculate pennation angle and fascicle length measurements.

The bars with the black and white lines refer to images of the rectus femoris and the solid black bars refers to images of the vastus lateralis. The percentage of total images are displayed above the bars. 60

Figure 14: The number of total fascicle length measurements removed, per transducer angle, due to lengths exceeding total muscle length. The bars with solid black bars and striped bars representing measurements for the vastus lateralis and the rectus femoris fascicle lengths, respectively. No black bars appear because no fascicle length measurements were removed from analysis. The percentages of total measurements are displayed above the respective bar. Estimated images, represented by “Est”, has a lower number of total measurements (180 total measurements) compared to other transducer angles (540 total measurements per measured transducer angle). 61

Figure 15: Measured transducer angles of estimated perpendicular transducer orientation for rectus femoris (Panel A) and vastus lateralis (Panel B), including data from both raters across all participants. Measured transducer angles of estimated perpendicular images taken by rater 1 are displayed with black bars, images taken by rater 2 are displayed with grey bars. 63

Figure 16: Bland-Altman plots comparing rectus femoris muscle thickness (A), fat thickness (B), pennation angle (C), and fascicle length (D) measurements from first and second measurements performed by rater 1 to assess intra-rater reliability. Data for all good-quality images of all participants taken by both raters at each transducer angle is displayed for muscle thickness, fat thickness and pennation angle (351 out of 360 data points for muscle and fat thickness, and 335 out of 360 data points for pennation angle).

Only fascicle length data within the length of the muscle is displayed for all participants (239 out of 360 data points) (D). The means are plotted along the X-axis and the differences between the measures are plotted on the Y-axis. The mean is displayed with a dashed grey line. The upper and lower agreements represent 1.96 standard deviations and are displayed as black lines. The data points represent the differences between 1st and 2nd measurements..... 72

Figure 17: Bland-Altman plots comparing vastus lateralis muscle thickness (A), fat thickness (B), pennation angle (C), and fascicle length (D) measurements from first and second measurements performed by rater 1 to assess intra-rater reliability. Data for images of all participants taken by both raters at each transducer angle is displayed with poor quality images removed (347 data points of 360). As no fascicle lengths exceeded the length of the muscle, all fascicle lengths from good quality images are included are included (347 data points). The means are plotted along the X-axis and the differences between the measures are plotted on the Y-axis. The mean is displayed with a grey dashed line. The upper and lower agreements represent 1.96 standard deviations and are displayed as two black lines. The data points represent the differences between 1st and 2nd measurements..... 73

Figure 18: Bland-Altman plots comparing rectus femoris muscle thickness (A), fat thickness (B), pennation angle (C), and fascicle length (D) measurements from images taken by rater 1 and rater 2. Data for all images of all participants at each transducer angle is displayed with poor-quality images and fascicle lengths which exceeded muscle length removed (174 data points for the muscle and fat thicknesses, 165 data points for the

pennation angles, and 111 data points for the fascicle lengths). The means are plotted along the X-axis and the differences between the measures are plotted on the Y-axis. The mean is displayed with a grey dashed line. The upper and lower agreements represent 1.96 standard deviations and are displayed as two black lines. The data points represent the differences between measurements from images taken by the first and second researcher. 75

Figure 19: Bland-Altman plots comparing vastus lateralis muscle thickness (A), fat thickness (B), pennation angle (C), and fascicle length (D) measurements from images taken rater 1 and rater 2. Data for all images of all participants at each transducer angle is displayed with poor quality images removed (172 data points). The means are plotted along the X-axis and the differences between the measures are plotted on the Y-axis. The mean is displayed with a grey dashed line. The upper and lower agreements represent 1.96 standard deviations and are displayed as two black lines. The data points represent the differences between measurements from images taken by the first and second researcher. 78

Figure 20: 3D scan of the ultrasound transducer. 110

Figure 21: Mean muscle architecture measurements with standard error bars for images of the rectus femoris: muscle thickness (A, B), fat thickness (C, D), pennation angle (E, F), and fascicle length (G, H). Data from rater 1s images are displayed in the left column (A, C, E, G) and data from rater 2s images are shown in the right column (B, D, F, H). The lone markers represent the average value of the measurement from the images taken with the transducer at an estimated (EST) perpendicular angle..... 128

Figure 22: Mean muscle architecture measurements with standard error bars for images of the vastus lateralis: muscle thickness (A, B), fat thickness (C, D), pennation angle (E, F), and fascicle length (G, H). Data from rater 1s images are displayed in the left column (A, C, E, G) and data from rater 2s images are shown in the right column (B, D, F, H). The lone markers represent the average value of the measurement from the images taken with the transducer at an estimated (EST) perpendicular angle..... 129

Figure 23: Bland-Altman plots comparing rectus femoris muscle thickness (A), fat thickness (B), pennation angle (C), and fascicle length (D) raw measurements from first and second measurements performed by rater 1 to assess intra-rater reliability. Data for all images of all participants taken by both raters at each transducer angle is displayed measurements. The means are plotted along the X-axis and the differences between the measures are plotted on the Y-axis. The mean is displayed with a dashed grey line. The upper and lower agreements represent 1.96 standard deviations and are displayed as black lines. The data points represent the differences between 1st and 2nd measurements. 133

Figure 24: Bland-Altman plots comparing vastus lateralis muscle thickness (A), fat thickness (B), pennation angle (C), and fascicle length (D) raw measurements from first and second measurements performed by rater 1 to assess intra-rater reliability. Data for all images of all participants taken by both raters at each transducer angle is displayed measurements. The means are plotted along the X-axis and the differences between the measures are plotted on the Y-axis. The mean is displayed with a dashed grey line. The upper and lower agreements represent 1.96 standard deviations and are displayed as black

lines. The data points represent the differences between 1st and 2nd measurements.

..... 135

Figure 25: Bland-Altman plots comparing rectus femoris muscle thickness (A), fat thickness (B), pennation angle (C), and fascicle length (D) measurements from images taken by rater 1 and rater 2. Data for all images of all participants at each transducer angle is displayed with poor-quality images and fascicle lengths which exceeded muscle length removed (174 data points for the muscle and fat thicknesses, 165 data points for the pennation angles, and 111 data points for the fascicle lengths). The means are plotted along the X-axis and the differences between the measures are plotted on the Y-axis. The mean is displayed with a grey dashed line. The upper and lower agreements represent 1.96 standard deviations and are displayed as two black lines. The data points represent the differences between measurements from images taken by the first and second researcher 137

Figure 26: Bland-Altman plots comparing vastus lateralis muscle thickness (A), fat thickness (B), pennation angle (C), and fascicle length (D) measurements from images taken by rater 1 and rater 2. Data for all images of all participants at each transducer angle is displayed with poor-quality images and fascicle lengths which exceeded muscle length removed (174 data points for the muscle and fat thicknesses, 165 data points for the pennation angles, and 111 data points for the fascicle lengths). The means are plotted along the X-axis and the differences between the measures are plotted on the Y-axis. The mean is displayed with a grey dashed line. The upper and lower agreements represent 1.96 standard deviations and are displayed as two black lines. The data points represent

the differences between measurements from images taken by the first and second
researcher 139

List of Tables

Table 1: Imaging parameters for ultrasound imaging summarizing ultrasound signal depth, frequency and the number of focus points.	44
Table 2: Total number of images taken for each muscle at each transducer angle.	44
Table 3: Parameter definitions, how they are typically measured, and how they were measured using our program.....	46
Table 4: Demographics for 30 participants. The right-hand columns described the same participants separated by sex.....	52
Table 5: Average rectus femoris muscle architecture values per transducer angle, separated by images taken by each rater. The sample size for each muscle architecture value is displayed beneath its respective cell.....	53
Table 6: Average vastus lateralis muscle architecture values per transducer angle, separated by images taken by each rater. The sample size for each muscle architecture value is displayed beneath its respective cell.....	54
Table 7: Rectus femoris standard error measurements (SEMs) of corrected data. Sample sizes are provided. SEMs compare measurements from images taken with the transducer at an estimated perpendicular angle and a measured 80°, 85°, 95°, and 100° transducer orientation to a measured 90° transducer angle. SEMs for images taken by each rater for each outcome at each transducer angle is displayed. Bolded cells show the highest error for each outcome.	66
Table 8: Rectus femoris intraclass correlation coefficients (ICCs) for corrected data. Sample sizes are provided. ICCs compare measurements from images taken with the	

transducer at an estimated perpendicular angle and a measured 80°, 85°, 95°, and 100° transducer orientation to a measured 90° transducer angle. ICCs for images taken by each rater for each outcome at each transducer angle is displayed. Dark green cells represent excellent agreements, light green cells represent good agreement, yellow cells represent fair agreement and red cells represent poor agreement..... 67

Table 9: Vastus lateralis standard error measurements (SEMs) of corrected data. Sample sizes are provided. SEMs compare measurements from images taken with the transducer at an estimated perpendicular angle and a measured 80°, 85°, 95°, and 100° transducer orientation to a measured 90° transducer angle. SEMs for images taken by each rater for each outcome at each transducer angle is displayed. Bolded cells show the highest error for each outcome. 68

Table 10: Vastus lateralis intraclass correlation coefficients (ICCs) for corrected data. Sample sizes are provided. ICCs compare measurements from images taken with the transducer at an estimated perpendicular angle and a measured 80°, 85°, 95°, and 100° transducer orientation to a measured 90° transducer angle. ICCs for images taken by each rater for each outcome at each transducer angle is displayed. Dark green cells represent excellent agreements, light green cells represent good agreement, yellow cells represent fair agreement and red cells represent poor agreement..... 69

Table 11: Intraclass correlation coefficients (ICCs) & standard error measurements (SEMs) for intra-rater reliability for muscle architecture measurements of the rectus femoris measure 1 and measure 2. For ICCs, dark green cells represent excellent agreements, light green cells represent good agreement, yellow cells represent fair

agreement and red cells represent poor agreement. These analyses contain images taken by both raters..... 71

Table 12: Vastus lateralis measure 1 vs. measure 2 intraclass correlation coefficients (ICCs) & standard error measurements (SEMs) for intra-rater reliability. For ICCs, Dark green cells represent excellent agreements, light green cells represent good agreement, yellow cells represent fair agreement and red cells represent poor agreement. These analyses contain images taken by both raters. 71

Table 13: Standard error measurements (SEMs) and intraclass correlation coefficients (ICCs) comparing rectus femoris measurements for images taken by rater 1 vs rater 2. For SEM, bold cells represent which transducer angle produced the largest error for each outcome. Dark green cells represent excellent agreements, light green cells represent good agreement, yellow cells represent fair agreement and red cells represent poor agreement. n=30 unless otherwise specified..... 76

Table 14: Vastus lateralis inter-rater reliability standard error measurements (SEMs) and intraclass correlation coefficients (ICCs). For SEMs, bold cells represent which transducer angle produced the largest error for each outcome. Dark green cells represent excellent agreements, light green cells represent good agreement, yellow cells represent fair agreement and red cells represent poor agreement..... 79

Table 15: 3D printing extruder properties..... 109

Table 16: Rectus femoris standard error measurements (SEMs) comparing measurements from images taken with the transducer at an estimated perpendicular angle and a measured 80°, 85°, 95°, and 100° transducer orientation to a measured 90° transducer

angle. SEMs for images taken by each rater for each outcome at each transducer angle is displayed. Bolded cells show the highest error for each outcome. 131

Table 17: Rectus femoris intraclass correlation coefficients (ICCs) comparing measurements from images taken with the transducer at an estimated perpendicular angle and a measured 80°, 85°, 95°, and 100° transducer orientation to a measured 90° transducer angle. ICCs for images taken by each rater for each outcome at each transducer angle is displayed. Dark green cells represent excellent agreements, light green cells represent good agreement, yellow cells represent fair agreement and red cells represent poor agreement. 131

Table 18: Vastus lateralis standard error measurements (SEMs) comparing measurements from images taken with the transducer at an estimated perpendicular angle and a measured 80°, 85°, 95°, and 100° transducer orientation to a measured 90° transducer angle. SEMs for images taken by each rater for each outcome at each transducer angle is displayed. Bolded cells show the highest error for each outcome. 132

Table 19: Vastus lateralis intraclass correlation coefficients (ICCs) comparing measurements from images taken with the transducer at an estimated perpendicular angle and a measured 80°, 85°, 95°, and 100° transducer orientation to a measured 90° transducer angle. ICCs for images taken by each rater for each outcome at each transducer angle is displayed. Dark green cells represent excellent agreements, light green cells represent good agreement, yellow cells represent fair agreement and red cells represent poor agreement. 132

Table 20: Intraclass correlation coefficients (ICCs) & standard error measurements (SEMs) for intra-rater reliability for muscle architecture measurements of the rectus femoris measure 1 and measure 2. For ICCs, dark green cells represent excellent agreements, light green cells represent good agreement, yellow cells represent fair agreement and red cells represent poor agreement. These analyses contain both rater 1 and rater 2 data..... 134

Table 21: Intraclass correlation coefficients (ICCs) & standard error measurements (SEMs) for intra-rater reliability for muscle architecture measurements of the vastus lateralis measure 1 and measure 2. For ICCs, dark green cells represent excellent agreements, light green cells represent good agreement, yellow cells represent fair agreement and red cells represent poor agreement. These analyses contain both rater 1 and rater 2 data..... 136

Table 22: Standard error measurements (SEMs) & intraclass correlation coefficients (ICCs) comparing rectus femoris measurements for images taken by rater 1 vs rater 2. For SEM, bold cells represent which transducer angle produced the largest error for each outcome. Dark green cells represent excellent agreements, light green cells represent good agreement, yellow cells represent fair agreement and red cells represent poor agreement..... 138

Table 23: Standard error measurements (SEMs) & intraclass correlation coefficients (ICCs) comparing rectus femoris measurements for images taken by rater 1 vs rater 2. For SEM, bold cells represent which transducer angle produced the largest error for each outcome. Dark green cells represent excellent agreements, light green cells represent

good agreement, yellow cells represent fair agreement and red cells represent poor agreement..... 140

List of Abbreviations and Symbols

6MWT: Six Minute Walk Test

ASIS: Anterior Superior Iliac Spine

CV: Coefficient of Variance

ICC: Intraclass Correlation Coefficient

NPRS: Numerical Pain Rating Scale

PART: Position, Alignment, Rotation, Tilt

RPE: Rating of Perceived Exertion

SEM: Standard Error Measurement

SE: Standard Error

SD: Standard Deviation

Chapter 1: Introduction

Skeletal muscle strength loss is a feature of numerous chronic health conditions, including musculoskeletal and neuromuscular diseases, as well as a hallmark of healthy aging (Roubenoff, 2001; Reardon et al., 2001; Narici et al., 2016). Regardless of the cause, the loss of skeletal muscle strength contributes to reduced physical function that limits productivity, recreation, and activities of daily living (Rosenberg, 1997; Roubenoff, 2001). The impact of these functional limitations can be debilitating (Rosenberg, 1997; Roubenoff, 2001). As a result, clinicians require reliable methods to track skeletal muscle strength over time; and researchers must explore the mechanisms that contribute to muscle strength in order to devise new strategies to prevent its loss.

Because muscle size is strongly associated with muscle strength, much research has been dedicated to tracking muscle size and volume using clinical tools, such as dual x-ray absorptiometry (DEXA), magnetic resonance imaging (MRI), and computerized tomography (CT) (e.g., physiological cross-sectional areas and lean muscle mass and volume) (Prado & Heymsfield, 2014); and research tools such as muscle biopsy (Suetta et al., 2008) to measure muscle and muscle fibre size. Relatively less work has focused on quantifying the physical arrangement of structures within the muscle (e.g., muscle fascicles); that is, muscle architecture (Blazevich, 2006; Narici, 1999; Gans, 1982). Yet, measurements of muscle architecture are related to force output and have been useful for tracking changes in muscle after interventions such as surgical procedures (Delp et al., 1990; Fridén et al., 2002; Lieber, 1993; Reardon et al., 2001), and strength training (Malas et al., 2013; Suetta et al., 2008; Vaz et al., 2013). However, traditional techniques

to capture measurements of muscle architecture include cadaveric dissection (Friederich et al., 1990; Cutts, 1988), and MRI (Prado & Heymsfield, 2014). Cadaveric studies are limited because tissue death alters architectural features (Friederich et al., 1990; Cutts, 1988) and MRI is costly (Reeves et al., 2004; Maden-Wilkenson et al., 2013). An inexpensive, non-invasive alternative is ultrasound imaging of muscle tissue (Prado & Heymsfield, 2014). However, the quality of measurements of muscle architecture acquired using ultrasonography depends heavily on the consistency of the protocol (Klimstra et al., 2007; Bénard et al., 2009; König et al., 2014). This thesis studied the sensitivity of muscle architecture measurements to one potential source of error in an ultrasonography protocol: the tilt of the ultrasound transducer relative to the skin. The following literature review provides relevant background on muscle structure and architecture, factors that influence muscle architecture, and measurement techniques used to capture this architecture.

1.1 Muscle Anatomy

Skeletal muscle is made up of contractile units called sarcomeres. These units are contained within bundles and are arranged within muscle based on its specific functional demands. Different muscle arrangements (organization of structural components within a muscle or muscle architecture) exist to optimize human movement. Variances in muscle architecture have implications for sarcomere location and therefore affect the force output and speed of muscle shortening (Bodine et al., 1982; Gans et al., 1987). Regardless of the specific arrangement, individual muscle components are comprised of the same basic

elements (Figure 1). These components are described hereafter in order from smaller, deeper elements to larger, more superficial elements.

1.1.1 Sarcomere

The sarcomere is the basic unit of muscle contraction and force production (Elder, 2007). As depicted in Figure 1d-c, sarcomeres are contained in series within long organelles called myofibrils (Damjanov, 2009; Elder, 2007). Sarcomeres are made up of fibrous proteins (principally, actin and myosin) that slide to overlap creating cross-bridges as the muscle contracts (Huxley et al., 1954; Huxley et al., 1954). Myosin is the component containing ATPase enzymes and cross-bridging heads that pull on the actin to allow the fibril to contract (Rode et al., 2016). The number of sarcomeres that can be packed within a muscle is largely reliant on the structural arrangement of the muscle (Kearns et al., 2000; Lieber & Fridén, 2000).

1.1.2 Muscle Fibre

Fibres, shown in Figure 1b, are made up of groups of myofibrils covered by endomysium sheath (Damjanov, 2009). The number of myofibrils contained within a fibre is dependent on the amount of force the muscle needs to be able to produce (Scott et al., 1993). Larger muscles contain more fibres with more myofibrils than smaller muscles that are responsible for movements which require lower force.

1.1.3 Muscle Fascicle

Fascicles are bundles of 10 – 100 muscle fibres bound together by a sheath of connective tissue called perimysium (Elder, 2007). Groups of muscle fascicles are held together alongside blood vessels with a continuous layer of connective tissue called the

epimysium, making up the whole muscle (Figure 1a). Fascicles can be viewed *in vivo* using ultrasound and appear dark compared to non-lean tissue (that is, tissue that is not muscle, such as fat). The arrangement of muscle fascicles infers the arrangement of its subunits (fibres, myofibrils, and sarcomeres).

There are two main arrangements of skeletal muscle fascicles: parallel (muscle fascicles are arranged parallel to the line of shortening) and pennate (muscle fascicles are arranged in an oblique feather-like pattern relative to the line of shortening) (Narici, 1999). Pennate muscles, like the rectus femoris and the vastus lateralis, are typically able to produce more force than parallel muscles, like the gracilis and the sartorius muscles because they can fit more fibres (and therefore sarcomeres) in parallel (Narici et al., 2016).

1.1.4 Aponeurosis

The aponeurosis is a tendon-like fibrous tissue that attaches broad muscles to its respective attachment site (Arellano et al., 2016). Separate from the previously mentioned epimysium, the aponeurosis functions to envelope muscle fascicles and separate individual muscles (Damjanov, 2009). This tissue can be imaged using ultrasound as it appears bright compared to muscle tissue. Aponeuroses can play an important part in quantifying muscle architectural properties by appearing as a border for muscles.

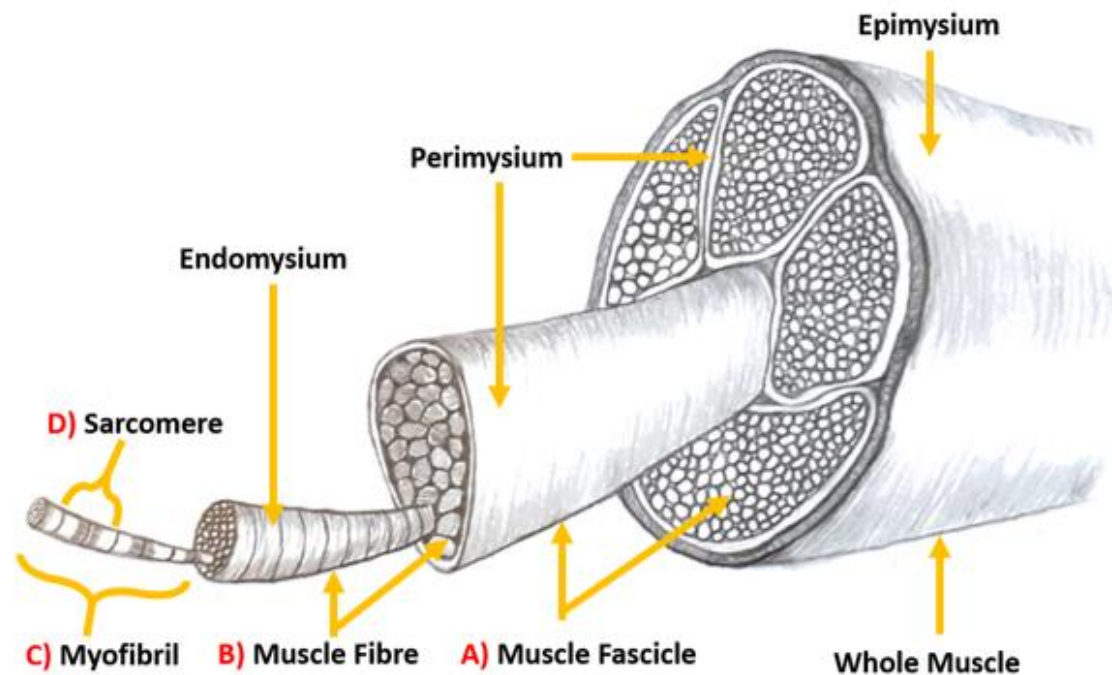


Figure 1: Anatomy of a muscle. Muscle fascicles, muscle fibres, myofibrils and sarcomeres are shown (a, b, c, d, respectively).

1.2 Muscle Architecture

The architecture of a muscle is often described in terms of whole muscle (muscle thickness), and individual fascicle properties (pennation angle, and fascicle length) (Blazevich, 2006; Narici, 1999). These architectural properties are useful in assessing physical adaptations that occur in response to muscle loading and unloading (Aagaard et al., 2001). Today, much research is dedicated to studying muscle characteristics such as hypertrophy and atrophy, with intentions of improving force output for activities of daily living, as well as occupational and athletic activities (Ikezoe et al., 2011; Puthoff et al., 2008). Muscle activity is often studied to evaluate muscle coordination and strength. Recently, more attention has focused on the physical arrangement of muscle fascicles.

The arrangement of fascicles has demonstrated direct influence upon contractile function. For example, a study by Thom et al. (2007) concluded that muscle architecture, specifically fascicle length, contributes to the torque and power-velocities of muscles in individuals both young and old. After normalization of velocity to fascicle length, differences in total contraction velocity decreased 15.9% (Thom et al., 2007). As well, Mitsukawa et al. (2009) concluded that changes in fascicle geometry occur in response to fatigue. As decreases in torque and tendon lengthening are observed during fatigue protocols, increases in fascicle lengths are seen (Mitsukawa et al., 2009). These changes occur more quickly in muscles with large proportions of fast-glycolytic fibres compared to synergistic muscles with greater proportions of slow-twitch fibres (Mitsukawa et al., 2009). Furthermore, a measurement often reported in musculoskeletal imaging literature is the quantification of the non-lean tissue above the muscle often referred to as fat thickness. Measurements of fat thickness provide information of site-specific body composition. Common muscle architecture characteristics that are easily observable using ultrasound are the following: muscle thickness, pennation angle, and fascicle length, along with measurements of subcutaneous fat.

1.2.1 Muscle Thickness

Muscle thickness is defined as the muscle belly thickness from superficial to deep aponeurosis (Figure 2) (Blazevich et al., 2007). The thickness of muscle is positively correlated to pennation angle such that muscles with larger pennation angles will be thicker (Fukunaga et al., 1997). This measurement can provide insight regarding atrophy and is often observed in immobility studies to quantify the effects of bed rest and space

flight on muscle shrinkage (de Boer et al., 2008). After only five weeks of horizontal bed rest, muscle thickness of the vastus lateralis declined by a mean of $8.0 \pm 9.1\%$ in otherwise healthy men (de Boer et al., 2008). Muscle thickness measurements are also useful in observing muscular gains (Blazevich et al., 2007).

1.2.2 Pennation Angle

The pennation angle of a muscle, shown in Figure 2, is the angle between an individual muscle fascicle and the deep aponeurosis of the muscle (Ema et al., 2013; Henriksson-Larsen et al., 1992; Rutherford et al., 1992). Hypertrophied muscles have pennation angles that are larger at rest compared to non-hypertrophied muscles (Kawakami et al., 1993). On the other hand, atrophy has been linked to decreases in pennation angle (Narici, 1999). The pennation angle of a muscle becomes larger as the muscle contracts (Fukunaga et al., 1997). Therefore, a muscle will have a smaller pennation angle at a rested state than it would in a contracted state. As fascicles of a pennate muscle shorten, they increase in angle and bring the aponeuroses towards one another (Narici, 1999). Pennate muscles contain more muscle fascicles arranged in parallel, allowing more sarcomeres in parallel. This increases the number of potential bridges that can be formed within the muscle ultimately allowing it to produce more force than a parallel muscle of equal size (Gans et al., 1987). This advantage, however, comes at a cost to contraction velocity. Muscles with larger pennation angles contract at a slower velocity than a muscle of equal volume with smaller pennation angles or no pennation at all (Narici, 1999).

1.2.3 Fascicle Length

Fascicle length is the length of the individual muscle fascicles within a muscle, extending from deep to superficial aponeurosis (Figure 2) (Blazevich et al., 2007). This measurement can provide evidence of atrophy, as atrophied muscles often have shorter fascicles than healthy muscles (Narici, 1999). Longer muscle fascicles are able to contain more sarcomeres arranged in series (Narici, 1999; Thom et al., 2007). Compared to shorter fascicles, greater lengths are associated with quicker absolute shortening speeds and increased power production (Lieber & Fridén, 2000). However, relative shortening velocity of shorter fascicles is higher than in longer fascicles (Narici, 1999). During contraction, the length of a fascicle decreases (Fukunaga et al., 1997).

1.2.4 Subcutaneous Fat Thickness

A common measure within muscle architecture literature is subcutaneous fat thickness. Fat thickness, shown in Figure 2, refers to the thickness of tissue beneath the dermal layer and superficial to the muscle fascia (subcutaneous tissue), which is considered to be mostly adipose tissue or fat (Prado & Heymsfield, 2014). Measuring fat thickness via ultrasound can provide a low cost, site specific, body composition assessment that can be reliably performed by individuals ranging in experience (Chirita-Emandi et al., 2015; Martinikorena et al., 2016). Such fat thickness assessments can be performed conveniently in both clinical or field settings as ultrasound systems can be portable (Chirita-Emandi et al., 2015). Burford et al. (2012) used a Short Physical Performance Battery (SPPB) test, a group of measurements that incorporates gait speed, chair stands and balance assessments, to separate participants into low functioning (participants who

scored 7 or less out of 12) and high functioning groups (participants who scored 11 or greater out of 12). Subcutaneous fat thickness, assessed using MRI, was shown to be larger in low functioning adults compared to high functioning adults (Buford et al., 2012).

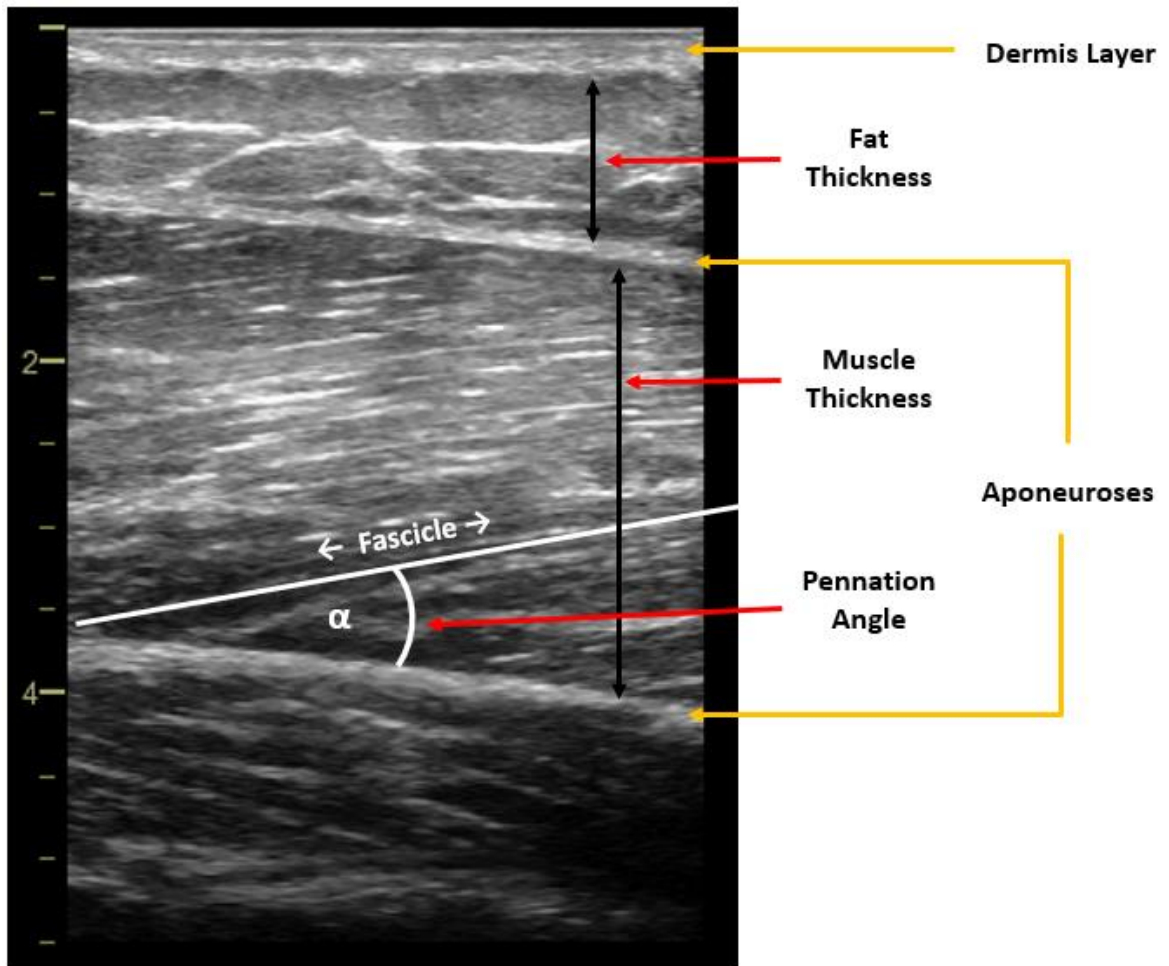


Figure 2: Representative ultrasound image of the vastus lateralis with an example of a muscle thickness, pennation angle (α), and fat thickness measurement. The dermis layer, as well as the aponeuroses are also shown using the orange lines.

1.3 Influence of Muscle Architecture on Muscle Function

Strength is the ability of a muscle to produce force (Sayers, 2007), while muscle power is the amount of force produced multiplied by the contraction velocity (Kraemer et al., 2000; Puthoff et al., 2010). Previous works have shown a relationship between muscle architecture (muscle thickness, fascicle length, and pennation angle) and strength (Alegre et al., 2006; Ando et al. 2015), as well as power (Thom et al., 2007). Muscle architecture properties are related to muscle capacity and are associated with force output (Lieber et al., 2000). Specifically, several studies have indicated that muscle thickness and pennation angle demonstrate good correlation to knee extension torque (Ando et al., 2015; Cadore et al., 2012; Fukumoto et al., 2012; Strasser et al., 2013; Watanabe et al., 2013). The force potential of a muscle is positively correlated to the number of sarcomeres in parallel and therefore is related to pennation angle, muscle thickness, and fascicle length (Gans et al., 1991; Lieber et al., 2000; Narici et al., 2016; Woittiez et al., 1983).

1.4 Factors Affecting Muscle Architecture

1.4.1 Aging

Features of muscle architecture, such as muscle thickness, have been related to the loss of dynamic torque with aging (Raj et al., 2017; Narici et al., 2003). Muscle capacity likely declines in response to a loss of contractile tissue which manifests as a decrease in muscle volume, fascicle length, and pennation angle (Narici et al., 2003). For example, myofibril length is shorter in older adults than in younger individuals (Melo et al., 2016; Suetta et

al., 2008). As well, in a study comparing the gastrocnemius muscle architecture of young and old individuals, fascicle lengths and pennation angles were both significantly smaller in the older sample (Narici et al., 2003). Other studies have indicated that muscle thickness (Fukumoto et al., 2012; Strasser et al., 2013) and pennation angles were significantly correlated to isometric strength in older adults (Strasser et al., 2013). A study by Thom et al. (2007) compared cross-sectional area (CSA) and fascicle length between older and younger men and found that both CSA and fascicle length were significantly correlated to torque-velocity in both groups. A different study by Morse and colleagues (2005) compared muscle architecture in older and younger men and found significantly smaller muscle volume (17 - 29%), and pennation angle (15 - 18%) in the calves of older men (Morse et al., 2005). Baroni et al. (2013), showed that, in the vastus lateralis, muscle thickness and fascicle length were significantly smaller in healthy older men compared to healthy younger men with similar physical activity levels. Together these findings suggest that changes in muscle architecture occur with aging regardless of maintained physical fitness throughout life (Baroni et al., 2013).

1.4.2 Disease

Several studies have shown altered muscle architecture outcomes in samples with disease compared to healthy counterparts (Chen et al., 2018; Kaya et al., 2013; Malas et al., 2013; Valle et al., 2016). Compared to children experiencing typical development, children with cerebral palsy have been shown to have alterations in their muscle architecture that appear similar to that observed during aging (smaller muscle thickness and fascicle lengths) (Chen et al., 2018; Moreau et al., 2009). On the contrary, individuals with

systemic lupus erythematosus had muscles characterized by increased muscle thickness and pennation angles in the vastus lateralis (Kaya et al., 2013). Since relative strength of the vastus lateralis and fascicle lengths were lower in individuals with systemic lupus erythematosus compared to controls, authors stated that the greater muscle thickness and pennation angle was likely a result of edema (Kaya et al., 2013). This highlights that the effects of both atrophy and inflammation resulting from pathology can be observed *in vivo* using ultrasound imaging.

Overall, most studies cite that diseases, such as spastic cerebral palsy and Down syndrome, are related to a loss in muscle volume and thickness (Valle et al., 2016), as well as a decline in pennation angle and fascicle length (Chen et al., 2018). However, one study observed relatively larger quadriceps cross-sectional area and larger pennation angle despite a relatively lower knee extension torque in an obese population (Rastelli et al., 2015). In obese individuals, absolute muscle strength is greater compared to healthy counterparts; however, when strength is normalized to body mass, people with obesity are not stronger than healthy individuals. This may be explained by a relatively larger muscle fat percentage (Rastelli et al., 2015). These relationships between muscle architecture and muscle capacity can help describe disease as well as its underlying risk factors.

Furthermore, this suggests that muscle fascicle arrangement differ depending on population characteristics.

1.4.3 Effect of Training on Muscle Architecture

It is well known that physical activity and exercise training influence muscle structure (such as hypertrophy) (Suetta et al., 2008; Potier et al., 2009; Blazevich et al., 2007; Ema

et al., 2013; Narici et al., 1996). However, not all training protocols effect the same properties of muscle architecture (muscle thickness, pennation angle, and fascicle length) to the same degree. Specific training protocols (for example, high resistance and low power versus low resistance and high power) influence the muscle architecture of each individual lower limb muscle differently (Blazevich et al., 2007; Alegre et al., 2014; Karamanidis et al., 2006). Heavy resistance training increases pennation angle in the vastus lateralis while plyometrics increases fascicle length but decreases pennation angle (Blazevich, 2006). Vastus lateralis fascicle length and pennation angle increases have been observed after five weeks of slow eccentric and concentric training programs, with pennation angle increases continuing up to ten weeks (Blazevich et al., 2007). Pennation angle of the vastus lateralis increased 35% with progressive, lower-limb, heavy resistance training after 14 weeks in young men (mean age of 27 years old) (Aagaard et al., 2001). Isometric training with quadriceps muscles at extended muscle lengths (compared to 90° flexion) improved pennation angle in 19 healthy young men and women (mean age of 19 years old) (Alegre et al., 2014). Muscle thickness increased with isometric training regardless of muscle length in 19 healthy young men and women compared to 10 healthy men and women in the control group (Alegre et al., 2014). Post-training, changes in pennation angle persist and remain above baseline in healthy young adults for a period of at least three months (Blazevich et al., 2007). Ultimately, studying muscle architecture responses to training and detraining protocols may allow us to design training programs to target specific muscle architecture characteristics (such as pennation angle and fascicle length).

1.5 Why Muscle Architecture is Important

1.5.1 Research Applications

It is important to study the underlying mechanisms responsible for reductions in muscle capacity that occur as a result of muscle dysfunction in order to explore potential solutions. Although muscle architecture has been studied for centuries, its implications on muscle function have only gained popularity in the literature within the last 40 years (Gans et al., 1987). Understanding the arrangement of muscle is a useful research tool for understanding muscle mechanics, for modeling (Holzbaur et al., 2005), as well as for measuring changes after a training program (Blazevich et al., 2007; Suetta et al., 2008).

1.5.2 Clinical Uses

Clinical applications of musculoskeletal imaging have evolved as our understanding of muscle architecture has improved. Several clinical applications of muscle architecture currently exist while future applications are becoming more apparent as new research emerges. Muscle architecture is used to plan and inform surgical procedures (Delp et al., 1990; Fridén et al., 2002; Lieber, 1993), for monitoring postoperative muscle wasting (Reardon et al., 2001), and to assess improvement in muscle after rehabilitation (Malas et al., 2013; Suetta et al., 2008; Vaz et al., 2013).

1.6 Ultrasound to Measure Muscle Architecture In Vivo

Cadavers have been used to examine muscle architecture in the past, but these measurements are typically limited to older adults and might underestimate muscle architecture due to tissue shrinkage that occurs over time (Friederich et al., 1990).

Importantly, the length of muscle fascicles is several millimetres (mm) shorter than that of dead fascicles, as the embalming chemicals used to preserve the tissue cause it to shrink (Cutts, 1988). Most importantly, these studies do not provide us with evidence of how muscle behaves *in vivo*.

MRI scanning has also been used to investigate muscle architecture (Scott et al., 1993), however this method is expensive, time-consuming, and can be uncomfortable for participants who experience claustrophobia. Further, not all MRI scanning systems can accommodate larger patients (Prado et al., 2014). This is of concern because, as previously mentioned, obesity is both a risk factor and a consequence of many diseases. It is important that we be able to study the muscle architecture of these individuals. Lastly, manual segmentation analysis of MRI scans to evaluate muscle architecture can be tedious and time consuming.

Ultrasonography provides a relatively non-expensive, non-invasive alternative that is capable of producing images that yield reliable and valid muscle architecture measurements in healthy adults for the vastus lateralis (Bleakney & Maffulli, 2002; Brancaccio et al., 2008; Chleboun et al., 2007; Fukunaga et al., 1997; Seiberl et al., 2010), and the rectus femoris (Moreau et al., 2009). Because acceptable reliability is reported consistently, ultrasound is commonly used to measure muscle architecture *in vivo*. Nonetheless, standardization of ultrasound imaging is crucial to boost accuracy, promote acceptable reliability and compare results across studies. Furthermore, previous findings have stated that excellent reliability (intraclass correlation coefficient (ICC) = 0.97) can be achieved between novice, intermediate, and experienced researchers (Correa-de-

Araujo et al., 2017). Novice operators were considered to be those with less than one month of experience, although, the quantity of practice scans was not specified by the authors (Correa-de-Araujo et al., 2017). Therefore, these measurements can be completed reliably by individuals with less than one month of experience. Although, without an aid, differences in applied pressure of the transducer head seems to be prevalent between these groups of imagers. Thus, the current barriers preventing the standardization of imaging include differences in transducer placement, and inter-rater imaging.

1.7 Limitations of Ultrasound

Differences in transducer position can introduce anisotropic error by parallax of images. This can occur if imaging region, pressure, imaging plane, and fascicle alignment are not constant. Muscle architecture is not uniform throughout the muscle (Kellis et al., 2010). Muscle thickness, pennation angle and fascicle length vary from proximal to distal portions of muscle (Kellis et al., 2010). Ideally, the thickest portion of the muscle belly would be imaged, however, this specific location may vary between participants. Imaging regions can be standardized by using relative scaling of imaging sites (e. g., 50% of the length between the anterior inferior iliac spine (ASIS) and the superior border of the patella) rather than absolute sites (e. g., 15 cm above the patella).

Muscle appearance can be altered as a result of varying pressure from the transducer head compressing the tissue. It is difficult to ensure consistent pressure of the transducer head between raters, and indeed, even within a single imager. Some studies

have suggested using a generous amount of gel can help to alleviate some of the pressure (Blazevich et al., 2006; Lixandrao et al., 2014; Valle et al., 2016). This is often done by allowing a thin space of gel above the skin surface to be visible within images (Lixandrao et al., 2014). This is a subjective method and may minimally attenuate the signal by increasing the depth that the ultrasound must penetrate (Narouze, 2011).

In order to standardize musculoskeletal ultrasound imaging, fascicle plane alignment is required (Bénard et al., 2009). This would require accurately positioning the head of the transducer parallel to the fascicles. *In vivo*, this positioning can be difficult to guarantee. A potential solution has been proposed by Bénard et al., 2009. Scout scanning can be performed with the ultrasound head in the transverse plane, the crest of the muscle can be identified and this can be marked as the imaging region (Bénard et al., 2009).

Orientation of the transducer (or transducer tilt) relative to the skin is also needed to ensure fascicle plane alignment (Bénard et al., 2009; König et al., 2014). A transducer orientation that is in line with and parallel to the muscle fascicles themselves is recommended for musculoskeletal imaging (Klimstra et al., 2007). Most studies image muscle with the transducer oriented perpendicular to the skin (Alegre et al., 2014; Bénard et al., 2009; Blazevich et al., 2006; Kwah et al., 2013; Thom et al., 2007; van den Hoorn et al., 2016). Methods to standardize the angle of the transducer against the skin are not common. To our knowledge, only one study has attempted to standardize transducer angle using a foam cast that was strapped around the gastrocnemius (König et al., 2014). However, several issues may arise from this method. First, the cast must be tightly

secured to the limb to prevent sliding of the transducer head. This may cause bulging or swelling of the muscle at the imaging region which could alter the muscle architecture measurements. Second, this method does not allow removal of the transducer head between scans. Removal of the transducer from the skin between individual scans is common practice as the constant transducer contact may compress tissue throughout the imaging session (Blazevich et al., 2006). From a practical perspective, the casting of the transducer against the skin may be cumbersome and time-consuming to implement into regular, clinical practice. Thus, a more convenient method to standardize the angle of the transducer is likely useful.

Finally, differences in sonographer performance and experience can interfere with direct comparisons between studies. As previously mentioned, pressure of the transducer likely varies between imagers and knowledge of anatomy is required to ensure correct imaging region, alignment, and orientation. Results may vary as a result of sonographer experience (novice imagers vs. trained sonographers). Therefore, a study that shows good intra- and inter-rater reliability by trained sonographers may not be applicable to imagers with novice training and experience.

Studies have investigated the intra-rater reliability in the vastus lateralis (Bleakney & Maffulli, 2002; Brancaccio et al., 2008; Chleboun et al., 2007; Fukunaga et al., 1997; Moreau et al., 2009; Seiberl et al., 2010), and the rectus femoris (Moreau et al., 2009). Three studies with similar designs investigated the intra-rater reliability of the pennation angle, fascicle length, and muscle thickness of the vastus lateralis in healthy young adults using a coefficient of variance equation (Bleakney & Maffulli, 2002; Brancaccio et al.,

2008; Fukunaga et al., 1997). All studies imaged the muscles using a perpendicular transducer angle, except for Bleakney & Maffulli (2002), who imaged the muscle with the transducer parallel to the floor (an explanation for this protocol decision was not provided). Chleboun et al. (2007) investigated the intra-rater reliability of measuring the fascicle lengths of the vastus lateralis in healthy young adults and was, seemingly, the only study to report absolute and relative reliability. Seiberl et al. (2010) performed ICC's (type unspecified) in order to control for intra-rater variations in measurements of the fascicle lengths and the pennation angles of the vastus lateralis in healthy young adults. Fascicle length was derived using an extrapolation technique (Finni et al., 2003). The intra-rater reliability of fascicle length using this technique was reported to be excellent (ICC = 0.80) (Seiberl et al., 2010).

The inter-rater reliability of in vivo muscle architecture measures of the vastus lateralis and the rectus femoris has been previously reported (Strasser et al., 2013). Strasser et al. (2013) used two-way random effect ICCs to assess the inter-rater reliability of the fascicle length and the muscle thickness in the rectus femoris, as well as the pennation angle, fascicle length, and muscle thickness within the vastus lateralis of healthy young adults. Strasser et al. (2013) did not report pennation angles of the rectus femoris because fascicle lengths were observed to be almost parallel to the aponeurosis and were considered to be 0°. Excellent reliability was reported for the muscle thickness measurements from both muscles (ICC = 0.97 for the rectus femoris and 0.96 for the vastus lateralis), fair reliability was reported for the fascicle lengths of each muscle (ICC = 0.57 for the rectus femoris and 0.62 for the vastus lateralis), and fair reliability was also

reported for the pennation angle measurements of the vastus lateralis (ICC = 0.53) (Strasser et al., 2013).

It is important to note that very few studies investigated the reliability of muscle architecture measures taken from the images of the rectus femoris. As well the majority of imaging from the previously mentioned sites were completed with the leg close to full extension (0-10°). To our knowledge, no studies have investigated the reliability of images taken of the vastus lateralis and rectus femoris when the knee is positioned such that these muscles are at optimal length. For these muscle groups, the optimal knee position is reported to be 60° (Lindahl et al., 1969; Ng et al., 1994; Welsch et al., 1998). Although we do not expect that imaging the quadriceps muscles at this angle will provide us with better quality images, most strength assessments are performed with the knee joint at the optimal angle of 60°. If reliable imaging of the vastus lateralis and the rectus femoris can be achieved from this knee joint angle, we can take images of the muscles at rest and during contraction while the leg is in the same position. Therefore, imaging at this angle may be ideal for understanding muscle architecture and fascicle behaviour at optimal angles.

1.8 Purpose and Hypothesis

The overarching aim of this work was to standardize musculoskeletal ultrasound imaging procedures of the rectus femoris and the vastus lateralis in healthy adults. The specific purpose of this study was to assess the level of agreement and quantify the error resulting from variations of the ultrasound transducer position relative to the surface of the skin, on measurements of muscle architecture acquired from the rectus femoris and vastus

lateralis, at rest, in healthy adults. This thesis has two secondary objectives. First, this study aimed to determine the intra-rater reliability of measuring muscle thickness, subcutaneous fat thickness, pennation angle, and fascicle length of two quadriceps from ultrasound images taken while the knee is positioned at the optimal length of the quadriceps, by a single researcher. Second, this study aimed to test the inter-rater reliability of ultrasound image acquisition of these two quadriceps muscles between two researchers with novice imaging experience.

1.8.1 Primary Hypothesis

We expected agreement of muscle architecture values (muscle thickness, fat thickness, pennation angle, and fascicle length) of the rectus femoris and vastus lateralis of healthy young adults to be highest, and error to be lowest, when the transducer was held at angles nearest to 90° to the skin (i.e., 85° and 95°).

1.8.2 Secondary Aim (A) Hypothesis

We hypothesized that, in healthy young adults, initial and repeated muscle architecture measurements (muscle thickness, fat thickness, pennation angle, and fascicle length) of the rectus femoris and vastus lateralis would be similar and therefore reliable.

1.8.3 Secondary Aim (B) Hypothesis

We hypothesized that muscle architecture outcomes (muscle thickness, fat thickness, pennation angle, and fascicle length) would be reliable between images taken by rater 1 (BDB) and rater 2 (JCH) in the rectus femoris and vastus lateralis of healthy young adults.

1.9 Contributions to Literature

This work will provide future researchers with a resource to aid in musculoskeletal ultrasound imaging. This work quantifies the error associated with imaging with different transducer angles as well as with different imagers. A device to assist in the standardization of transducer angle has been proposed and implemented in this study. Lastly, the reliability of data produced while using this device has been assessed in this study. This investigation has provided the literature with a comprehensive resource assessing the reliability of measuring muscle architecture of two commonly imaged muscles in a healthy young adult population.

References

- Aagaard, P., Andersen, J. L., Dyhre-Poulsen, P., Leffers, A. M., Wagner, A., Magnusson, S. P., Halkjær-Kristensen, J., Simonsen, E. B. (2001). A mechanism for increased contractile strength of human pennate muscle in response to strength training: Changes in muscle architecture. *Journal of Physiology*, 534(2), 613–623. <https://doi.org/10.1111/j.1469-7793.2001.t01-1-00613.x>
- Alegre, L. M., Ferri-Morales, A., Rodriguez-Casares, R., & Aguado, X. (2014). Effects of isometric training on the knee extensor moment - angle relationship and vastus lateralis muscle architecture. *European Journal of Applied Physiology*, 114(11), 2437–2446. <https://doi.org/10.1007/s00421-014-2967-x>
- Alegre, L. M., Jiménez, F., Gonzalo-Orden, J. M., Martín-Acero, R., & Aguado, X. (2006). Effects of dynamic resistance training on fascicle length and isometric strength. *Journal of Sports Sciences*, 24(5), 501–508. <https://doi.org/10.1080/02640410500189322>
- Ando, R., Saito, A., Umemura, Y., & Akima, H. (2015). Local architecture of the vastus intermedius is a better predictor of knee extension force than that of the other quadriceps femoris muscle heads. *Clinical Physiology and Functional Imaging*, 35(5), 376–382. <https://doi.org/10.1111/cpf.12173>
- Arellano, C. J., Gidmark, N. J., Konow, N., Azizi, E., & Roberts, T. J. (2016). Determinants of aponeurosis shape change during muscle contraction. *Journal of Biomechanics*, 49(9), 1812–1817. <https://doi.org/10.1016/j.jbiomech.2016.04.022>
- Baroni, B. M., Geremia, J. M., Rodrigues, R., Borges, M. K., Jinha, A., Herzog, W., Vaz, M. A. (2013). Functional and morphological adaptations to aging in knee extensor muscles of physically active men. *Journal of Applied Biomechanics*, 29(5), 535–542.
- Bénard, M. R., Becher, J. G., Harlaar, J., Huijing, P. A., & Jaspers, R. T. (2009). Anatomical information is needed in ultrasound imaging of muscle to avoid potentially substantial errors in measurement of muscle geometry. *Muscle and Nerve*, 39(5), 652–665. <https://doi.org/10.1002/mus.21287>
- Blazevich, A. J. (2006). Effects of Physical Training and Detraining, Immobilisation, Growth and Aging on Human Fascicle Geometry. *Sports Med*, 36(12), 1003–1017.
- Blazevich, A. J., Cannavan, D., Coleman, D. R., & Horne, S. (2007). Influence of concentric and eccentric resistance training on architectural adaptation in human quadriceps muscles. *Journal of Applied Physiology*, 103(5), 1565–1575. <https://doi.org/10.1152/jappphysiol.00578.2007>
- Blazevich, A. J., Gill, N. D., & Zhou, S. (2006). Intra- and intermuscular variation in human quadriceps femoris architecture assessed in vivo. *Journal of Anatomy*, 209(3), 289–310. <https://doi.org/10.1111/j.1469-7580.2006.00619.x>
- Bleakney, R., & Maffulli, N. (2002). Ultrasound changes to intramuscular architecture of the quadriceps following intramedullary nailing. *Journal of Sports Medicine and Physical Fitness*, 42(1), 120–125.
- Bodine, S., Roy, R., Meadows, D., Zernicke, R., Sacks, R., Fournier, M., & Edgerton, V.

- (1982). Architectural, histochemical, and contractile characteristics of a unique biarticular muscle: the cat semitendinosus. *Journal of Neurophysiology*, 48(1), 192–201. <https://doi.org/10.1152/jn.1982.48.1.192>
- Brancaccio, P., Limongelli, F. M., D'Aponte, A., Narici, M., & Maffulli, N. (2008). Changes in skeletal muscle architecture following a cycloergometer test to exhaustion in athletes. *Journal of Science and Medicine in Sport*, 11(6), 538–541. <https://doi.org/10.1016/j.jsams.2007.05.011>
- Buford, T. W., Lott, D. J., Marzetti, E., Wohlgemuth, S. E., Vandenborne, K., Pahor, M., Leeuwenburgh, C., Manini, T. M. (2012). Age-related differences in lower extremity tissue compartments and associations with physical function in older adults. *Experimental Gerontology*, 47(1), 38–44. <https://doi.org/10.1016/j.exger.2011.10.001>
- Cadore, E. L., Izquierdo, M., Conceição, M., Radaelli, R., Pinto, R. S., Baroni, B. M., Vaz, M. A., Alberton, C. L., Pinto, S. S., Cunha, G., Bottaro, M., Krueel, L. F. M. (2012). Echo intensity is associated with skeletal muscle power and cardiovascular performance in elderly men. *Experimental Gerontology*, 47(6), 473–478. <https://doi.org/10.1016/j.exger.2012.04.002>
- Chen, Y., He, L., Xu, K., Li, J., Guan, B., & Tang, H. (2018). Comparison of calf muscle architecture between Asian children with spastic cerebral palsy and typically developing peers. *PLoS ONE*, 13(1), 1–14. <https://doi.org/10.1371/journal.pone.0190642>
- Chirita-Emandi, A., Dobrescu, A., Papa, M., Puiu, M., & Emandi, A. C. (2015). Reliability of Measuring Subcutaneous Fat Tissue Thickness Using Ultrasound in Non-Athletic Young Adults. *Maedica - a Journal of Clinical Medicine*, 10(103), 204–209.
- Chleboun, G. S., Basic, A. B., Graham, K. K., & Stuckey, H. A. (2007). Fascicle Length Change of the Human Tibialis Anterior and Vastus Lateralis During Walking. *Journal of Orthopaedic & Sports Physical Therapy*, 37(7), 372–379. <https://doi.org/10.2519/jospt.2007.2440>
- Correa-de-Araujo, R., Harris-Love, M. O., Miljkovic, I., Fragala, M. S., Anthony, B. W., & Manini, T. M. (2017). The Need for Standardized Assessment of Muscle Quality in Skeletal Muscle Function Deficit and Other Aging-Related Muscle Dysfunctions: A Symposium Report. *Frontiers in Physiology*, 8, 1–19. <https://doi.org/10.3389/fphys.2017.00087>
- Cutts, (1988). Shrinkage of muscle fibres during the fixation of cadaveric tissue. *Journal of Anatomy*, 160, 75-78.
- Damjanov, I. (2009). Skeletal muscles. In *Pathology Secrets* 3rd edition (pp. 434–447). <https://doi.org/10.1016/B978-0-323-05594-9.00021-0>
- de Boer, M. D., Seynnes, O. R., di Prampero, P. E., Pišot, R., Mekjavić, I. B., Biolo, G., & Narici, M. V. (2008). Effect of 5 weeks horizontal bed rest on human muscle thickness and architecture of weight bearing and non-weight bearing muscles. *European Journal of Applied Physiology*, 104(2), 401–407. <https://doi.org/10.1007/s00421-008-0703-0>
- Delp, S. L. L., Loan, J. P. P., Hoy, M. G. G., Zajac, F. E., Topp, E. L., & Rosen, J. M.

- (1990). An interactive graphics-based model of the lower extremity to study orthopedic surgical procedures. *IEEE Transactions on Biomedical Engineering*, 37(8), 757–767. <https://doi.org/10.1109/10.102791>
- Elder, J. B. (2007). *THIEME Atlas of Anatomy Series. Neurosurgery* (Vol. 61). <https://doi.org/10.1227/01.NEU.0000290923.01213.93>
- Ema, R., Wakahara, T., Miyamoto, N., Kanehisa, H., & Kawakami, Y. (2013). Inhomogeneous architectural changes of the quadriceps femoris induced by resistance training. *European Journal of Applied Physiology*, 113(11), 2691–2703. <https://doi.org/10.1007/s00421-013-2700-1>
- Finni, T., Ikegawa, S., Lepola, V., & Komi, P. V. (2003). Comparison of force-velocity relationships of vastus lateralis muscle in isokinetic and in stretch-shortening cycle exercises. *Acta Physiologica Scandinavica*, 177(4), 483–491. <https://doi.org/10.1046/j.1365-201X.2003.01069.x>
- Fridén, J., & Lieber, R. L. (2002). Mechanical considerations in the design of surgical reconstructive procedures. *Journal of Biomechanics*, 35(8), 1039–1045. [https://doi.org/10.1016/S0021-9290\(02\)00045-3](https://doi.org/10.1016/S0021-9290(02)00045-3)
- Friederich, J. A., & Brand, R. A. (1990). Muscle fiber architecture in the human lower limb. *Journal of Biomechanics*, 23(1), 91–95. <https://doi.org/10.1227/01.NEU.0000297048.04906.5B0>
- Fukumoto, Y., Ikezoe, T., Yamada, Y., Tsukagoshi, R., Nakamura, M., Mori, N., Kimura, M., Ichihashi, N. (2012). Skeletal muscle quality assessed from echo intensity is associated with muscle strength of middle-aged and elderly persons. *European Journal of Applied Physiology*, 112(4), 1519–1525. <https://doi.org/10.1007/s00421-011-2099-5>
- Fukunaga, T., Ichinose, Y., Masamitsu, I., Kawakami, Y., & Fukashiro, S. (1997). Determination of fascicle length and pennation in a contracting human muscle in vivo. *The American Physiology Society*, 378–381.
- Fukunaga, T., Kawakami, Y., Kuno, F., & Fukashiro, S. (1997). Muscle Architecture and Function in Humans. *Journal of Biomechanics*, 30(5), 457–463.
- Gans, C. (1982). Fiber Architecture and Muscle Function. *Exercise & Sport Sciences Reviews*, 10, 160–207.
- Gans, C., & de Vree, F. (1987). Functional bases of fibre length and angulation in muscle. *Journal of Morphology*, 192, 63–85.
- Gans, C., & Gaunt, A. S. (1991). Muscle architecture in relation to function. *Journal of Biomechanics*, 24(Supplementary 1), 53–65. [https://doi.org/10.1016/0021-9290\(91\)90377-Y](https://doi.org/10.1016/0021-9290(91)90377-Y)
- Henriksson-Larsen, K., Wretling, M. L., Lorentzon, R., & Öberg, L. (1992). Do muscle fibre size and fibre angulation correlate in pennated human muscles? *European Journal of Applied Physiology and Occupational Physiology*, 64(1), 68–72. <https://doi.org/10.1007/BF00376443>
- Holzbour, K. R. S., Murray, W. M., & Delp, S. L. (2005). A model of the upper extremity for simulating musculoskeletal surgery and analyzing neuromuscular control. *Annals of Biomedical Engineering*, 33(6), 829–840. <https://doi.org/10.1007/s10439-005-3320-7>

- Huxley, A.F., Niedergerke, R., (1954). Structural Changes in Muscle During Contraction: Interference Microscopy of Living Muscle Fibres. *Nature*, 173, 971-973.
- Huxley, H., Hanson, J., (1954). Changes in the Cross-Striation of Muscle During Contraction and Stretch and their Structural Interpretation. *Nature*, 173, 973-976.
- Ikezoe, T., Mori, N., Nakamura, M., & Ichihashi, N. (2011). Age-related muscle atrophy in the lower extremities and daily physical activity in elderly women. *Archives of Gerontology and Geriatrics*, 53(2). <https://doi.org/10.1016/j.archger.2010.08.003>
- Karamanidis, K., & Arampatzis, A. (2006). Mechanical and morphological properties of human quadriceps femoris and triceps surae muscle-tendon unit in relation to aging and running. *Journal of Biomechanics*, 39(3), 406–417. <https://doi.org/10.1016/j.jbiomech.2004.12.017>
- Kawakami, Y., Abe, T., & Fukunaga, T. (1993). Muscle-fiber pennation angles are greater in hypertrophied than in normal muscles. *Journal of Applied Physiology*, 74(6), 2740–2744. <https://doi.org/10.1152/jap.1993.74.6.2740>
- Kaya, A., Kara, M., Tiftik, T., Tezcan, M. E., Özel, S., Ersöz, M., Göker, B., Haznedaroğlu, Ş., Özçakar, L. (2013). Ultrasonographic evaluation of the muscle architecture in patients with systemic lupus erythematosus. *Clinical Rheumatology*, 32(8), 1155–1160. <https://doi.org/10.1007/s10067-013-2249-8>
- Kearns, C. F., Abe, T., & Brechue, W. F. (2000). Muscle enlargement in sumo wrestlers includes increased muscle fascicle length. *European Journal of Applied Physiology*, 83(4–5), 289–296. <https://doi.org/10.1007/s004210000298>
- Kellis, E., Galanis, N., Natsis, K., & Kapetanios, G. (2010). Muscle architecture variations along the human semitendinosus and biceps femoris (long head) length. *Journal of Electromyography and Kinesiology*, 20(6), 1237–1243. <https://doi.org/10.1016/j.jelekin.2010.07.012>
- Klimstra, M., Dowling, J., Durkin, J. L., & MacDonald, M. (2007). The effect of ultrasound probe orientation on muscle architecture measurement. *Journal of Electromyography and Kinesiology*, 17(4), 504–514. <https://doi.org/10.1016/j.jelekin.2006.04.011>
- König, N., Cassel, M., Intziagianni, K., & Mayer, F. (2014). Inter-rater reliability and measurement error of sonographic muscle architecture assessments. *Journal of Ultrasound in Medicine*, 33(5), 769–777. <https://doi.org/10.7863/ultra.33.5.769>
- Kraemer, W. J., & Newton, R. U. (2000). Training for Muscular Power. *Physical Medicine and Rehabilitation Clinics of North America*, 11(2), 341–368.
- Kwah, L. K., Pinto, R. Z., Diong, J., & Herbert, R. D. (2013). Reliability and validity of ultrasound measurements of muscle fascicle length and pennation in humans: a systematic review. *Journal of Applied Physiology*, 114(6), 761–769. <https://doi.org/10.1152/jap.1993.74.6.2740>
- Lieber, R. L. (1993). Skeletal Muscle Architecture: Implications for Muscle Function and Surgical Tendon Transfer. *Journal of Hand Therapy*, 6(2), 105–113. [https://doi.org/10.1016/S0894-1130\(12\)80291-2](https://doi.org/10.1016/S0894-1130(12)80291-2)
- Lieber, R. L., & Fridén, J. (2000). Functional and Clinical Significance of Skeletal

- Muscle Architecture. *Muscle Nerve*, 23(November), 1647–1666.
[https://doi.org/10.1002/1097-4598\(200011\)23:11<1647::AID-MUS1>3.0.CO;2-M](https://doi.org/10.1002/1097-4598(200011)23:11<1647::AID-MUS1>3.0.CO;2-M)
 [pii]
- Lindahl, O., Movin, A., & Ringqvist, I. (1969). Knee extension: Measurement of the isometric force in different positions of the knee-joint. *Acta Orthopaedica*, 40(1), 79–85. <https://doi.org/10.3109/17453676908989487>
- Lixandrao, M. E., Ugrinowitsch, C., Bottaro, M., Chacon-Mikahil, M., Cavaglieri, C. R., Min, L. L., DeSouza, E. O., Laurentino, G. C., Libardi, C. A. (2014). Vastus Lateralis Muscle Cross-Sectional Area Ultrasonography Validity for Image Fitting in Humans. *Journal of Strength and Conditioning Research*, 28(11), 3293–3297.
- Maden-Wilkinson, T., Degens, H., Jones, D. A., McPhee, J. S., (2013). Comparison of MRI and DXA to measure muscle size and age-related atrophy in thigh muscles. *Journal of Musculoskeletal & Neuronal Interactions*. 13(3), 320-328.
- Malas, F. Ü., Özçakar, L., Kaymak, B., Ulaşlı, A., Güner, S., Kara, M., & Akinci, A. (2013). Effects of different strength training on muscle architecture: Clinical and ultrasonographic evaluation in knee osteoarthritis. *PM and R*, 5(8), 655–662. <https://doi.org/10.1016/j.pmrj.2013.03.005>
- Martinikorena, I., Martínez-Ramírez, A., Gómez, M., Lecumberri, P., Casas-Herrero, A., Cadore, E. L., Millor, N., Zambom-Ferraresi, F., Idoate, F., Izquierdo, M. (2016). Gait Variability Related to Muscle Quality and Muscle Power Output in Frail Nonagenarian Older Adults. *Journal of the American Medical Directors Association*, 17(2), 162–167. <https://doi.org/10.1016/j.jamda.2015.09.015>
- Melo, R. C., Takahashi, A. C. M., Quiterio, R. J., Salvini, T. F., & Catai, A. M. (2016). Eccentric Torque-Producing Capacity is Influenced by Muscle Length in Older Healthy Adults. *Journal of Strength and Conditioning Research*, 30(1), 259–266.
- Mitsukawa, N., Sugisaki, N., Kanehisa, H., Fukunaga, T., & Kawakami, Y. (2009). Fatigue-related changes in fascicle-tendon geometry over repeated contractions: Difference between synergist muscles. *Muscle and Nerve*, 40(3), 395–401. <https://doi.org/10.1002/mus.21303>
- Moreau, N. G., Teefey, S. A., & Damiano, D. L. (2009). In vivo muscle architecture and size of the rectus femoris and vastus lateralis in children and adolescents with cerebral palsy. *Developmental Medicine and Child Neurology*, 51(10), 800–806. <https://doi.org/10.1111/j.1469-8749.2009.03307.x>
- Morse, C. I., Thom, J. M., Birch, K. M., & Narici, M. V. (2005). Changes in triceps surae muscle architecture with sarcopenia. *Acta Physiologica Scandinavica*, 183(3), 291–298. <https://doi.org/10.1111/j.1365-201X.2004.01404.x>
- Narici, M., Hoppeler, H., Kayser, B., Landoni, L., Classen, H., Gavardi, C., Conti, M., Cerretelli, P., (1996). Human Quadriceps Cross-Sectional Area, Torque and Neural Activation during 6 Month Strength Training. *Acta Physiologica Scandanavica*. 157(2), 175 – 186. [10.1046/j.1365-201X.1996.483230000.x](https://doi.org/10.1046/j.1365-201X.1996.483230000.x)
- Narici, M., (1999). Human skeletal muscle architecture studied in vivo by non-invasive imaging techniques: functional significance and applications. *J Electromyogr Kinesiol*, 9(2), 97–103. [https://doi.org/10.1016/S1050-6411\(98\)00041-8](https://doi.org/10.1016/S1050-6411(98)00041-8)
- Narici, M., Franchi, M., & Maganaris, C. (2016). Muscle structural assembly and

- functional consequences. *Journal of Experimental Biology*, 219(2), 276–284. <https://doi.org/10.1242/jeb.128017>
- Narici, M. V., Maganaris, C. N., Reeves, N. D., & Capodaglio, P. (2003). Effect of Aging on Human Muscle Architecture. *Journal of Applied Physiology*, 95(6), 2229–2234. <https://doi.org/10.1152/jappphysiol.00433.2003>
- Narouze, S. N. (2011). Atlas of ultrasound-guided procedures in interventional pain management. *Atlas of Ultrasound-Guided Procedures in Interventional Pain Management*, 1–372. <https://doi.org/10.1007/978-1-4419-1681-5>
- Ng, A. V., Agre, J. C., Hanson, P., Harrington, M. S., & Nagle, F. J. (1994). Influence of muscle length and force on endurance and pressor responses to isometric exercise. *Journal of Applied Physiology*, 76(6), 2561–2569.
- Potier, T., Alexander, C. M., Seynnes, O. R., (2009). Effects of eccentric strength training on biceps femoris muscle architecture and knee joint range of movement. *European Journal of Applied Physiology*. 105(6), 939-944. 10.1007/s00421-008-0980-7
- Prado, C. M. M., & Heymsfield, S. B. (2014). Lean Tissue Imaging: A New Era for Nutritional Assessment and Intervention. *Journal of Parenteral and Enteral Nutrition*, 38(8), 940–953. <https://doi.org/10.1177/0148607114550189>
- Puthoff, M. L., Janz, K. F., & Nielsen, D. H. (2008). The relationship between lower extremity strength and power to everyday walking behaviors in older adults with functional limitations. *Journal of Geriatric Physical Therapy*, 31(1), 24–31. <https://doi.org/10.1519/00139143-200831010-00005>
- Puthoff, M. L., & Nielsen, D. H. (2010). Relationships Among Impairments in Lower-Extremity Strength and Power, Functional Limitations, and Disability in Older Adults. *Physical Therapy Journal*, 87(October 2010), 1–2. Retrieved from [http://report.nih.gov/nihfactsheets/Pdfs/DisabilityinOlderAdults\(NIA\).pdf](http://report.nih.gov/nihfactsheets/Pdfs/DisabilityinOlderAdults(NIA).pdf)
- Raj, S. I., Bird, S., Shield, A., (2017). Ultrasound Measurements of Skeletal Muscle Architecture are Associated with Strength and Functional Capacity in Older Adults. *Ultrasound in Medicine & Biology*. 43(3), 586 – 594. 10.1016/j.ultrasmedbio.2016.11.013
- Rastelli, F., Capodaglio, P., Orgiu, S., Santovito, C., Caramenti, M., Cadioli, M., Falini, A., Rizzo, G., Lafortuna, C. L. (2015). Effects of muscle composition and architecture on specific strength in obese older women. *Experimental Physiology*, 100(10), 1159–1167. <https://doi.org/10.1113/EP085273>
- Reardon, K., Galea, M., Dennett, X., Choong, P., & Byrne, E. (2001). Quadriceps muscle wasting persists 5 months after total hip arthroplasty for osteoarthritis of the hip: a pilot study. *Intern Med J*, 31(1), 7–14. <https://doi.org/10.1046/j.1445-5994.2001.00007.x>
- Reeves, N. D., Maganaris, C. N., Narici, M. V., (2004). Ultrasonographic assessment of human skeletal muscle size. *European Journal of Applied Physiology*. 91(1), 116-118. 10.1007/s00421-003-0961-9
- Rode, C., Siebert, T., Tomalka, A., & Blickhan, R. (2016). Myosin filament sliding

- through the Z-disc relates striated muscle fibre structure to function. *Proceedings of the Royal Society B: Biological Sciences*, 283(1826), 10–13.
<https://doi.org/10.1098/rspb.2015.3030>
- Rosenberg, I. H., (1997). Sarcopenia: Origins and Clinical Relevance. *American Society for Nutritional Sciences*. 127, 990S – 991S.
- Roubenoff, R., (2001). Origins and Clinical Relevance of Sarcopenia. *Canadian Journal of Applied Physiology*. 26(1), 78 – 89.
- Rutherford, O. M., & Jones, D. A. (1992). Measurement of fibre pennation using ultrasound in the human quadriceps in vivo. *European Journal of Applied Physiology and Occupational Physiology*, 65(5), 433–437.
<https://doi.org/10.1007/BF00243510>
- Sayers, S. P. (2007). High-speed power training: a novel approach to resistance training in older men and women. A brief review and pilot study. *Journal of Strength & Conditioning Research*, 21(2), 518–526. <https://doi.org/10.1519/R-20546.1>
- Scott, S. H., Engstrom, C. M., & Loeb, G. E. (1993). Morphometry of human thigh muscles. Determination of fascicle architecture by magnetic resonance imaging. *Journal of Anatomy*, 182, 249–257.
- Seiberl, W., Hahn, D., Kreuzpointner, F., Schwirtz, A., & Gastmann, U. (2010). Force enhancement of quadriceps femoris in vivo and its dependence on stretch-induced muscle architectural changes. *Journal of Applied Biomechanics*, 26(3), 256–264.
<https://doi.org/10.1123/jab.26.3.256>
- Strasser, E. M., Draskovits, T., Praschak, M., Quittan, M., & Graf, A. (2013). Association between ultrasound measurements of muscle thickness, pennation angle, echogenicity and skeletal muscle strength in the elderly. *Age*, 35(6), 2377–2388.
<https://doi.org/10.1007/s11357-013-9517-z>
- Suetta, C., Andersen, J. L., Dalgas, U., Berget, J., Koskinen, S., Aagaard, P., Magnusson, S. P., Kjaer M. (2008). Resistance training induces qualitative changes in muscle morphology, muscle architecture, and muscle function in elderly postoperative patients. *Journal of Applied Physiology*, 105, 180–186.
<https://doi.org/10.1152/jappphysiol.01354.2007>
- Thom, J. M., Morse, C. I., Birch, K. M., & Narici, M. V. (2007). Influence of muscle architecture on the torque and power-velocity characteristics of young and elderly men. *European Journal of Applied Physiology*, 100(5), 613–619.
<https://doi.org/10.1007/s00421-007-0481-0>
- Valle, M. S., Casabona, A., Micale, M., & Cioni, M. (2016). Relationships between Muscle Architecture of Rectus Femoris and Functional Parameters of Knee Motion in Adults with Down Syndrome. *BioMed Research International*, 2016.
<https://doi.org/10.1155/2016/7546179>
- van den Hoorn, W., Coppeters, M. W., van Dieën, J. H., & Hodges, P. W. (2016). Development and Validation of a Method to Measure Lumbosacral Motion Using Ultrasound Imaging. *Ultrasound in Medicine and Biology*, 42(5), 1221–1229.
<https://doi.org/10.1016/j.ultrasmedbio.2016.01.001>
- Vaz, M. A., Baroni, B. M., Geremia, J. M., Lanferdini, F. J., Mayer, A., Arampatzis, A.,

- & Herzog, W. (2013). Neuromuscular electrical stimulation (NMES) reduces structural and functional losses of quadriceps muscle and improves health status in patients with knee osteoarthritis. *Journal of Orthopaedic Research*, 31(4), 511–516. <https://doi.org/10.1002/jor.22264>
- Watanabe, Y., Yamada, Y., Fukumoto, Y., Ishihara, T., Yokoyama, K., Yoshida, T., Miyake, M., Yamagata, E., Kimura, M. (2013). Echo intensity obtained from ultrasonography images reflecting muscle strength in elderly men. *Clinical Interventions in Aging*, 8, 993–998. <https://doi.org/10.2147/CIA.S47263>
- Welsch, M. A., Williams, P. A., Pollock, M. L., Graves, J. E., Foster, D. N., & Fulton, M. N. (1998). Quantification of full-range-of-motion unilateral and bilateral knee flexion and extension torque ratios. *Archives of Physical Medicine and Rehabilitation*, 79(8), 971–978. [https://doi.org/10.1016/S0003-9993\(98\)90097-1](https://doi.org/10.1016/S0003-9993(98)90097-1)
- Woittiez, R. D., Huijing, P. A., & Rozendal, R. H. (1983). Influence of muscle architecture on the length-force diagram - A model and its verification. *European Journal of Physiology*, 397(1), 73–74. <https://doi.org/10.1007/BF00585173>

Chapter 2: Reliability of Muscle Architecture Measurements of the Vastus Lateralis and the Rectus Femoris Acquired Using a Novel 3D-Printed Device

2.1 Introduction

Muscle thickness, pennation angle, and fascicle length are often used to characterize the architecture of a muscle (Blazevich, 2006; Narici, 1999). Muscle architecture is relevant to functional capabilities of muscle, such as strength and contraction velocity (Bodine et al., 1982; Gans & de Vree, 1987). As a result, muscle architecture assessments are commonly studied. Despite the many applications of muscle architecture (e.g., muscle thickness, pennation angle, and fascicle length), comparison between muscle architecture studies is difficult due to the lack of reporting specific standardization between protocols.

Ultrasound can be used to assess muscle architecture, as well as surrounding tissues, such as subcutaneous fat. However, ultrasound imaging is sensitive to the position of the transducer around the x-, y-, and z- axes (shown in Figure 3) (Klimstra et al., 2007; Prado et al., 2014). Rotation around the x-axis adjusts the tilt of the transducer relative to the skin. Rotation around the z-axis adjusts alignment of the transducer head to the muscle fascicles. Rotation around the y-axis adjusts the transducer's contact with the skin and is sometimes referred to as "heel-toe rotation." Alignment of the transducer in the y- and z-axes can be standardized between images by drawing a line on the skin around the head of the transducer to ensure the same placement for each image within a participant. In the literature, there lacks a technique to standardize the angle of the transducer around the x-axis (Figure 3). This is concerning because inconsistent transducer positions can

potentially alter the appearance of thickness, pennation angle, and fascicle lengths. Some studies report that the transducer was held perpendicular to the skin, however methods to ensure a 90° position have often not been outlined in current literature.

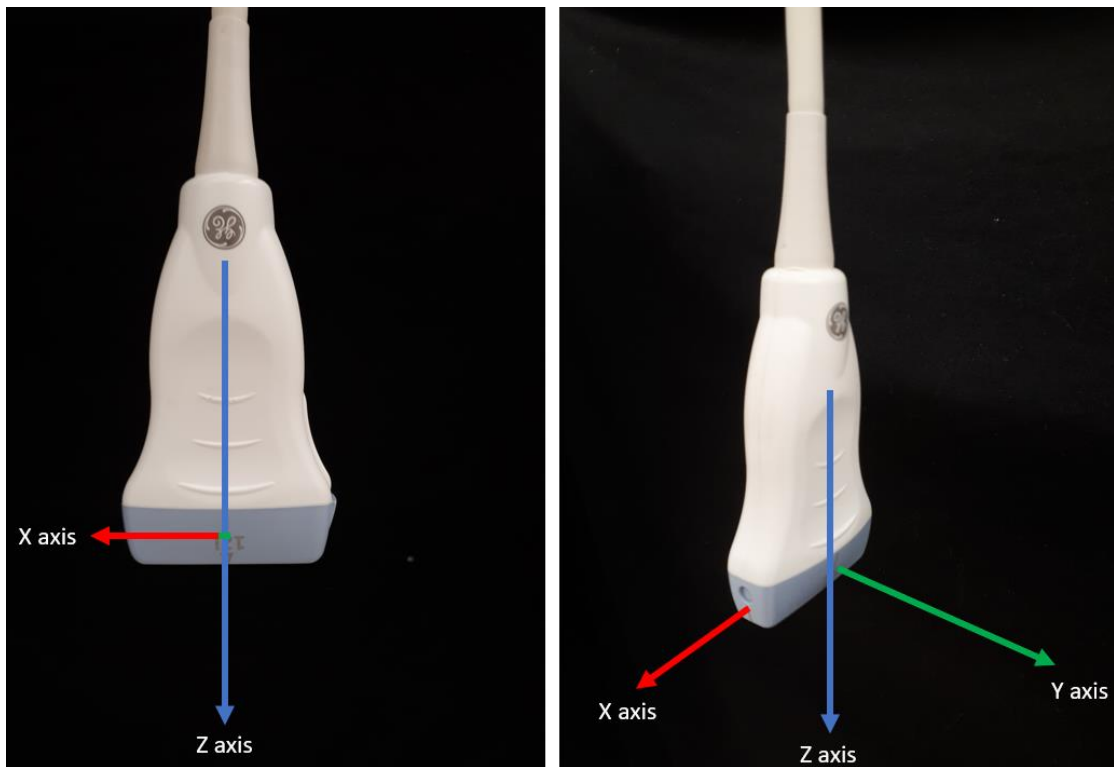


Figure 3: A 12L ultrasound transducer with the x, y, and z axis of the transducer labeled in red, green, and blue respectively.

When imaging the muscle longitudinally, the face of the transducer should be held parallel lengthwise to the muscle fascicles (Figure 4) to limit parallax and ensure optimal imaging (Klimstra et al., 2007). Parallax is a phenomenon that describes a difference in appearance due to a difference in perspective. Consistent positioning of the transducer along the x-axis is crucial to avoid imaging parallax errors and subsequent underestimation or overestimation of muscle architecture properties. The plane parallel to

the fascicles would produce the largest pennation angle and thickness relative to the other positions along the x-axis of the transducer. Imaging the muscle at any other angle would produce anisotropy artifacts (differences of image appearance as a result of parallax).



Figure 4: An image of the thigh showing the relative positioning of the transducer (the grey block) to the muscle fascicles (the black lines).

Consistent transducer positioning is also necessary to allow for comparison of data across studies. Given the non-invasive nature of ultrasonography, it is difficult to ensure exact alignment to fascicles. Most protocols attempt to achieve this by holding the transducer perpendicular to the skin (Alegre et al., 2014; Bénard et al., 2009; Blazeovich et al., 2006; Kwah et al., 2013; Thom et al., 2007; van den Hoorn et al., 2016). However, variation in transducer angle during imaging is likely. To our knowledge, only one study

has attempted to standardize the tilt of the transducer against the skin. König and colleagues (2014) used a foam cast to standardize the angle of the transducer in a 90° position relative to the skin when imaging the gastrocnemius muscle in healthy adults. Images taken using the cast demonstrated lower error (SEM = 0.05 cm) than without the cast (SEM = 0.1 cm). This cast succeeded in maintaining probe position but may have sacrificed quality of images due to sustained compression of the transducer head against the tissue. Nonetheless, this study concluded that using a device to standardize probe position is beneficial to ultrasound imaging. Despite potential modest deviations from a perpendicular position that may occur without standardization, few studies have demonstrated the measurement error associated with 5-10° deviations from the perpendicular orientation of the transducer relative to the skin. Furthermore, even when a perpendicular placement has been achieved, this transducer position does not ensure that images will be acquired perpendicular to the muscle belly.

2.1.1 Purpose

The primary purpose of this study was to determine the agreement of muscle architecture measures from images taken with the transducer held at 80°, 85°, 95° and 100° relative to the skin, compared with a reference position of perpendicular (90°) to the rectus femoris and vastus lateralis in healthy adults. Muscle architectural properties included muscle thickness, pennation angle, fascicle length, and subcutaneous fat thickness.

A secondary purpose was to determine the intra-rater reliability of architectural measurements from the same set of images within one researcher. As well, another secondary purpose was to determine inter-rater reliability of the muscle architecture

measurements from images acquired by two different researchers with novice imaging experience.

2.1.2 Hypotheses

For the primary hypothesis, we hypothesized that there would be a higher standard error and smaller ICC associated with architecture measurements from images of the rectus femoris and vastus lateralis taken at 80° and 100°; and lower error and higher ICC associated with 85° and 95° transducer angles. We expected that the direction of error would be predictable, such that muscle thickness, and pennation angle would be larger than measurements acquired at 90°, while fascicle length would be smaller when images were taken at 90° due to an expected anisotropic effect associated with a misaligned transducer angle. Further, we expected poor agreement between estimated and measured angles 90° transducer tilt.

For the secondary hypotheses, we hypothesized acceptable agreement of measurements taken from the same set of images by one researcher; and acceptable agreement of muscle architectural measurements from images acquired by two different researchers.

2.2 Methods

2.2.1 Study Design

This study was conducted at McMaster University in Hamilton, Ontario, Canada and was approved by the Hamilton Integrated Research Ethics Board (# 3472). All participants received a detailed explanation of the study purpose, protocol, risks and benefits; and had

an opportunity to seek answers to any questions that arose. All participants provided written consent prior to study participation.

2.2.2 Participants

Participants were recruited locally through the institutional social network and an introductory email sent to the Kinesiology Department at the university. Participants were screened with an online questionnaire by one researcher prior to scheduling their visit. Participants were included if they reported no recent leg injuries or significant leg pain in the past year and demonstrated a healthy status according to the Get Active Questionnaire (Canadian Society of Exercise Physiology, Ottawa, ON., Canada). Individuals who reported comorbidities or injuries that may limit their participation in the study were excluded. Eligible participants were scheduled for a lab visit and were asked to wear loose shorts and avoid strenuous physical activity on the day of their visit.

Thirty healthy participants (15 men, 15 women) between the ages of 20 - 29 years old were recruited locally. Demographics are summarized in Table 4. Reliability studies typically require 30 participants to estimate absolute reliability (Koo & Li, 2016; Riddle & Stratford, 2013).

2.2.3 Protocol

Fifteen right legs and 15 left legs were examined. Each participant's height and mass was measured while they were in bare feet. To identify the dominant leg, participants were asked which leg they would kick a ball with.

Then, participants were familiarized with a 10-point BORG rating of perceived exertion (RPE) scale and performed a six-minute walk test (6MWT). The RPE scale is a

validated scale that allows the participant to self report how exerted they feel on a scale from 0-10, 0 being not exerted at all and 10 representing maximal exertion (Borg, 1982). The 6MWT produces reliable data for healthy adults aged 18 - 43 years (ICC = 0.93 ranging between 0.79 and 0.97) (Wilken et al., 2012). During the 6MWT, participants were instructed to walk as fast as they could comfortably for 6 minutes without running in a tiled, well-lit, level hallway (Crapo et al., 2002). Throughout this walk, standardized statements were used to motivate the participant. A researcher followed behind the participant with an odometer to avoid influencing the participant's pace. The 6MWT was intended as a standardized warm-up for the protocol.

2.2.4 Positioning

Participants were invited to sit on a commercial isokinetic dynamometer seat (Biodex System 4, Biodex Medical Systems, Shirley, NY, USA). Ultrasound imaging of the leg was done while seated in the dynamometer to ensure sitting position remained standard between participants and trials. The seat was adjusted so that the lateral aspect of the lateral femoral condyle of the knee joint was centred to the axis of rotation of the dynamometer. The leg was secured the dynamometer lever arm using a strap positioned above their lateral malleolus. The dynamometer arm was set to 90° as a reference point; this angle was confirmed with a universal goniometer. During imaging, the dynamometer attachment arm was held at 60° of flexion (from a straight leg position). Sixty degrees has been identified as the optimal knee joint angle for extension in individuals between 20 to 48 years old (Lindahl et al., 1969; Ng et al., 1994; Welsch et al., 1998).

2.2.5 Imaging Land-Marking

Architecture differs across scanning sites of the muscle (Ando et al., 2015); thus, care was taken to ensure that scanning sites remained consistent throughout the collection and between participants. The greater trochanter, lateral femoral condyle, anterior superior iliac spine (ASIS), and the superficial border of the patella were palpated, and the overlaying skin was marked with indelible ink by one researcher for every participant (Figure 5). Imaging regions were marked while participants were seated in the dynamometer (Figure 5). The vastus lateralis was imaged at the midpoint between the greater trochanter and the lateral femoral epicondyle in the sagittal plane of the thigh (Baroni et al., 2013; Csapo et al., 2011; Scanlon et al., 2014). The length between the greater trochanter and the lateral femoral condyle was recorded as the vastus lateralis length. The thigh circumference at this vastus lateralis imaging region was recorded. The rectus femoris was imaged at the midpoint of the ASIS and the superior border of the patella in the axial plane (Ando et al., 2015; Arts et al., 2010; Ema et al., 2013; Scanlon et al., 2014). The septum of the rectus femoris was first located in the transverse view for reference, if the septum interfered with the imaging clarity of the longitudinal images, the transducer was placed medially, and this new placement was marked. The length between the ASIS and the superior border of the patella was recorded as the rectus femoris length. The thigh circumference at the midpoint of the rectus femoris was recorded.



Figure 5: Image land-marking for the rectus femoris and vastus lateralis. A marking was drawn to identify the superior border of the patella and the lateral femoral condyle. A mark was made at the half point between the anterior superior iliac spine and the superior border of the patella and another mark halfway between the greater trochanter and the lateral femoral condyle.

2.2.6 Image Acquisition

A high frequency linear probe (12L-RS) was used to image the vastus lateralis and rectus femoris quadriceps muscles (Vivid Q, General Electric, WI, USA). A generous amount of water-soluble gel was used for acoustic coupling and to minimize pressure of the transducer against the tissue (Blazevich et al., 2006; Lixandrao et al., 2014). Researchers were cautious to apply minimal pressure during imaging to limit compression of the tissues by the ultrasound transducer.

To standardize the angle of the transducer, a 3D printed transducer attachment was created with an affixed protractor (Figure 6A-D). The 3D printed attachment was created using a model produced from a 3D scan of the ultrasound transducer (Artec Eva,

Artec 3D, CA, USA). An open source modeling software facilitated the 3D model that was printed (MeshMixer, Autodesk Inc., CA, United States). The attachment is held together against the transducer by 4 small neodymium magnets and features a wedge that can be magnetically attached to the protractor and adjusted to accommodate the curvature of each participant's thigh. The purpose of the wedge is to limit rotation of the protractor around the thigh.

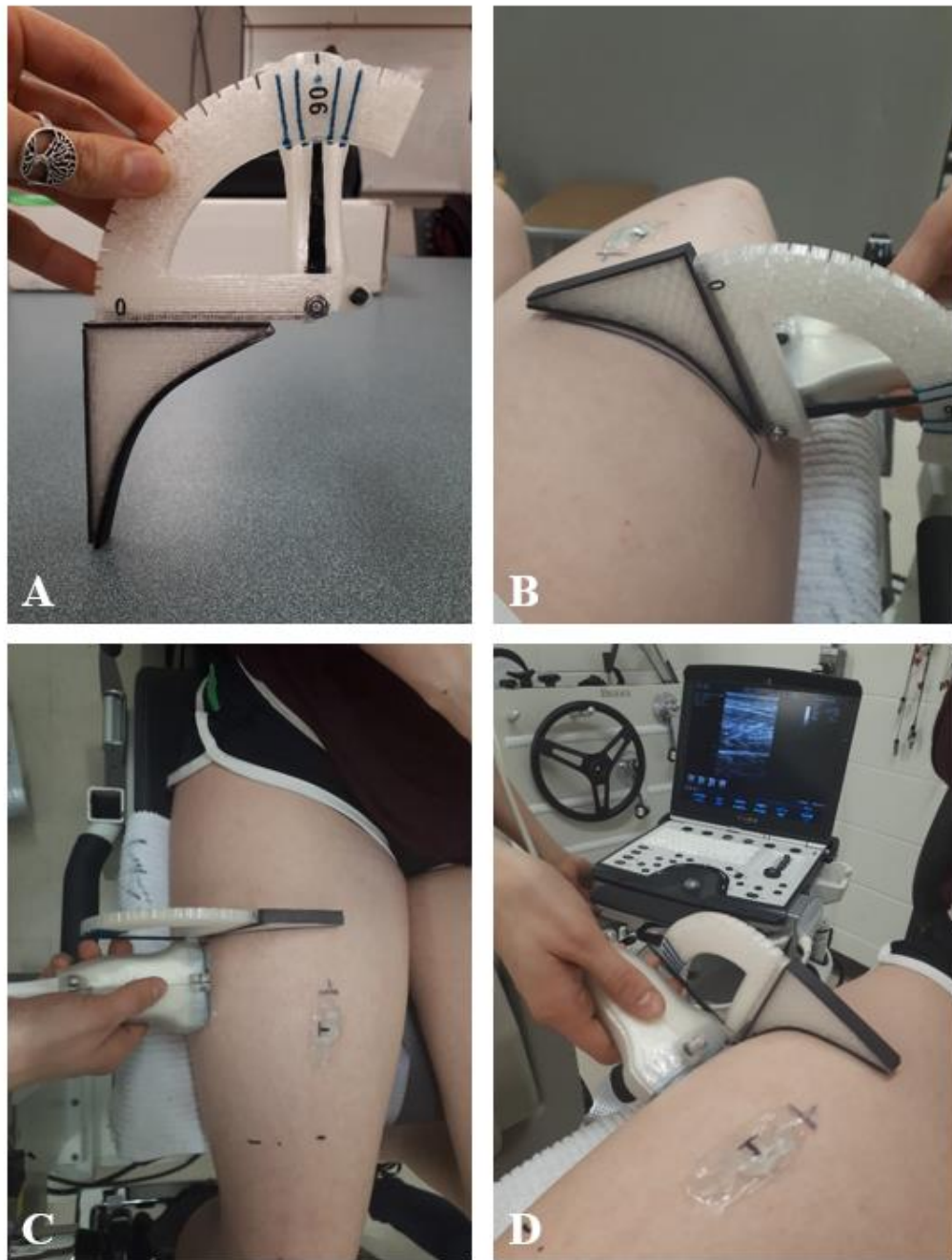


Figure 6: Figure 6A shows the 3D-printed transducer attachment device with a protractor marked with blue lines at 80°, 85°, 90°, 95°, and 100°. A black wedge attaches to the protractor using magnets. The bottom of the wedge fits along the thigh to limit movement of the protractor and to distribute pressure. Figures 6B, C, and D show the transducer with the attachment in use imaging the vastus lateralis.

Participants were asked to relax their muscles as much as possible. Images were taken in B-mode and the gain was set to mid range. Imaging parameters are summarized in Table 1. Images were taken with the transducer in the longitudinal plane for both muscles. For each site, three images were acquired as is often done (Rutherford et al., 1992; Noorkoiv et al., 2010; Narici et al., 2003). Two researchers acquired images of the rectus femoris and vastus lateralis in the study leg. As described below, acquisition of an image at an angle estimated to be 90° to the skin surface was conducted first by both researchers; otherwise, the orders of muscles, transducer angle, and researcher were all block-randomized with a random number generator.

The first researcher placed the transducer over the imaging region of the randomly assigned first muscle and adjusted the transducer position until it was aligned with the muscle and the image appeared clear. A mark was traced on the skin along the top of the transducer. The researcher then held the transducer at an angle they perceived to be perpendicular to the skin and acquired an image. The angle of the transducer against the skin was measured by a third researcher (EGW). This was repeated for the second muscle. Finally, this process was repeated by the second imager for both muscles using the participant positioning and region markings of the first rater. Both ultrasound operators were blinded to their measured angles until completion of the study to avoid training over the period of the study.

Then, using the 3D printed protractor attachment, both muscles were imaged at five transducer angles (80°, 85°, 90°, 95°, 100° to the skin) randomly. The edge of the protractor and wedge were traced on the skin to ensure that the same placement was used

for each image and only the transducer angle was changing. Each angle was imaged 3 times, the transducer was removed from the skin between images. The number of images taken for each transducer angle is summarized in Table 2. The depth of the imaging system was kept at 5.5 cm when possible; this was changed when required to image the full muscle. The frequency of the ultrasound is related to the depth of view, and this was kept at 11 MHz when possible but was decreased if a depth of 6.5 cm or greater was required. The ultrasound signal is emitted in an hourglass shape, the smallest point of this shape is known as the focus. This focuses the signal toward the tissue of interest. The number and position of focus points can be adjusted. For this study, the number and positioning of focus points was kept the same when possible but was sometimes changed to accommodate different participant anthropometrics. In all instances, the researcher aimed to obtain the clearest image of the entire region of interest.

Table 1: Imaging parameters for ultrasound imaging summarizing ultrasound signal depth, frequency and the number of focus points.

	Main Parameters	Range
Depth (cm)	5.5 (n=26)	5 - 7
Frequency (MHz)	11 (n=28)	10 - 11
Focus Points (#)	2 (n= 25)	2 - 5

Table 2: Total number of images taken for each muscle at each transducer angle.

Images per muscle	Rectus Femoris	Vastus Lateralis
Estimation image	2 (1 by each rater)	2 (1 by each rater)
80°	6 (3 by each rater)	6 (3 by each rater)
85°	6 (3 by each rater)	6 (3 by each rater)
90°	6 (3 by each rater)	6 (3 by each rater)
95°	6 (3 by each rater)	6 (3 by each rater)
100°	6 (3 by each rater)	6 (3 by each rater)
Total	32 images	32 images

2.2.7 Muscle Architecture Measurements

Images were exported from the ultrasound software as a jpeg file. Rater 1 analyzed images twice in random order separated by approximately 3 weeks. During this analysis, the researcher was blinded to participant, muscle, and transducer angle.

The superficial and deep aponeuroses appear as 2 thick hyperechoic lines that run horizontally across the image in a longitudinal plane (Figure 7). These lines were used as top and bottom muscle boundaries (aponeuroses) for the pennation angle measurements and the extrapolation of fascicle length. The white striations within the aponeuroses of the muscle depict hyperechoic connective tissue within the muscle, between the fascicles.

The diagonal hypoechoic striations within the aponeuroses are muscle fascicles. Muscle architecture measurement techniques are summarized in Table 3.

A custom Python program was used to extract measures of muscle and fat thicknesses, fascicle length, and pennation angle from jpeg images. The semi-automated program measured the four muscle architecture outcomes using user identified points on the image. Guidelines were temporarily appended to each image to ensure that measurements were taken in the same place on each image. Specific guidelines used to measure these architectural features are summarized in Table 3.

Table 3: Parameter definitions, how they are typically measured, and how they were measured using our program.

Parameter	Definition	Measurement	Measurement in Analysis Program
Muscle Thickness (cm)	The thickness of the whole muscle at thickest region of the muscle.	Measured as the distance from the superficial to the deep aponeurosis. The mean value of single measurements acquired at three standardized locations was analyzed.	Three lines were placed by clicking the guide lines beneath the dermis layer and above the muscle's superficial aponeurosis border. Only the y-coordinates of the image were used to ensure a straight line. (Figure 7, red lines)
Fat Thickness (cm)	The thickness of the subcutaneous tissue.	The distance between the superficial layer of skin to the outer border of the superficial aponeurosis. The mean of single measurements acquired at three standardized locations was analyzed.	Fat thickness was measured the same way as muscle thickness, only within the dermis layer and above the border of the muscle's superficial aponeurosis. (Figure 7, green lines)
Pennation Angle (°)	The angle between the fascicle and the deep aponeurosis.	The angle between the fascicle and deep aponeurosis. A mean of three angles was analyzed.	The lines produced from the top and bottom points of the muscle thickness measures were used as the borders for the pennation angle. Three visible fascicles were traced. The angle between the traces and the deep aponeurosis border was recorded as the pennation angle. (Figure 7, blue and yellow lines)
Fascicle Length (cm)	The length of a full fascicle.	The length of the line extrapolated from fascicle tracings to the superficial aponeurosis border. The mean of three was analyzed.	Fascicle lengths were extrapolated. From the fascicle traces used to measure pennation angle, an extrapolation line was created that continued until an intercept with the superficial aponeurosis was met. (Figure 7b, orange lines)

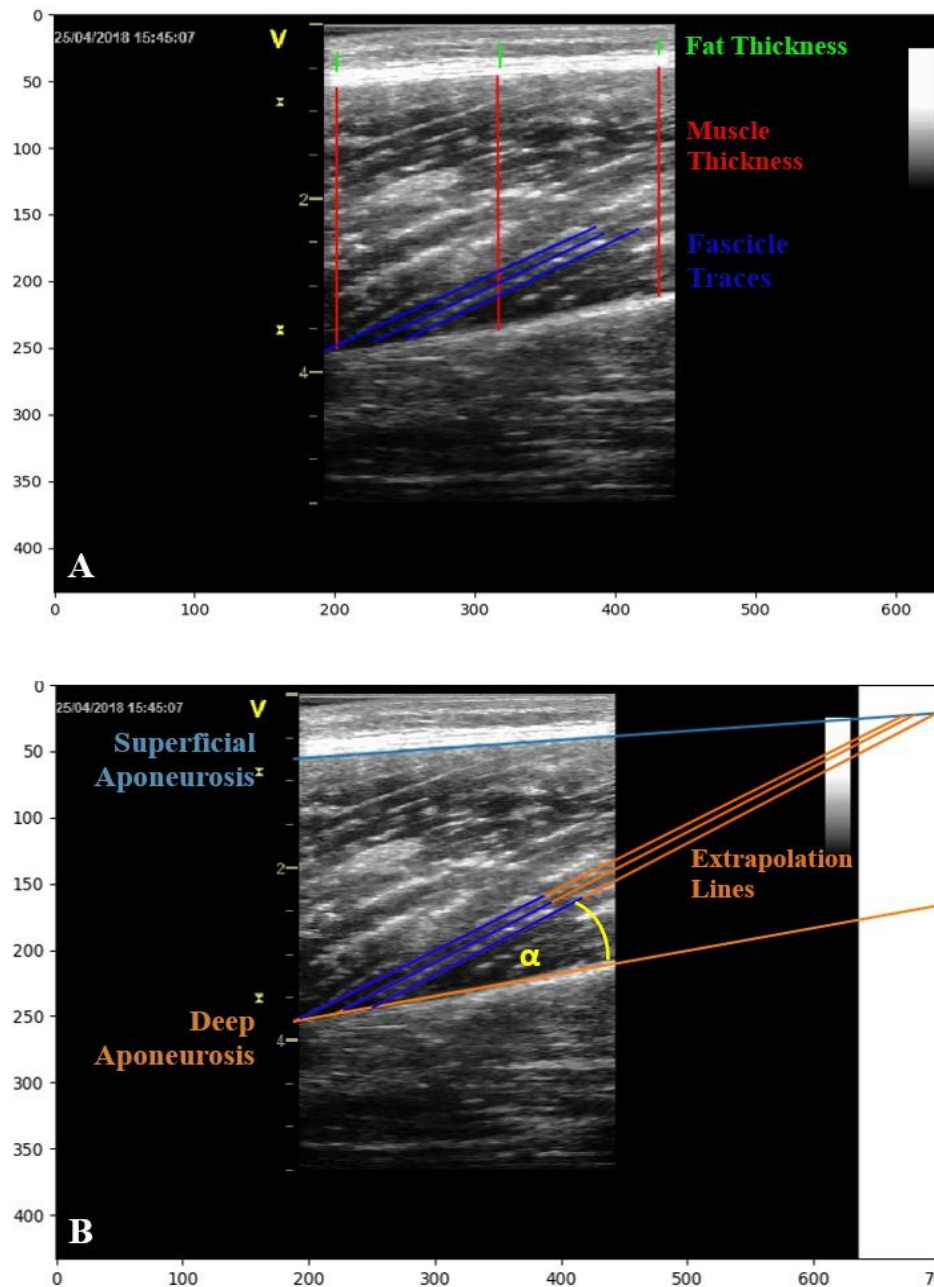


Figure 7: Muscle architecture measurements made with a custom Python program. (A) Red lines represent the muscle thickness measurements. Green lines represent fat thickness measurements. Blue lines are traces of fascicles. (B) From muscle thickness measurements, a boundary for the superficial and deep aponeurosis were drawn (light blue and orange lines respectively). From the traces, the angle between the fascicles and the deep aponeurosis (shown in yellow) was recorded as the pennation angles. Finally, to define the fascicle length, an extrapolation line was created from the fascicle traces that continued until the superficial aponeurosis border (light blue line) was met.

2.2.8 Statistical Analyses

Every image acquired was reviewed to ensure all statistical analyses were completed using data measured from quality images. SPSS was used to calculate the statistics (IBM Corp. Released 2017. IBM SPSS Statistics for Windows, Version 25.0. Armonk, NY: IBM Corp.). Demographics were summarized to describe the sample. A paired t-test was used to compare muscle thickness, fat thickness, pennation angles, and fascicle length means between men and women.

For the primary purpose, both relative and absolute agreement was assessed. Two-way random, intraclass correlation coefficients (ICCs) (2, k) were used to assess the relative agreement between transducer angles (estimated perpendicular tilt, 80°, 85°, 95°, and 100°) and a perpendicular transducer position (90°) for each of the measurements (muscle thickness, fat thickness, pennation angle, and fascicle length). Interpretation of ICC has been determined by Cicchetti (1994). If the ICC < 0.40 the level of agreement is considered poor, if the ICC is 0.4-0.59 the agreement is fair, an ICC of 0.6-0.74 is good and an ICC above 0.75 demonstrates excellent agreement (Cicchetti, 1994). For absolute agreement, SEM was used to quantify the error associated with alternative transducer tilts (other than 90° such as 80°, 85°, 95°, and 100°). Measured transducer angles of 80° and 85° were lateral to perpendicular (90°), and 95° and 100° were medial to perpendicular. SEM was calculated as $SEM = \text{Standard Deviation (SD) of Differences} / \sqrt{2}$. Graphs are displayed with custom standard error (SE) bars calculated using the following equation: $SE = SD / \sqrt{n}$.

For secondary purposes, ICCs, SEMs, and Bland-Altman plots were used to determine the intra-rater reliability for muscle architecture measurements. As well, ICCs, SEMs and Bland-Altman plots were used to determine the inter-rater reliability for image acquisition using raw data. For inter-rater reliability, ICC and SEM analyses were separated by transducer angle and muscle, while for intra-rater, the data was only separated by muscle.

2.2.9 Data Quality

Before conducting analyses to address the primary and secondary objectives, it was evident that some images were not of sufficient quality for measurement, due to poor visibility of the whole image, aponeuroses, or fascicles. In participants with larger fat thicknesses, many images did not show one or more of the structures needed to measure the muscles architecture (e.g., the deep aponeurosis or the muscle fascicles). An example of an image of the vastus lateralis that is not usable is shown in Figure 8. These images were considered to be “unusable images”.

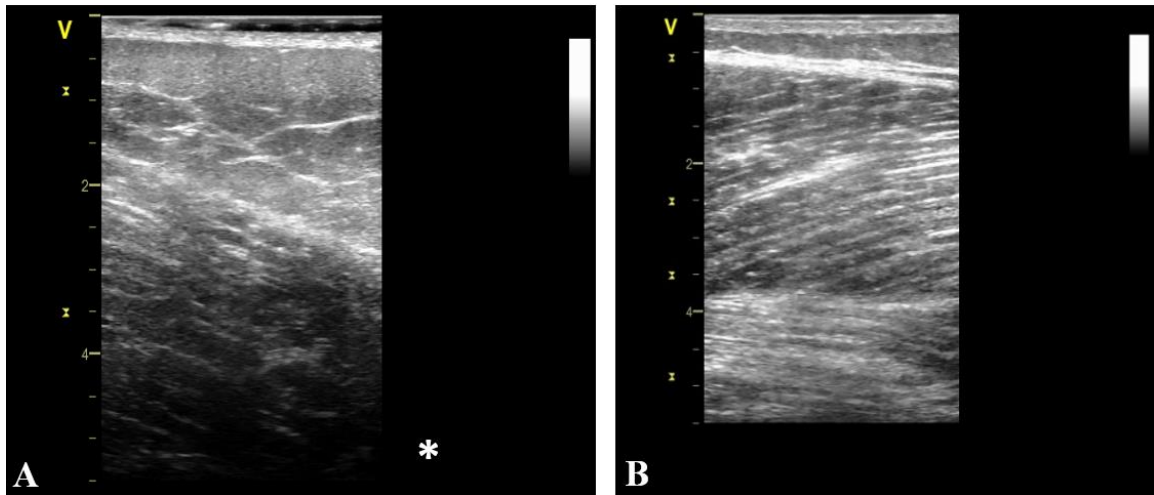


Figure 8: Panel A presents an example of a vastus lateralis image that is not usable compared to a usable image shown in Panel B. *In Panel A, the deep aponeurosis is not visible, and the fascicles are unclear.

As well, due to the automatic extrapolation used in this study, many fascicle lengths exceeded the recorded lengths of the muscle as a result of small pennation angles. The fascicle length outcomes for these images were considered to be erroneous. Raw data analyses, which include these “erroneous” outcomes, are available in Appendix H. In the raw data analysis, the unusable images were included with muscle architecture measurements recorded as zero for muscle thickness, fat thickness, pennation angle, and fascicle length. The analysis of primary and secondary purposes was repeated with unusable images and erroneous fascicle lengths removed from the data set. The results of these analyses are presented in the results section of this thesis.

To determine which variables could indicate if a participant were more likely to produce “unusable images”, linearity of the relationship between the independent variables (fat thickness, sex, thigh circumference, and BMI) and the dependent variable (number of unusable images) was tested. Sex was input as “2” for men and “1” for

women. These potential indicators were tested for multicollinearity for each of the rectus femoris and the vastus lateralis using a bivariate correlation test. Variables that showed a high level of collinearity ($r > 0.6$) were removed from the subsequent regression analysis. Normal distribution of error between observed and predicted values were tested. A forward regression analysis ($\alpha = 0.05$) was used to determine the correlation between fat thickness, sex, and thigh circumference (independent variables, in that order) and the number of unusable images for the rectus femoris and vastus lateralis (the dependent variable).

2.3 Results

2.3.1 Participants

Thirty healthy, right leg dominant participants (25 ± 2.5 years old) participated in this study. Participant demographics are summarized across the entire sample and separated by sex in Table 4.

Table 4: Demographics for 30 participants. The right-hand columns described the same participants separated by sex.

	All Participants (n = 30)			Women = (n = 15)			Men = (n = 15)		
	Mean (SD)	Min	Max	Mean (SD)	Min	Max	Mean (SD)	Min	Max
Age (years)	25 (2.5)	20	29	25 (2.6)	22	29	24 (2.2)	20	29
BMI (kg*m ²)	22.6 (3.0)	17.2	29.4	22.2 (2.5)	19.4	27.5	23.0 (13.0)	17.2	29.4
Rectus Femoris Length (cm)	44.2 (2.9)	36.4	49.3	42.9 (2.4)	36.4	46	45.6 (2.6)	40.4	49.3
Vastus Lateralis Length (cm)	46.1 (3.0)	40.3	55.5	45.1 (2.6)	40.3	48.7	47.1 (3.1)	40.8	55.5
Rectus Femoris Thigh Circ. (cm)	53.9 (4.5)	42.3	65.9	53.0 (3.0)	47.7	57.3	54.9(5.6)	42.3	65.9
Vastus Lateralis Thigh Circ. (cm)	55.6 (4.9)	43	69.8	55.1 (3.3)	48.8	60.4	56.2 (6.1)	43	69.8
6MWT (m)	679 (91)	453	940	662 (67)	537	762	697 (110)	453	940

SD = standard deviation; Min = minimum; Max = maximum; Circ. = circumference; 6MWT = six-minute walk test

Mean muscle architecture measurements for the rectus femoris and vastus lateralis are summarized in Table 5 and Table 6, respectively. Figures 9 and 10 display the mean muscle architecture values taken by rater 1 and rater 2 at each transducer angle for the rectus femoris and the vastus lateralis, respectively. Muscle and fat thickness means were similar for both muscles. Mean pennation angles of the vastus lateralis were larger compared to the rectus femoris. Mean pennation angle was largest at 95° and 100° transducer angles for the rectus femoris and at an 80° transducer angle for the vastus lateralis. Meanwhile, mean fascicle lengths of the rectus femoris were larger than the vastus lateralis fascicle lengths. Mean fascicle lengths were largest at an 80° transducer angle for the rectus femoris and at 95° and 100° transducer angles for the vastus lateralis.

Table 5: Average rectus femoris muscle architecture values per transducer angle, separated by images taken by each rater. The sample size for each muscle architecture value is displayed beneath its respective cell.

		Est.	80°	85°	90°	95°	100°
Muscle Thickness (cm)	Rater 1	2.3	2.4	2.3	2.2	2.3	2.2
	n	30	27	30	29	30	29
Fat Thickness (cm)	Rater 2	2.3	2.3	2.3	2.3	2.2	2.2
	n	30	29	29	30	30	30
Fat Thickness (cm)	Rater 1	0.7	0.7	0.7	0.7	0.7	0.7
	n	30	27	30	29	30	29
Pennation Angle (°)	Rater 2	0.8	0.7	0.7	0.7	0.7	0.7
	n	30	29	29	30	30	30
Pennation Angle (°)	Rater 1	12.2	7.4	8.1	9.8	12.2	11.5
	n	28	26	29	28	29	28
Fascicle Length (cm)	Rater 2	11.4	7.7	8.7	9.4	11.2	11.7
	n	29	29	29	30	28	27
Fascicle Length (cm)	Rater 1	21.5	27.7	25.0	21.5	21.0	18.6
	n	26	10	16	20	27	25
Fascicle Length (cm)	Rater 2	18.2	27.6	23.4	22.1	18.1	16.7
	n	25	11	19	22	24	23

Table 6: Average vastus lateralis muscle architecture values per transducer angle, separated by images taken by each rater. The sample size for each muscle architecture value is displayed beneath its respective cell.

		Est.	80°	85°	90°	95°	100°
Muscle Thickness (cm)	Rater 1	2.8	2.9	2.9	2.8	2.8	2.8
	n	30	30	30	30	29	24
	Rater 2	2.8	3.0	2.9	2.9	2.8	2.7
	n	30	30	30	30	30	26
Fat Thickness (cm)	Rater 1	0.8	0.8	0.8	0.7	0.7	0.6
	n	30	30	30	30	29	24
	Rater 2	0.8	0.8	0.8	0.8	0.7	0.7
	n	30	30	30	30	30	26
Pennation Angle (°)	Rater 1	16.0	18.5	17.2	17.0	15.4	15.2
	n	30	30	30	30	29	24
	Rater 2	16.7	17.3	16.8	16.8	15.9	15.3
	n	30	30	30	30	30	26
Fascicle Length (cm)	Rater 1	10.9	9.4	9.8	10.5	12.4	14.1
	n	30	30	30	30	29	24
	Rater 2	9.5	9.6	11.1	11.9	13.3	9.5
	n	30	30	30	30	30	26

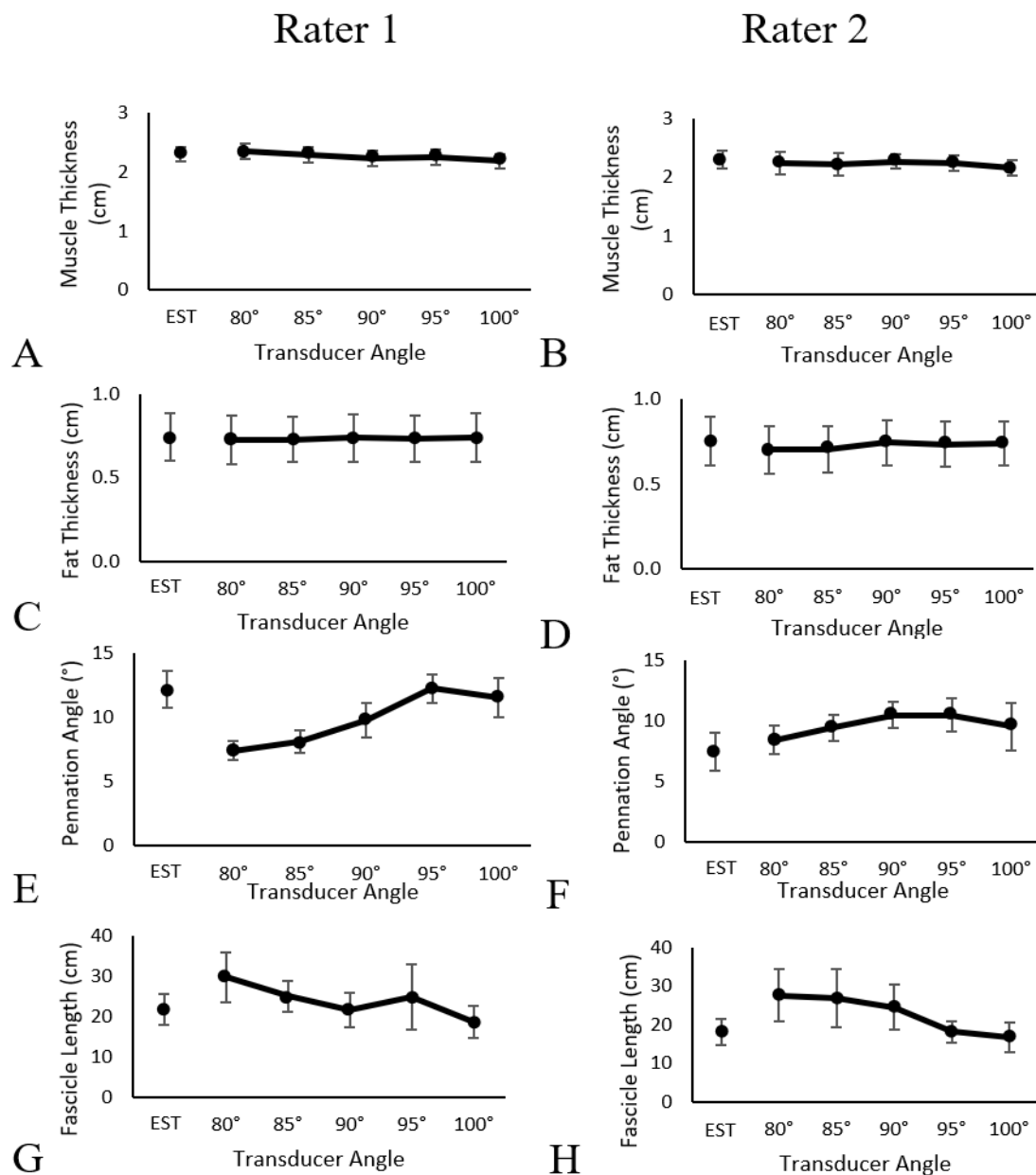


Figure 9: Mean muscle architecture measurements (and standard error bars) for the rectus femoris with unusable images removed and fascicle lengths exceeding the muscle lengths removed: muscle thickness (A, B), fat thickness (C, D), pennation angle (E, F), and fascicle length (G, H). Data from rater 1's images are displayed in the left column (A, C, E, G) and data from rater 2's images are shown in the right column (B, D, F, H). The lone markers represent the average value of the measurement from the images taken with the transducer at an estimated (EST) perpendicular angle.

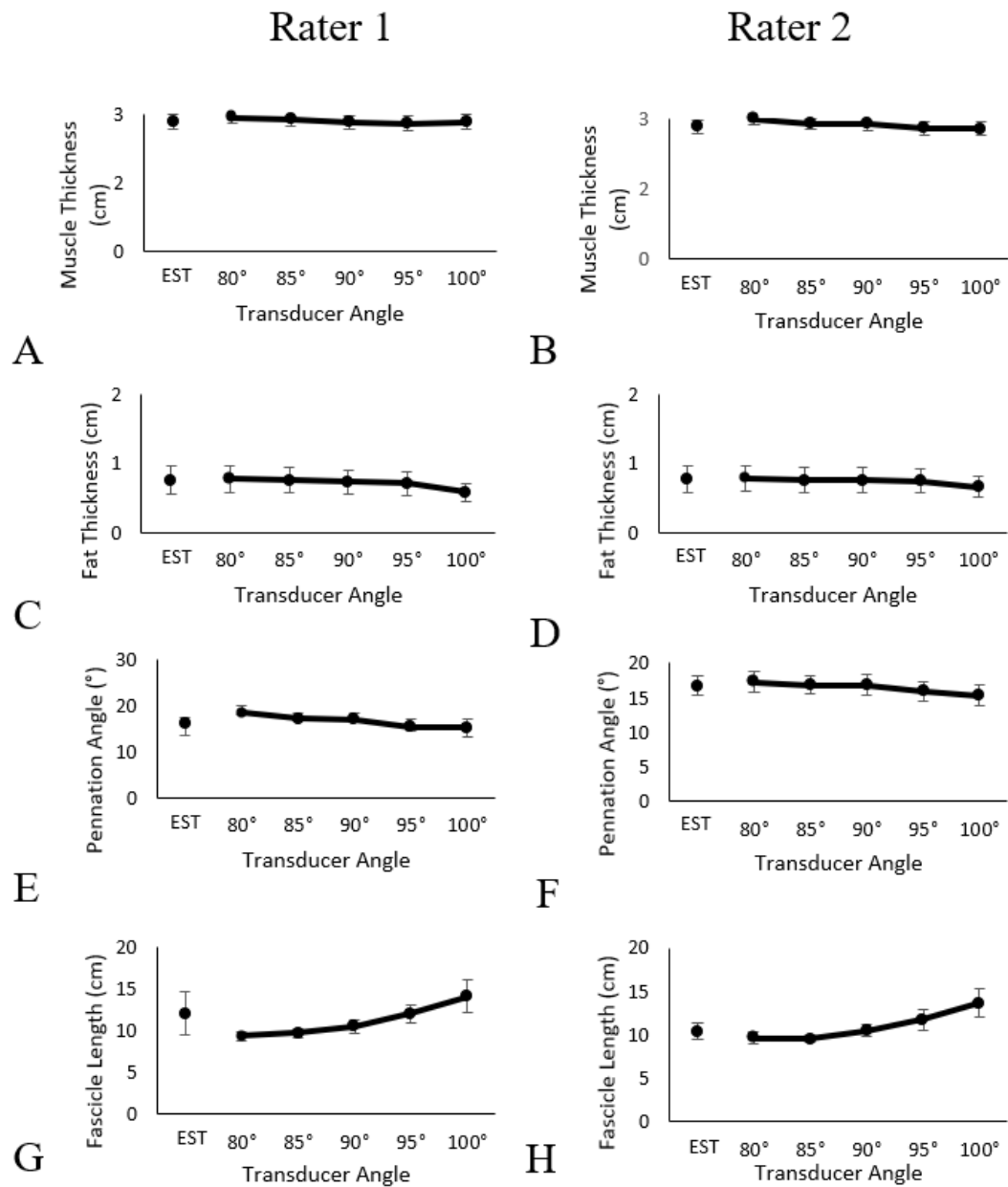


Figure 10: Mean muscle architecture measurements with unusable images and fascicle lengths exceeding the vastus lateralis removed: muscle thickness (A, B), fat thickness (C, D), pennation angle (E, F), and fascicle length (G, H). Data from rater 1's images are displayed in the left column (A, C, E, G) and data from rater 2's images are shown in the right column (B, D, F, H). The lone markers represent the average value of the measurement from the images taken with the transducer at an estimated (EST) perpendicular angle.

2.3.2 Sex Differences

Muscle architecture differences between male and female participants are shown in Figure 11. Mean rectus femoris muscle thickness was significantly larger in men than in women at all transducer angles (2.5 and 2.1 cm, respectively; $p = 0.002$). The mean subcutaneous fat thickness above the rectus femoris was significantly smaller in men than in women at all transducer angles (0.5 cm and 1.0 cm, respectively; $p < 0.001$). However, no significant differences were found between men and women for mean pennation angles (10.0° and 10.5° , respectively; $p = 0.92$) or mean fascicle lengths (23.3 cm and 20.3 cm, respectively; $p = 0.67$) of the rectus femoris. Although overall means were the same, vastus lateralis muscle thickness was larger in men (mean = 2.9 cm) than in women (mean = 2.9 cm) at all transducer angles ($p = 0.002$), this may be explained by larger SD for men (SD = 2.3 cm) than women (SD = 0.4 cm). Mean subcutaneous fat tissue above the vastus lateralis was smaller in men than in women at all transducer angles (1.1 cm and 1.5 cm, respectively; $p < 0.001$). No significant differences were seen between males and females for mean pennation angles (15.0° and 13.6° , respectively; $p = 0.62$) or mean fascicle lengths (10.3 cm and 9.9 cm, respectively; $p = 0.16$) of the vastus lateralis.

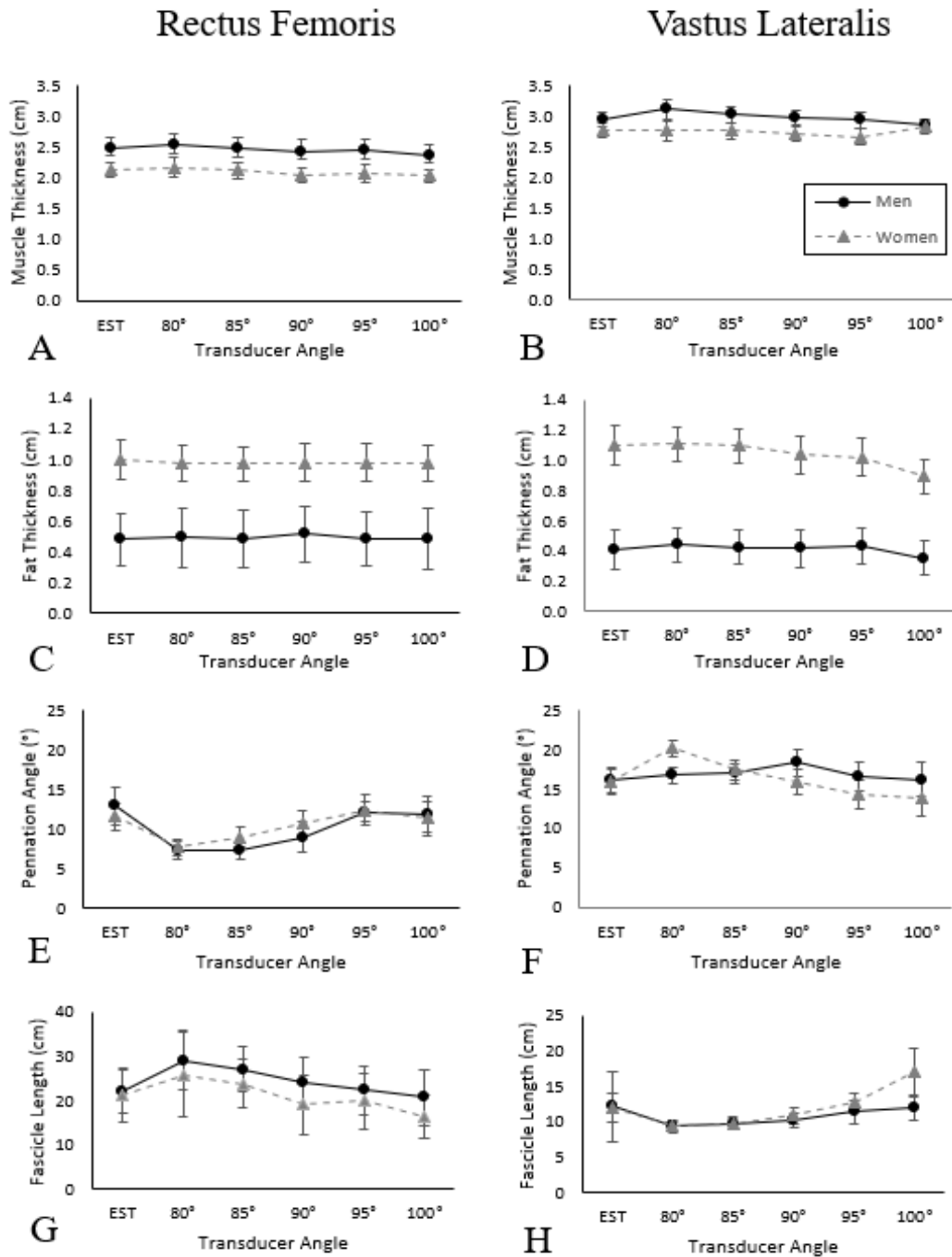


Figure 11: Means (with standard error bars) for muscle thickness, fat thickness, pennation angle, and fascicle length separated by sex. Muscle architecture data from men participants are displayed with circle markers and solid lines; data from women are displayed with triangle markers and dashed lines. Rectus femoris data is shown in panels 10A, 10C, 10E, and 10G, respectively. Vastus lateralis data is shown in panels 10B, 10D, 10F, and 10H.

2.3.3 Assessment of Image Quality and Unusable Images

A total of 1,920 ultrasound images were taken. Of the 1,920 images, 1,732 images (90%) were able to facilitate all four muscle architecture measurements (i.e., muscle thickness, fat thickness, pennation angle, and fascicle length). There were 99 images (5%) out of 1,920 that could not facilitate any of the muscle architecture measurements because the aponeuroses were unclear or not visible (Figure 12). Another 89 could not facilitate measures of pennation angle and fascicle length (even though muscle and fat thickness could be measured) because the fascicles alone were not clear (Figure 13).

In some cases, recorded fascicle lengths exceeded the length of the muscle and tendon (from origin to insertion). This only occurred for images of the rectus femoris. Of 960 total images of the rectus femoris, 155 (16% of total images) were removed as a result of fascicle length measurements exceeding the muscle length. The number of fascicle lengths which were removed because they exceeded the length of the muscle for each transducer angle are displayed in Figure 14. Clearly erroneous fascicle lengths were observed in greater numbers when the images were taken with the transducer held at 80°, 85°, and 90° to the skin. Only 8% of fascicle lengths were removed from images taken at angles estimated to be perpendicular to the skin; however, there were fewer measurements taken at this transducer angle (2 images taken at an estimated perpendicular angle :6 images taken at each other angle) and the percentage of total measurements removed was similar to 95° and 100° transducer angles.

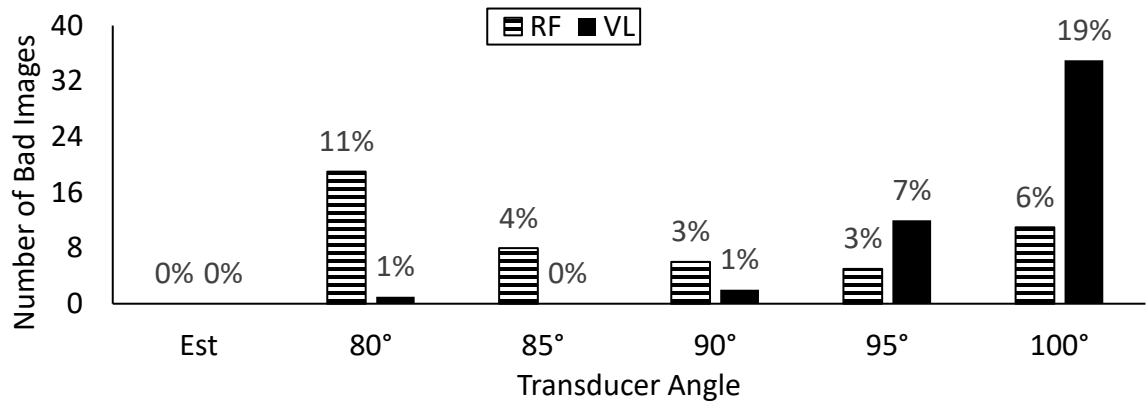


Figure 12: The number of unusable images because the aponeurosis was not visible, per muscle and transducer angle. “Est” stands for the images taken at an angle that was estimated to be perpendicular. Only 60 images were taken in this condition per muscle, whereas 180 images were taken per muscle at all other measured transducer angles. These unusable images could not be used to calculate muscle thickness, fat thickness, pennation angle, and fascicle length. The bars with the black and white lines refer to images of the rectus femoris (RF) and bars with the solid black lines refer to images of the vastus lateralis (VL). The percentage of total images are displayed above the bars.

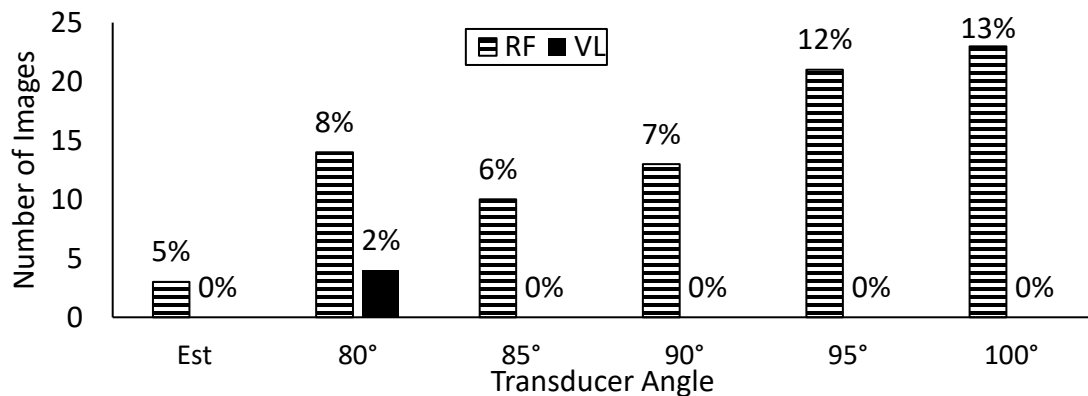


Figure 13: Number of unusable images because the fascicles were not clear, per muscle and transducer angle. “Est” stands for the images taken at an angle that was estimated to be perpendicular. Only 60 images were taken in this condition per muscle, whereas 180 images were taken per muscle at all other measured transducer angles. These unusable images could not be used to calculate pennation angle and fascicle length measurements. The bars with the black and white lines refer to images of the rectus femoris and the solid black bars refers to images of the vastus lateralis. The percentage of total images are displayed above the bars.

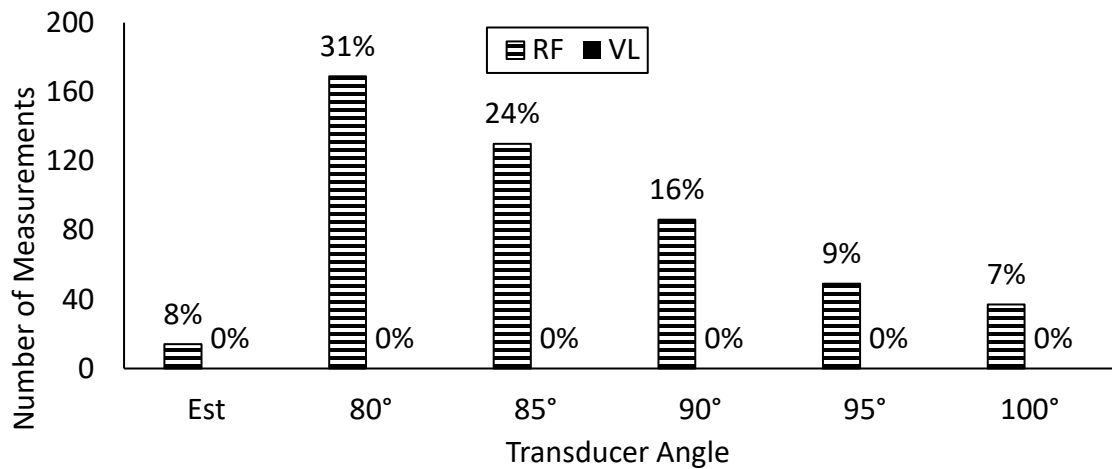


Figure 14: The number of total fascicle length measurements removed, per transducer angle, due to lengths exceeding total muscle length. The bars with solid black bars and striped bars representing measurements for the vastus lateralis and the rectus femoris fascicle lengths, respectively. No black bars appear because no fascicle length measurements were removed from analysis. The percentages of total measurements are displayed above the respective bar. Estimated images, represented by “Est”, has a lower number of total measurements (180 total measurements) compared to other transducer angles (540 total measurements per measured transducer angle).

Because a substantial proportion of images acquired were unusable, additional analyses were completed to explore potential indicators of poor-quality ultrasound images. First, for the rectus femoris, rectus femoris fat thickness, sex, thigh circumference at the rectus femoris imaging site, and BMI were explored as potential features that may correlate to the acquisition of unusable images. These variables were tested for normality and then collinearity. A Pearson’s correlation was conducted between rectus femoris fat thickness, sex, thigh circumference at the rectus femoris site and BMI. BMI and thigh circumference at the rectus femoris were strongly, positively correlated ($R = 0.88$, $p < 0.01$). Fat thickness was significantly higher in women than in men ($R = -0.65$, $p < 0.01$). To avoid multicollinearity, BMI and sex were removed from the regression analysis for

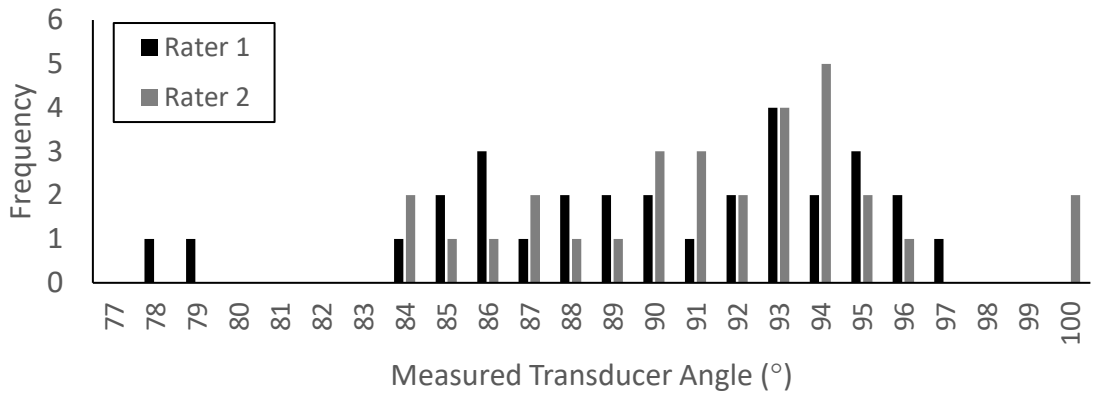
rectus femoris. A forward regression was conducted with a 95% confidence interval and a significance of 0.05 using fat thickness and thigh circumference as independent variables and the designation of usable versus unusable images as the dependent variable. There was no significant association ($R^2 = 0.096$).

Fat thickness of the vastus lateralis, sex, thigh circumference at the imaging site of the vastus lateralis, and BMI were tested for normality. Vastus lateralis fat thickness data were not normally distributed based on the Shapiro-Wilk test, where the p-value (0.044) was less than the alpha value (0.05). After log transforming, vastus lateralis fat thickness data were normally distributed. The log transformed vastus lateralis fat thickness data, sex, and thigh circumference at the site of the vastus lateralis were tested for collinearity using a bivariate correlation. Again, fat thickness was larger in women than in men ($R = -0.722$, $p < 0.01$) and weakly correlated to thigh circumference ($R = 0.409$, $p < 0.01$). BMI was significantly correlated to thigh circumference (0.898, $p < 0.01$). BMI and sex were removed from the regression. A forward multiple regression was conducted (95% confidence interval; threshold $\alpha = 0.05$) using fat thickness and thigh circumference as independent variables and the number of unusable images as the dependent variable. Only fat thickness was significantly associated with the designation of unusable images for the vastus lateralis ($R^2 = 0.626$, $p < 0.01$).

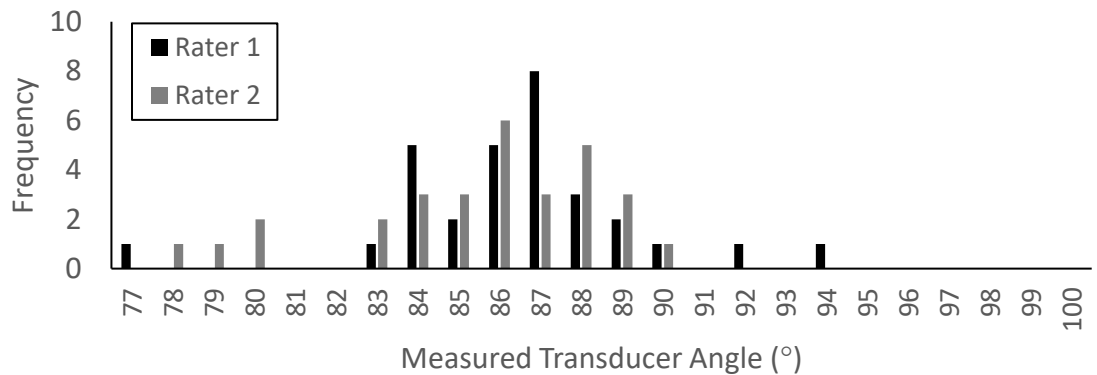
2.3.4 Effect of Transducer Angle on Muscle Architecture

Figure 15 shows the measured transducer angle for the images that were acquired at an angle estimated to be perpendicular. Measured angles from estimated perpendicular transducer positions were similar for rater 1 and rater 2. When measured, transducer

angles estimated to be a perpendicular position were near 90° for the rectus femoris (90.0° ± 4.8° by rater 1 and 91.5° ± 4.0° by rater 2) and the vastus lateralis (86.5° ± 3.0° by rater 1 and 85.5° ± 3.0° by rater 2). The mode transducer angle for an estimated perpendicular position for rectus femoris was 93° for rater 1 and 94° for rater 2. The mode transducer angle for vastus lateralis was 87° for rater 1 and 86° for rater 2. Although the central tendencies were around 90°, there was a range in transducer angle between participants (78°-100° for rectus femoris and 77°-94° for vastus lateralis).



A



B

Figure 15: Measured transducer angles of estimated perpendicular transducer orientation for rectus femoris (Panel A) and vastus lateralis (Panel B), including data from both raters across all participants. Measured transducer angles of estimated perpendicular images taken by rater 1 are displayed with black bars, images taken by rater 2 are displayed with grey bars.

Table 7 displays SEMs from images of the rectus femoris taken by rater 1 and rater 2. For the rectus femoris fat thicknesses, 80° transducer positions were associated with relatively high SEM. Very high SEM for muscle thickness was associated with 80° and 85° transducer angles for rater 1 and rater 2, respectively. Very high fascicle length SEM was shown for transducer positions closer to perpendicular (85° for rater 1 and 95° for rater 2).

Table 8 displays ICCs assessing the agreement of a measured 90° transducer angle to an estimated perpendicular position and measured 80°, 85°, 95°, and 100° for the rectus femoris. Muscle thickness and fat thickness displayed excellent agreement between all angles and a 90° position. Notably, pennation angles and fascicle lengths, from images taken at transducer positions that were estimated to be perpendicular showed poor agreement to a measured perpendicular transducer angle. Compared to other transducer angles, images of the rectus femoris taken at 85° transducer angles displayed the most consistent results (fair to excellent agreement) for all outcomes and raters.

Table 9 shows SEMs from images of the vastus lateralis taken by rater 1 and rater 2. For the vastus lateralis, transducer angles of 80° produced the highest error for muscle thickness, while transducer angles of 100° produced the highest error for pennation angle and fascicle length. Transducer angles that were estimated to be perpendicular showed the highest error for fat thickness of the vastus lateralis.

ICCs assessing agreement of a measured 90° transducer angle to an estimated perpendicular angle and measured 80°, 85°, 95°, and 100° transducer angles of images taken of the vastus lateralis by rater 1 and rater 2 are summarized in Table 10. Muscle

thickness and fat thickness demonstrated good to excellent agreement at all transducer angles except when the transducer was held at 80° by rater 2. Transducer angles of 100° demonstrated poor reliability to a 90° position for fascicle length and pennation angle outcomes. The best reliability (where most measurements demonstrated at least good to excellent reliability) was achieved at 85° and 95° transducer positions.

Table 7: Rectus femoris standard error measurements (SEMs) of corrected data. Sample sizes are provided. SEMs compare measurements from images taken with the transducer at an estimated perpendicular angle and a measured 80°, 85°, 95°, and 100° transducer orientation to a measured 90° transducer angle. SEMs for images taken by each rater for each outcome at each transducer angle is displayed. Bolded cells show the highest error for each outcome.

	Rater	Est vs. 90°	80° vs. 90°	85° vs. 90°	95° vs. 90°	100° vs. 90°
Muscle Thickness (cm)	1	0.15	0.44	0.07	0.16	0.09
	n	27	28	29	29	28
	2	0.16	0.29	0.38	0.10	0.12
	n	30	29	28	30	20
Fat Thickness (cm)	1	0.06	0.07	0.05	0.06	0.05
	n	29	26	29	29	28
	2	0.09	0.16	0.16	0.07	0.05
	n	29	29	29	30	30
Pennation Angle (°)	1	3.03	2.56	1.84	2.18	2.85
	n	26	24	28	28	27
	2	3.47	2.82	2.35	2.00	3.49
	n	29	29	29	28	27
Fascicle Length (cm)	1	8.32	8.74	5.98	19.20	9.00
	n	19	9	15	19	19
	2	11.46	11.86	13.38	4.76	4.90
	n	19	11	20	20	18

Table 8: Rectus femoris intraclass correlation coefficients (ICCs) for corrected data. Sample sizes are provided. ICCs compare measurements from images taken with the transducer at an estimated perpendicular angle and a measured 80°, 85°, 95°, and 100° transducer orientation to a measured 90° transducer angle. ICCs for images taken by each rater for each outcome at each transducer angle is displayed. Dark green cells represent excellent agreements, light green cells represent good agreement, yellow cells represent fair agreement and red cells represent poor agreement.

	Rater	Est vs. 90°	80° vs. 90°	85° vs. 90°	95° vs. 90°	100° vs. 90°
Muscle Thickness	1	0.90	0.95	0.98	0.90	0.96
	n	27	28	29	29	28
	2	0.91	0.92	0.98	0.96	0.92
	n	30	29	28	30	30
Fat Thickness	1	0.99	0.99	0.99	0.99	0.99
	n	29	26	29	29	28
	2	0.97	0.99	0.97	0.98	0.99
	n	29	29	29	30	30
Pennation Angle	1	0.39	0.18	0.71	0.60	0.52
	n	26	24	28	28	27
	2	0.26	0.16	0.59	0.67	0.61
	n	29	29	29	28	27
Fascicle Length	1	0.34	0.10	0.61	0.07	0.03
	n	19	9	15	19	19
	2	0.25	0.60	0.48	0.63	0.67
	n	19	11	20	20	18

Table 9: Vastus lateralis standard error measurements (SEMs) of corrected data. Sample sizes are provided. SEMs compare measurements from images taken with the transducer at an estimated perpendicular angle and a measured 80°, 85°, 95°, and 100° transducer orientation to a measured 90° transducer angle. SEMs for images taken by each rater for each outcome at each transducer angle is displayed. Bolded cells show the highest error for each outcome.

	Rater	Est vs. 90°	80° vs. 90°	85° vs. 90°	95° vs. 90°	100° vs. 90°
Muscle Thickness (cm)	1	0.15	0.21	0.12	0.12	0.16
	n	30	30	29	29	24
	2	0.22	0.25	0.20	0.15	0.16
	n	30	30	30	30	26
Fat Thickness (cm)	1	0.09	0.07	0.06	0.07	0.05
	n	30	30	29	29	24
	2	0.09	0.05	0.06	0.08	0.04
	n	30	30	30	30	26
Pennation Angle (°)	1	2.78	3.68	2.46	2.99	5.09
	n	30	30	29	29	24
	2	3.77	3.51	3.23	3.10	4.03
	n	30	30	30	30	26
Fascicle Length (cm)	1	2.19	1.16	1.24	1.52	3.08
	n	30	30	29	29	24
	2	3.12	3.00	2.58	1.74	3.61
	n	30	30	30	30	26

Table 10: Vastus lateralis intraclass correlation coefficients (ICCs) for corrected data. Sample sizes are provided. ICCs compare measurements from images taken with the transducer at an estimated perpendicular angle and a measured 80°, 85°, 95°, and 100° transducer orientation to a measured 90° transducer angle. ICCs for images taken by each rater for each outcome at each transducer angle is displayed. Dark green cells represent excellent agreements, light green cells represent good agreement, yellow cells represent fair agreement and red cells represent poor agreement.

	Rater	Est vs. 90°	80° vs. 90°	85° vs. 90°	95° vs. 90°	100° vs. 90°
Muscle Thickness	1	0.93	0.84	0.95	0.96	0.91
	n	30	30	29	29	24
	2	0.83	0.66	0.82	0.91	0.89
	n	30	30	30	30	26
Fat Thickness	1	0.98	0.99	0.99	0.99	0.99
	n	30	30	29	29	24
	2	0.99	0.99	0.99	0.99	0.99
	n	30	30	30	30	26
Pennation Angle	1	0.72	0.37	0.76	0.62	0.00
	n	30	30	29	29	24
	2	0.18	0.40	0.42	0.53	0.00
	n	30	30	30	30	26
Fascicle Length	1	0.00	0.63	0.63	0.78	0.33
	n	30	30	29	29	24
	2	0.49	0.52	0.77	0.76	0.30
	n	30	30	30	30	26

2.3.5 Secondary Purposes

2.3.5.1 Intra-Rater Reliability

SEM and ICCs for intra-rater reliability of rectus femoris muscle architecture measurements are displayed in Table 11. Excellent agreement and low error are displayed for all outcomes. SEM and ICC's for intra-rater reliability of rectus femoris muscle architecture measurements are displayed in Table 12. For the vastus lateralis, excellent agreement and low error is shown for intra-rater reliability.

Bland Altman plots for the agreement between rectus femoris muscle architecture measurement 1 and measurement 2 for the assessment of intra-rater reliability are shown in Figure 16. The majority of the data lies within two SD for all outcomes. For muscle fat thicknesses, data beyond two SD tend to lie above the upper agreement border. When poor quality images were excluded, there were 11 disagreements between measurement 1 and measurement 2 for the rectus femoris. That is, during the first or second round of measurements, one time the image was determined to be unusable, and the other time, measurements were taken.

Bland Altman plots for the agreement between vastus lateralis muscle architecture measurement 1 and measurement 2 for intra-rater reliability are shown in Figure 17. For the vastus lateralis, there is a small bias in the positive direction in the mean differences for muscle thickness and pennation angle measurements. When poor quality images were excluded, there were only 2 disagreements between measurement 1 and measurement 2 for the vastus lateralis.

Table 11: Intraclass correlation coefficients (ICCs) & standard error measurements (SEMs) for intra-rater reliability for muscle architecture measurements of the rectus femoris measure 1 and measure 2. For ICCs, dark green cells represent excellent agreements, light green cells represent good agreement, yellow cells represent fair agreement and red cells represent poor agreement. These analyses contain images taken by both raters.

	Muscle Thickness (cm) n = 351	Fat Thickness (cm) n = 351	Pennation Angle (°) n = 335	Fascicle Length (cm) n = 239
SEM	0.17	0.08	1.25	4.42
ICC	0.90	0.98	0.95	0.87

Table 12: Vastus lateralis measure 1 vs. measure 2 intraclass correlation coefficients (ICCs) & standard error measurements (SEMs) for intra-rater reliability. For ICCs, Dark green cells represent excellent agreements, light green cells represent good agreement, yellow cells represent fair agreement and red cells represent poor agreement. These analyses contain images taken by both raters.

	Muscle Thickness (cm) n = 347	Fat Thickness (cm) n = 347	Pennation Angle (°) n = 347	Fascicle Length (cm) n = 347
SEM	0.20	0.10	1.36	1.42
ICC	0.89	0.98	0.95	0.87

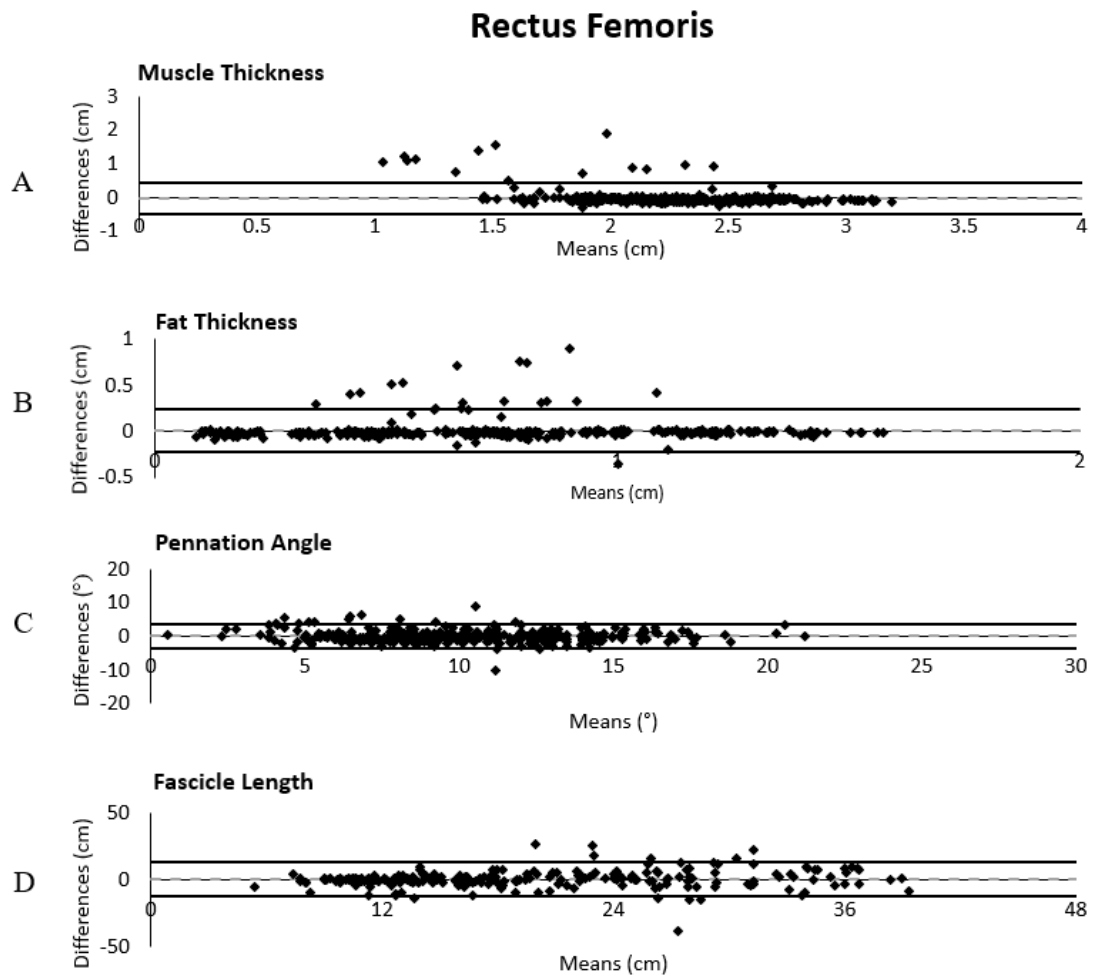


Figure 16: Bland-Altman plots comparing rectus femoris muscle thickness (A), fat thickness (B), pennation angle (C), and fascicle length (D) measurements from first and second measurements performed by rater 1 to assess intra-rater reliability. Data for all good-quality images of all participants taken by both raters at each transducer angle is displayed for muscle thickness, fat thickness and pennation angle (351 out of 360 data points for muscle and fat thickness, and 335 out of 360 data points for pennation angle). Only fascicle length data within the length of the muscle is displayed for all participants (239 out of 360 data points) (D). The means are plotted along the X-axis and the differences between the measures are plotted on the Y-axis. The mean is displayed with a dashed grey line. The upper and lower agreements represent 1.96 standard deviations and are displayed as black lines. The data points represent the differences between 1st and 2nd measurements.

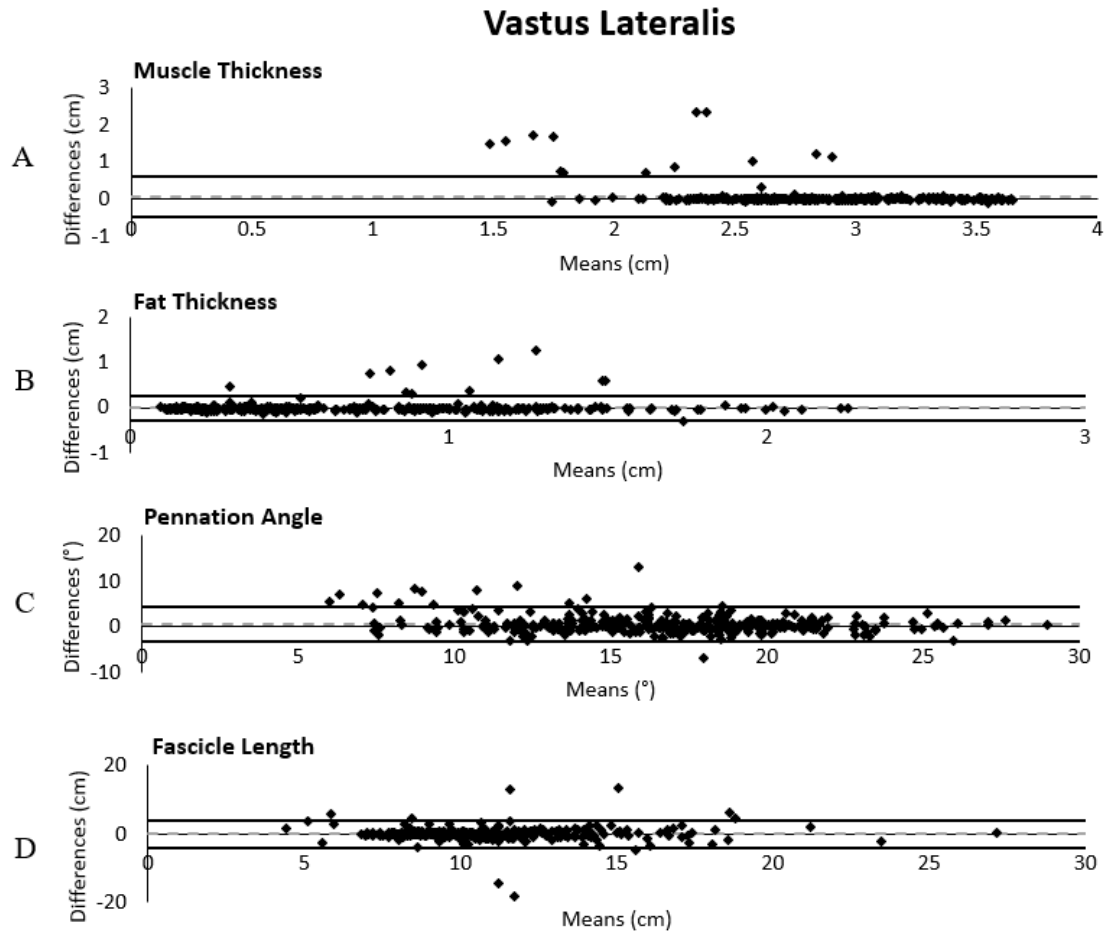


Figure 17: Bland-Altman plots comparing vastus lateralis muscle thickness (A), fat thickness (B), pennation angle (C), and fascicle length (D) measurements from first and second measurements performed by rater 1 to assess intra-rater reliability. Data for images of all participants taken by both raters at each transducer angle is displayed with poor quality images removed (347 data points of 360). As no fascicle lengths exceeded the length of the muscle, all fascicle lengths from good quality images are included are included (347 data points). The means are plotted along the X-axis and the differences between the measures are plotted on the Y-axis. The mean is displayed with a grey dashed line. The upper and lower agreements represent 1.96 standard deviations and are displayed as two black lines. The data points represent the differences between 1st and 2nd measurements.

2.3.5.2 Inter-Rater Image Acquisition

Bland-Altman graphs comparing the features of rectus femoris muscle architecture (muscle thickness, fat thickness, pennation angle and fascicle length) from images acquired by rater 1 and rater 2 are displayed in Figure 18. For all outcomes, most differences lie within two SD. The spread of the means for muscle thickness are generally between 1.5 cm and 3 cm and within two SD for differences between raters. The majority of fat thickness means are spread between 0 cm and 1.6 cm. Wider spreads of data are displayed for the pennation angle ($3 - 20^\circ$) and fascicle length measurements (6 – 44 cm).

ICCs and SEMs assessing inter-rater reliability of rectus femoris images are displayed in Table 13. Inter-rater reliability was excellent at all transducer angles for rectus femoris muscle and fat thicknesses. Good to excellent reliability was shown for rectus femoris pennation angles at all transducer angles. As well, Good to excellent agreement was displayed for fascicle length measurements at all transducer angles except 85° which showed poor agreement between raters for the rectus femoris.

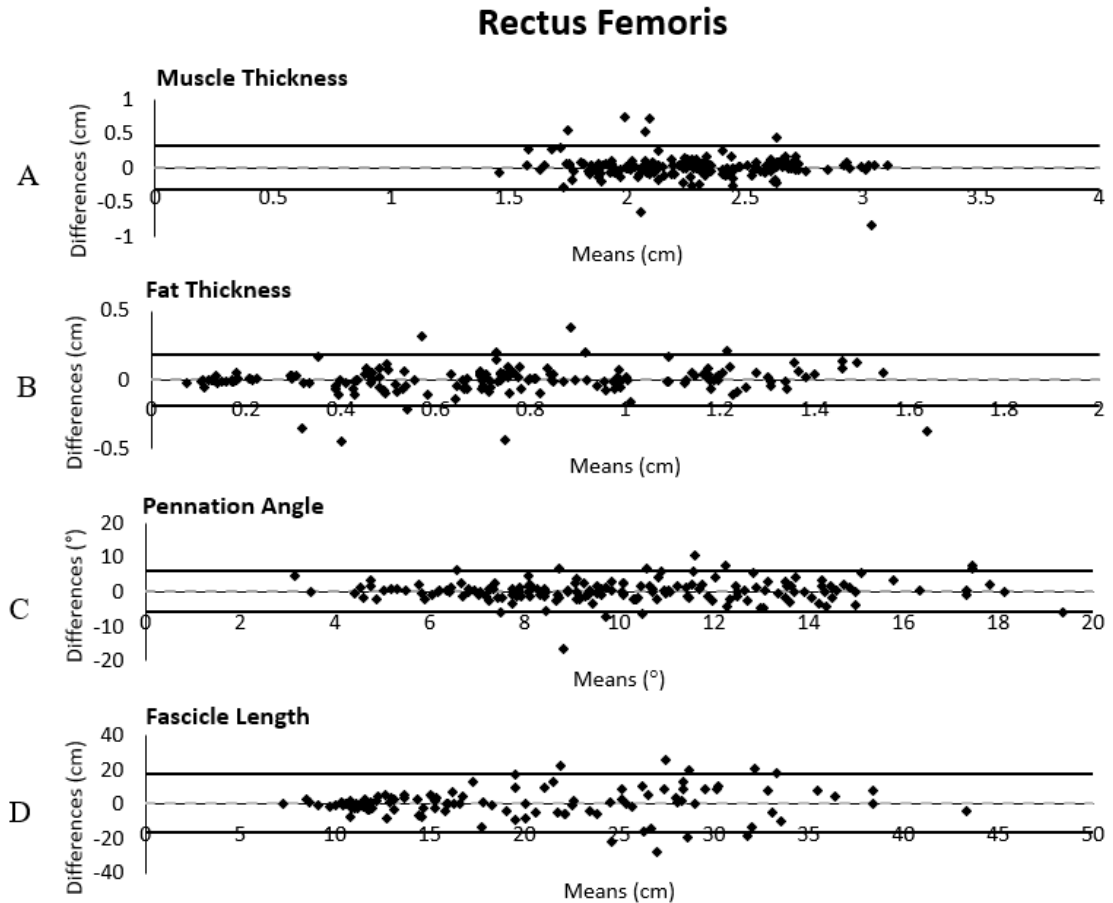


Figure 18: Bland-Altman plots comparing rectus femoris muscle thickness (A), fat thickness (B), pennation angle (C), and fascicle length (D) measurements from images taken by rater 1 and rater 2. Data for all images of all participants at each transducer angle is displayed with poor-quality images and fascicle lengths which exceeded muscle length removed (174 data points for the muscle and fat thicknesses, 165 data points for the pennation angles, and 111 data points for the fascicle lengths). The means are plotted along the X-axis and the differences between the measures are plotted on the Y-axis. The mean is displayed with a grey dashed line. The upper and lower agreements represent 1.96 standard deviations and are displayed as two black lines. The data points represent the differences between measurements from images taken by the first and second researcher.

Table 13: Standard error measurements (SEMs) and intraclass correlation coefficients (ICCs) comparing rectus femoris measurements for images taken by rater 1 vs rater 2. For SEM, bold cells represent which transducer angle produced the largest error for each outcome. Dark green cells represent excellent agreements, light green cells represent good agreement, yellow cells represent fair agreement and red cells represent poor agreement. n=30 unless otherwise specified.

		Est ₁ vs. Est ₂	80° ₁ vs. 80° ₂	85° ₁ vs. 85° ₂	90° ₁ vs. 90° ₂	95° ₁ vs. 95° ₂	100° ₁ vs. 100° ₂
Muscle Thickness	SEM (cm)	0.17	0.11	0.06	0.10	0.10	0.12
	ICC	0.90	0.95	0.99	0.96	0.96	0.93
	n	30	27	29	29	30	29
Fat Thickness	SEM (cm)	0.07	0.06	0.07	0.09	0.05	0.07
	ICC	0.99	0.99	0.98	0.98	0.99	0.98
	n	30	27	29	29	30	29
Pennation Angle	SEM (°)	2.86	1.18	1.62	2.03	1.92	3.15
	ICC	0.65	0.82	0.71	0.75	0.68	0.72
	n	28	26	28	28	28	28
Fascicle Length	SEM (cm)	6.51	5.67	7.24	7.07	4.86	5.50
	ICC	0.66	0.82	0.33	0.64	0.82	0.83
	n	24	6	14	17	24	23

Bland-Altman graphs comparing means and differences for the muscle thickness, fat thickness, pennation angle, and fascicle length of vastus lateralis ultrasound images taken by rater 1 and rater 2 are shown in Figure 19. The majority of data lies between 2 SD for all outcomes. There is a small bias in the negative direction in the mean differences of the fat thickness measurements.

SEM and ICC values comparing vastus lateralis images taken by rater 1 and rater 2 are shown in Table 14. Good to excellent agreement was demonstrated for muscle thickness and fat thickness outcomes at all transducer angles. For images taken at an angle estimated to be perpendicular, fair reliability was shown for pennation angle (ICC = 0.58) and fascicle length (ICC = 0.51). Other than the estimated transducer angle, excellent reliability was observed for pennation angle and good to excellent agreement for fascicle lengths from images taken at all measured transducer angles. Error measurements were largest for images taken at 100° transducer angles for muscle thicknesses and fascicle lengths of the vastus lateralis. Vastus lateralis pennation angles showed larger SEM at estimated perpendicular angles compared to measured angles.

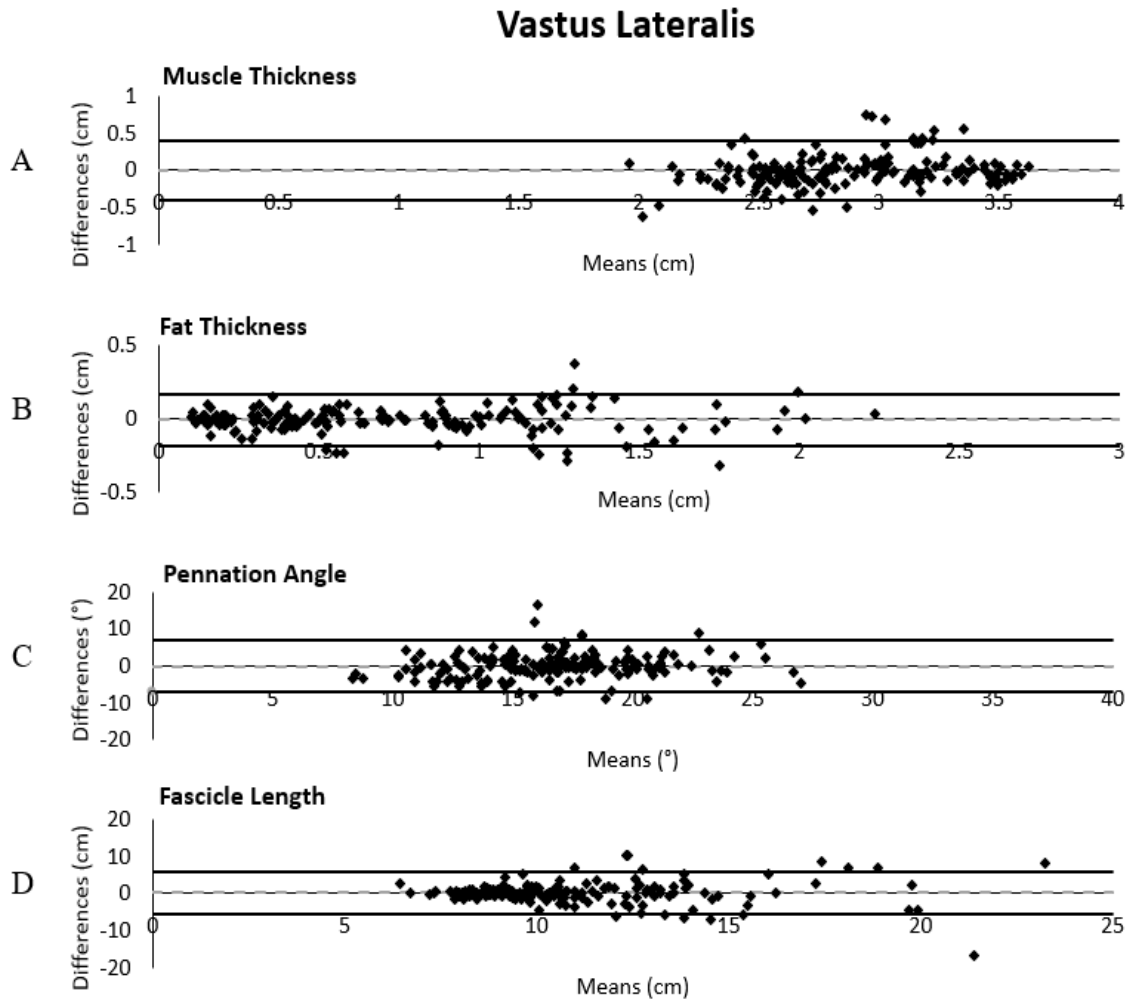


Figure 19: Bland-Altman plots comparing vastus lateralis muscle thickness (A), fat thickness (B), pennation angle (C), and fascicle length (D) measurements from images taken rater 1 and rater 2. Data for all images of all participants at each transducer angle is displayed with poor quality images removed (172 data points). The means are plotted along the X-axis and the differences between the measures are plotted on the Y-axis. The mean is displayed with a grey dashed line. The upper and lower agreements represent 1.96 standard deviations and are displayed as two black lines. The data points represent the differences between measurements from images taken by the first and second researcher.

Table 14: Vastus lateralis inter-rater reliability standard error measurements (SEMs) and intraclass correlation coefficients (ICCs). For SEMs, bold cells represent which transducer angle produced the largest error for each outcome. Dark green cells represent excellent agreements, light green cells represent good agreement, yellow cells represent fair agreement and red cells represent poor agreement.

		Est ₁ vs. Est ₂	80° ₁ vs. 80° ₂	85° ₁ vs. 85° ₂	90° ₁ vs. 90° ₂	95° ₁ vs. 95° ₂	100° ₁ vs. 100° ₂
Muscle Thickness	SEM (cm)	0.12	0.14	0.16	0.14	0.15	0.18
	ICC	0.96	0.91	0.90	0.94	0.94	0.88
	n	30	30	30	30	29	23
Fat Thickness	SEM (cm)	0.07	0.04	0.05	0.08	0.06	0.07
	ICC	0.99	1.00	1.00	0.99	0.99	0.98
	n	30	30	30	30	29	23
Pennation Angle	SEM (°)	3.20	2.38	1.84	2.41	2.29	2.60
	ICC	0.58	0.79	0.85	0.79	0.80	0.79
	n	30	30	30	30	29	23
Fascicle Length	SEM (cm)	2.31	1.25	0.85	2.41	2.16	3.23
	ICC	0.51	0.62	0.76	0.61	0.76	0.66
	n	30	30	30	30	29	23

2.4 Discussion

Current literature describing muscle architecture measurements acquired with ultrasound can benefit from standardization methods for ultrasound imaging protocols (Prado et al., 2014). Specifically, the angle at which the ultrasound transducer is placed relative to the tissue of interest (Klimstra et al., 2007). This thesis demonstrated that estimated perpendicular angles may not be consistent or accurate. Therefore, confirmation of a true 90° transducer angle is likely necessary. Although transducer angle did not influence muscle and fat thickness measurements in this study, differences in agreement and error were seen for pennation angles and fascicle lengths of the vastus lateralis and the rectus

femoris. This suggests these measurements are sensitive to the ultrasound acquisition protocol. If pennation angle and fascicle length are of interest, it is recommended that the angle of the transducer be standardized for musculoskeletal imaging. When imaging the vastus lateralis, it is recommended to acquire images of the muscle at 85° relative to the skin surface. For the rectus femoris, it is recommended that the muscle be imaged at 95° to the skin surface. If an ultrasound system which does not support extended fields of view is used, extrapolation of fascicle length is not recommended.

Estimated perpendicular angles showed poor agreement to a measured 90° position (ICC = 0.25 – 0.39) for pennation angle and fascicle length of the rectus femoris muscle. As well, estimated perpendicular transducer angles for ultrasound imaging of the rectus femoris and vastus lateralis without the aid resulted in greater variability in measurements acquired between participants and between imagers. Using a device to standardize the angle of the transducer against the skin improved the reliability and reduced the variability of muscle architecture measurements.

Overall, the data suggests that, compared to traditional techniques of estimating the best position of the ultrasound transducer head relative to the skin, a simple device to standardize the ultrasound transducer angle produced data with greater reliability and smaller error for the pennation angle and fascicle length measurements of both the rectus femoris and vastus lateralis in healthy, young adults. As the angle of the transducer deviates from perpendicular to the skin, the SEM of the vastus lateralis pennation angle and fascicle length measurements increase, and the ICCs for the pennation angle and the fascicle length measurements become poorer. For the vastus lateralis, fascicle length

appears to decrease as the transducer is tilted laterally (80° and 85°). Agreement between pennation angles and fascicle lengths improve when the angle of the transducer is standardized with the device and held at 85° or 95° . Our results are similar to a study which investigated the effect of transducer tilt on the muscle architectural appearance of the medial gastrocnemius (Bénard et al., 2009). This study found that five degree deviations from a perpendicular transducer position in the lateral and medial directions produced muscle architecture values (muscle thickness, pennation angle, and fascicle length) with low error (4%) (Bénard et al., 2009). Transducer tilts which exceeded 5 degrees produced higher error in muscle architecture measurements (up to 25%) (Bénard et al., 2009).

In spite of 90° being consistently cited as the angle of the transducer in previous studies (Alegre et al., 2014; Bénard et al., 2009; Blazeovich et al., 2006; Kwah et al., 2013; Thom et al., 2007; van den Hoorn et al., 2016), this may not be the best angle to image all muscles. Based on the results of this study, a 95° transducer angle may be recommended in order to reliably measure the rectus femoris. Although an 85° transducer angle demonstrated low error and excellent to fair agreement to a 90° position, it was associated with more erroneous fascicle lengths and unusable images for the rectus femoris. When the rectus femoris was imaged at 95° transducer angles, agreement to a perpendicular position was good to excellent for all but one condition, mean pennation angles appeared largest, and image quality was superior. However, when imaging the vastus lateralis, either an 85° or 95° transducer angle may be optimal. Inter-rater reliability was highest at these transducer angles. As well, images taken at these angles demonstrated low error and

excellent reliability to a 90° transducer angle. However, images taken at an 85° transducer angle may retrieve higher quality images as no images taken at this angle were determined to be unusable. It is not surprising that a transducer position perfectly perpendicular to the skin was not ideal. Though, it may be necessary to utilize a 90° position to limit attenuation of the ultrasound signal caused by reflection at an angle (Narouze, 2011), particularly in the presence of large subcutaneous fat thicknesses. This layer of fat may cause a wedge of tissue (as opposed to an evenly dispersed layer) that may offset the alignment of the transducer to the muscle. Thus, the anthropometry of the participants should be considered when designing a protocol. From this perspective, it is important to consider that women had significantly larger subcutaneous fat thicknesses above the rectus femoris and vastus lateralis than men.

Careful review and removal of poor-quality images was important to improve the inter-rater reliability of mean muscle architecture outcomes. The most important example was the impact of the extrapolation methodology on representing fascicle length. In the analyses of the raw data, the large number of erroneous fascicle lengths systematically altered the muscle architecture outcomes for the rectus femoris, such that fascicle length was erroneously longer. For rectus femoris, our average lengths far exceed what has been cited in previous literature (Kwah et al., 2013; Ward et al., 2009). For example, Moreau and colleagues (2009) reported mean fascicle lengths in the rectus femoris (9.75 ± 2.3 cm) which are far exceeded by our findings (16.7 – 27.7 cm) (Moreau et al., 2009). This error was not as obvious in the vastus lateralis as values remained within plausible ranges (9.4 cm – 14.1 cm) similar to those found in the literature (9.9 cm - 15.21 cm) (Ward et

al., 2009; Chleboun et al., 2007; Baroni et al., 2013). The extrapolation technique may not be useful in muscles with small pennation angles ($< 12^\circ$), such as that observed in the resting position of the rectus femoris. We believe that our study produced large lengths as a result of the small pennation angles observed in the rectus femoris while the muscle is in a relaxed position (Strasser et al., 2013). From this perspective, our strategy of removing fascicle lengths exceeding muscle lengths will not have completely addressed error due to overestimated fascicle lengths. The best strategy to correct this error in future ultrasound studies of the muscle groups is to either image the muscle while the knee is in full extension or use an ultrasound system which facilitates extended fields of view so that full fascicles can be observed. Finally, it is important to note that measurements of subcutaneous fat thickness, muscle thickness, and pennation angle of the vastus lateralis and rectus femoris match that reported in previous literature (Ward et al., 2009; Kwah et al., 2013).

2.4.1 Intra-rater reliability

Excellent intra-rater reliability was demonstrated for all measurements of muscle architecture measurements of both muscles (rectus femoris: ICC = 0.87 – 0.98; vastus lateralis: ICC = 0.87 – 0.98). Excellent agreement between measurements suggests that muscle and fat thickness, pennation angle, and fascicle length measurements are reproducible in this sample. Our intra-rater ICC values for fat thickness above the rectus femoris are the same as a previously reported ICC (ICC = 0.98) (Welsch et al., 1998). Previous studies which included intra-rater reliability of measuring the fascicle lengths of the vastus lateralis using an extrapolation method found an ICC of 0.9 and an SEM of

0.10 cm (Chleboun et al., 2007). This is similar to our vastus lateralis fascicle length ICC of 0.89, however our SEM was much higher (1.42 cm). Moreau et al. (2009) reported the relative reliability of the muscle thickness, fascicle lengths, and pennation angles of the vastus lateralis (ICCs 0.96- 0.99) and the rectus femoris (ICCs 0.95- 0.98) in healthy young individuals. These values are higher than that found in the current study for fascicle lengths and muscle thicknesses of the rectus femoris (ICCs 0.87-0.90) and fascicle lengths of the vastus lateralis (ICCs 0.89) but not pennation angles (ICC = 0.95 for rectus femoris and vastus lateralis). The differences in the ICC values most likely reflect the use of different ICC equations. Our study investigated two-way random effects for agreement, while Moreau et al (2009), and Chleboun et al. (2007) reported two-way mixed effects of consistency. For the purpose of our study, the two-way random effects measurement was more appropriate to analyze our data and answer our research question as we intend for our results to be generalizable to a larger set of researchers with similar knowledge, experience, and equipment (Koo & Li, 2016). Furthermore, previous studies have imaged the quadriceps with the knee joint in near full extension. Differences in results may, in part, be due to differences in the knee joint angle during imaging, as pennation angles and fascicle lengths have been shown to change as knee joint angle changes (Fukunaga et al., 1997).

2.4.2 Inter-rater reliability

Inter-rater reliability was better when imaging the vastus lateralis than when imaging the rectus femoris. Agreement of pennation angle and fascicle length measurements from images taken by two raters showed higher variability across transducer angles (rectus

femoris: ICC range = 0.33 – 0.83; vastus lateralis: ICC range = 0.51 – 0.85) than muscle and fat thickness measurements (rectus femoris: ICC range = 0.90 – 0.99; vastus lateralis: ICC range = 0.88 – 1.00). This suggests that muscle architecture assessments of pennation angle and fascicle length measurements are more sensitive to error caused by transducer position than muscle and fat thickness are. This has been previously shown by Strasser et al. (2013) who reported high reliability for muscle thickness (ICC = 0.97 and 0.96 for the rectus femoris and vastus lateralis, respectively), and lower ICC values for fascicle length and pennation angle measurements (ICC = 0.57 and 0.62 for fascicle lengths of the rectus femoris and the vastus lateralis, respectively; ICC = 0.53 for the pennation angle measurements of the vastus lateralis). Additionally, our study yielded similar inter-rater ICC values for fat thickness to a previous study which reported an ICC of 0.98 (Welsch et al., 1998).

2.4.3 Limitations

This study had limitations. The pressure of the transducer was not quantified, and differences in pressure may have hindered reliability between images due to compression of underlying tissues. Excessive pressure of the transducer against the skin was minimized as much as possible by using a generous amount of gel (Blazevich et al., 2006; Lixandrao et al., 2014; Valle et al., 2016). Additionally, given the 2D, *in vivo*, nature of ultrasound, there was no way to confirm that the transducer head was aligned exactly to the fascicles. An attempt to overcome this was made by scout-scanning to find an optimal alignment before images were collected. Furthermore, the ultrasound system that was used did not support extended fields of view, as such, no full fascicles were visible. As

well, the participants were imaged while seated on a dynamometer at 60° of knee joint flexion. As a result, the seat cushion may have added additional compression of the thigh tissue, especially in the region of the vastus lateralis. This may have affected the images. The measurements of this study were completed semi-automatically on a laptop and were subject to human error. To minimize this error, a custom program was created by a researcher assistant to automatically overlay ultrasound images with three equally spaced guidelines to ensure that measurements were performed in the same relative positions for each image. Lastly, participants in this study were recruited locally at McMaster University. The sample consisted of recreationally active graduate students of similar age whom all had sedentary jobs. Consequently, results from this study may not be generalizable to other populations. As well, large SEM and high ICC suggest high variability between participant measurements which may have influenced reliability.

2.4.4 Future directions

Use of the transducer attachment should be tested on muscles which were not examined in this study to determine if the results can be repeated in different muscles. Afterwards, these tools can be used to assist in research and clinical examinations of muscle architecture. Future studies may also focus on determining the usefulness of a device such as the one that we have used in measuring other muscle architecture parameters, such as cross sectional areas and echogenicity. This protocol should be performed in individuals who are not considered to be young and healthy in order to determine the applicability of this device in imaging muscles within broader samples. This device may be useful to other researchers investigating muscle architecture, particularly with repeated measure

design. Reliable imaging is important in order to monitor muscle changes and to test the effectiveness of interventions to prevent muscle loss. Lastly, this apparatus should be tested during contractions in order to determine the feasibility of sustaining a consistent transducer angle during contraction without the need to affix the transducer probe to the thigh using a strap or a cast.

2.5 Conclusions

Findings from this study suggest that, compared to traditional techniques of estimating the best position of the ultrasound transducer head relative to the skin, a simple device to standardize the ultrasound transducer angle produced data with greater reliability and smaller error for the pennation angle and fascicle length measurements of both the rectus femoris and vastus lateralis in healthy, young adults. However, muscle and fat thickness measurements appeared to be more robust as these measurements were not altered by varying transducer angles. Furthermore, the intra-rater reliability of muscle architecture measurements was acceptable, except for fascicle length for rectus femoris. Inter-rater reliability analyses for fascicle length and pennation angle showed variance between novice raters. Finally, we conclude that, when imaging the rectus femoris and vastus lateralis in healthy young adults, an extended field of view is necessary in order to accurately measure fascicle lengths of the muscle.

References

- Alegre, L. M., Ferri-Morales, A., Rodriguez-Casares, R., & Aguado, X. (2014). Effects of isometric training on the knee extensor moment - angle relationship and vastus lateralis muscle architecture. *European Journal of Applied Physiology*, 114(11), 2437–2446. <https://doi.org/10.1007/s00421-014-2967-x>
- Ando, R., Saito, A., Umemura, Y., & Akima, H. (2015). Local architecture of the vastus intermedius is a better predictor of knee extension force than that of the other quadriceps femoris muscle heads. *Clinical Physiology and Functional Imaging*, 35(5), 376–382. <https://doi.org/10.1111/cpf.12173>
- Arts, I. M. P., Pillen, S., Schelhaas, H. J., Overeem, S., & Zwarts, M. J. (2010). Normal values for quantitative muscle ultrasonography in adults. *Muscle and Nerve*, 41(1), 32–41. <https://doi.org/10.1002/mus.21458>
- Baroni, B. M., Geremia, J. M., Rodrigues, R., Borges, M. K., Jinha, A., Herzog, W., Vaz, M. A. (2013). Functional and morphological adaptations to aging in knee extensor muscles of physically active men. *Journal of Applied Biomechanics*, 29(5), 535–542.
- Bénard, M. R., Becher, J. G., Harlaar, J., Huijing, P. A., & Jaspers, R. T. (2009). Anatomical information is needed in ultrasound imaging of muscle to avoid potentially substantial errors in measurement of muscle geometry. *Muscle and Nerve*, 39(5), 652–665. <https://doi.org/10.1002/mus.21287>
- Blazevich, A. J. (2006). Effects of Physical Training and Detraining, Immobilisation, Growth and Aging on Human Fascicle Geometry. *Sports Med*, 36(12), 1003–1017.
- Blazevich, A. J., Gill, N. D., & Zhou, S. (2006). Intra- and intermuscular variation in human quadriceps femoris architecture assessed in vivo. *Journal of Anatomy*, 209(3), 289–310. <https://doi.org/10.1111/j.1469-7580.2006.00619.x>
- Bodine, S., Roy, R., Meadows, D., Zernicke, R., Sacks, R., Fournier, M., & Edgerton, V. (1982). Architectural, histochemical, and contractile characteristics of a unique biarticular muscle: the cat semitendinosus. *Journal of Neurophysiology*, 48(1), 192–201. <https://doi.org/10.1152/jn.1982.48.1.192>
- Borg, G. A. V. (1982). Psychophysical bases of perceived exertion. *Medicine and Science in Sports and Exercise*, 14(5), 377–381.
- Chen M.J., Fan X., Moe, S. T. (2002). Criterion-related validity of the Borg rating of perceived exertion scale in healthy individuals. *Journal of Sports Sciences*, 20(11), 873–899.
- Chleboun, G. S., Basic, A. B., Graham, K. K., & Stuckey, H. A. (2007). Fascicle Length Change of the Human Tibialis Anterior and Vastus Lateralis During Walking. *Journal of Orthopaedic & Sports Physical Therapy*, 37(7), 372–379. <https://doi.org/10.2519/jospt.2007.2440>
- Cicchetti, D. V. (1994). Guidelines, Criteria, and Rules of Thumb for Evaluating Normed

- and Standardized Assessment Instruments in Psychology. *Psychological Assessment*, 6(4), 284–290. <https://doi.org/10.1037/1040-3590.6.4.284>
- Craig, C. L., Marshall, A. L., Sjöström, M., Bauman, A. E., Booth, M. L., Ainsworth, B. E., Pratt, M., Ekelund, U., Yngve, A., Sallis, J. F. Oja, P. (2003). International physical activity questionnaire: 12-Country reliability and validity. *Medicine and Science in Sports and Exercise*, 35(8), 1381–1395. <https://doi.org/10.1249/01.MSS.0000078924.61453.FB>
- Crapo, R. O., Casaburi, R., Coates, A. L., Enright, P. L., MacIntyre, N. R., McKay, R. T., Johnson, D., Wanger, J. S., Zeballos, R. J., Bittner, V., Mottram, C. (2002). ATS statement: Guidelines for the six-minute walk test. *American Thoracic Society*, 166(1), 111–117. <https://doi.org/10.1164/rccm.166/1/111>
- Csapo, R., Alegre, L. M., & Baron, R. (2011). Time kinetics of acute changes in muscle architecture in response to resistance exercise. *Journal of Science and Medicine in Sport*, 14(3), 270–274. <https://doi.org/10.1016/j.jsams.2011.02.003>
- Ema, R., Wakahara, T., Miyamoto, N., Kanehisa, H., & Kawakami, Y. (2013). Inhomogeneous architectural changes of the quadriceps femoris induced by resistance training. *European Journal of Applied Physiology*, 113(11), 2691–2703. <https://doi.org/10.1007/s00421-013-2700-1>
- Fukunaga, T., Ichinose, Y., Masamitsu, I., Kawakami, Y., & Fukashiro, S. (1997). Determination of fascicle length and pennation in a contracting human muscle in vivo. *The American Physiology Society*, 378–381.
- Gans, C. (1982). Fiber Architecture and Muscle Function. *Exercise & Sport Sciences Reviews*, 10, 160–207.
- Gans, C., & de Vree, F. (1987). Functional bases of fibre length and angulation in muscle. *Journal of Morphology*, 192, 63–85.
- Klimstra, M., Dowling, J., Durkin, J. L., & MacDonald, M. (2007). The effect of ultrasound probe orientation on muscle architecture measurement. *Journal of Electromyography and Kinesiology*, 17(4), 504–514. <https://doi.org/10.1016/j.jelekin.2006.04.011>
- König, N., Cassel, M., Intziagianni, K., & Mayer, F. (2014). Inter-rater reliability and measurement error of sonographic muscle architecture assessments. *Journal of Ultrasound in Medicine*, 33(5), 769–777. <https://doi.org/10.7863/ultra.33.5.769>
- Koo, T. K., & Li, M. Y. (2016). A Guideline of Selecting and Reporting Intraclass Correlation Coefficients for Reliability Research. *Journal of Chiropractic Medicine*, 15(2), 155–163. <https://doi.org/10.1016/j.jcm.2016.02.012>
- Kwah, L. K., Pinto, R. Z., Diong, J., & Herbert, R. D. (2013). Reliability and validity of ultrasound measurements of muscle fascicle length and pennation in humans: a systematic review. *Journal of Applied Physiology*, 114(6), 761–769. <https://doi.org/10.1152/jappphysiol.01430.2011>
- Lindahl, O., Movin, A., & Ringqvist, I. (1969). Knee extension: Measurement of the

- isometric force in different positions of the knee-joint. *Acta Orthopaedica*, 40(1), 79–85. <https://doi.org/10.3109/17453676908989487>
- Lixandrao, M. E., Ugrinowitsch, C., Bottaro, M., Chacon-Mikahil, M., Cavaglieri, C. R., Min, L. L., DeSouza, E. O., Laurentino, G. C., Libardi, C. A. (2014). Vastus Lateralis Muscle Cross-Sectional Area Ultrasonography Validity for Image Fitting in Humans. *Journal of Strength and Conditioning Research*, 28(11), 3293–3297.
- Moreau, N. G., Teefey, S. A., & Damiano, D. L. (2009). In vivo muscle architecture and size of the rectus femoris and vastus lateralis in children and adolescents with cerebral palsy. *Developmental Medicine and Child Neurology*, 51(10), 800–806. <https://doi.org/10.1111/j.1469-8749.2009.03307.x>
- Narici, M. (1999). Human skeletal muscle architecture studied in vivo by non-invasive imaging techniques: functional significance and applications. *J Electromyogr Kinesiol*, 9(2), 97–103. [https://doi.org/10.1016/S1050-6411\(98\)00041-8](https://doi.org/10.1016/S1050-6411(98)00041-8)
- Narici, M. V, Maganaris, C. N., Reeves, N. D., & Capodaglio, P. (2003). Effect of Aging on Human Muscle Architecture. *Journal of Applied Physiology*, 95(6), 2229–2234. <https://doi.org/10.1152/jappphysiol.00433.2003>
- Narouze, S. N. (2011). Atlas of ultrasound-guided procedures in interventional pain management. *Atlas of Ultrasound-Guided Procedures in Interventional Pain Management*, 1–372. <https://doi.org/10.1007/978-1-4419-1681-5>
- Ng, A. V, Agre, J. C., Hanson, P., Harrington, M. S., & Nagle, F. J. (1994). Influence of muscle length and force on endurance and pressor responses to isometric exercise. *Journal of Applied Physiology*, 76(6), 2561–2569.
- Noorkoiv, M., Stavnsbo, A., Aagaard, P., & Blazevich, A. J. (2010). In vivo assessment of muscle fascicle length by extended field-of-view ultrasonography. *Journal of Applied Physiology*, 109(6), 1974–1979. <https://doi.org/10.1152/jappphysiol.00657.2010>
- Prado, C. M. M., & Heymsfield, S. B. (2014). Lean Tissue Imaging: A New Era for Nutritional Assessment and Intervention. *Journal of Parenteral and Enteral Nutrition*, 38(8), 940–953. <https://doi.org/10.1177/0148607114550189>
- Riddle, D. L., & Stratford, P. W. (2013). How Confident Can I Be About the Outcome Measurement on My Patient? In *Is This Change Real? Interpreting Patient Outcomes in Physical Therapy* (pp. 43–58).
- Rutherford, O. M., & Jones, D. A. (1992). Measurement of fibre pennation using ultrasound in the human quadriceps in vivo. *European Journal of Applied Physiology and Occupational Physiology*, 65(5), 433–437. <https://doi.org/10.1007/BF00243510>
- Scanlon, T. C., Fragala, M. S., Stout, J. R., Emerson, N. S., Beyer, K. S., Oliveira, L. P., & Hoffman, J. R. (2014). Muscle architecture and strength: Adaptations to short-term resistance training in older adults. *Muscle and Nerve*, 49(4), 584–592. <https://doi.org/10.1002/mus.23969>
- Strasser, E. M., Draskovits, T., Praschak, M., Quittan, M., & Graf, A. (2013). Association

- between ultrasound measurements of muscle thickness, pennation angle, echogenicity and skeletal muscle strength in the elderly. *Age*, 35(6), 2377–2388. <https://doi.org/10.1007/s11357-013-9517-z>
- Thom, J. M., Morse, C. I., Birch, K. M., & Narici, M. V. (2007). Influence of muscle architecture on the torque and power-velocity characteristics of young and elderly men. *European Journal of Applied Physiology*, 100(5), 613–619. <https://doi.org/10.1007/s00421-007-0481-0>
- Valle, M. S., Casabona, A., Micale, M., & Cioni, M. (2016). Relationships between Muscle Architecture of Rectus Femoris and Functional Parameters of Knee Motion in Adults with Down Syndrome. *BioMed Research International*, 2016. <https://doi.org/10.1155/2016/7546179>
- van den Hoorn, W., Coppieters, M. W., van Dieën, J. H., & Hodges, P. W. (2016). Development and Validation of a Method to Measure Lumbosacral Motion Using Ultrasound Imaging. *Ultrasound in Medicine and Biology*, 42(5), 1221–1229. <https://doi.org/10.1016/j.ultrasmedbio.2016.01.001>
- Ward, S. R., Eng, C. M., Smallwood, L. H., & Lieber, R. L. (2009). Are current measurements of lower extremity muscle architecture accurate? *Clinical Orthopaedics and Related Research*, 467(4), 1074–1082. <https://doi.org/10.1007/s11999-008-0594-8>
- Welsch, M. A., Williams, P. A., Pollock, M. L., Graves, J. E., Foster, D. N., & Fulton, M. N. (1998). Quantification of full-range-of-motion unilateral and bilateral knee flexion and extension torque ratios. *Archives of Physical Medicine and Rehabilitation*, 79(8), 971–978. [https://doi.org/10.1016/S0003-9993\(98\)90097-1](https://doi.org/10.1016/S0003-9993(98)90097-1)
- Wilken, J. M., Darter, B. J., Goffar, S. L., Ellwein, J. C., Snell, R. M., Tomalis, E. A., & Shaffer, S. W. (2012). Physical Performance Assessment in Military Service Members. *Journal of American Academy of Orthopaedic Surgeons*, 20(S1), S42–S47.

Chapter 3: Discussion

Ultrasound imaging can be a powerful tool in assessing features of muscle architecture to advance studies of muscle capacity; however, measurements derived from ultrasound images, such as pennation angle, appear sensitive to protocol deviations (Bénard et al., 2009; Klimstra et al., 2007). One important example of a protocol deviation is the angle at which the ultrasound transducer is placed relative to the tissue of interest (Klimstra et al., 2007). Traditionally, musculoskeletal imaging to observe muscle architecture is performed with the ultrasound transducer perpendicular to the skin (Alegre et al., 2014; Bénard et al., 2009; Blazevich et al., 2006; Kwah et al., 2013; Thom et al., 2007; van den Hoorn et al., 2016). Though, transducer angles estimated to be perpendicular to the skin, without aid or confirmation of the transducer angle, may not be in an exact 90° position. Consequentially, reporting of muscle architecture variables may not be consistent across studies. The purpose of this work was to investigate the effect of the ultrasound transducer angle on four muscle architecture measurements of the rectus femoris and the vastus lateralis in healthy adults: muscle thickness, pennation angle, fascicle length, and subcutaneous fat thickness. This was accomplished using a custom transducer attachment that quantified the transducer angle against the skin's surface. Secondly, intra- and inter-rater reliability of muscle architecture measures were determined. When compared to a measured 90° angle, 10° deviations from perpendicular positions negatively influenced pennation angle and fascicle length measurements of the rectus femoris and the vastus lateralis in healthy, young participants. Intra-rater reliability was high for all measures, except fascicle length of the rectus femoris muscle. However, inter-rater

reliability analyses for fascicle length and pennation angle showed variance between novice raters.

3.1 Transducer Tilt

Transducer angle did not have significant influence on the muscle and fat thicknesses within our sample. This is likely indicative of the muscle geometry. The whole muscle thickness of the vastus lateralis and the rectus femoris are uniform in the region of the tissue that was imaged between 80° and 100° transducer angles. Our finding that muscle thickness is not sensitive to transducer angle is corroborated by the literature. A study by Dankel et al. (2018) tested the reliability of muscle thickness measurements of ultrasound images taken of the biceps brachii and the tibialis anterior at six transducer angles (2° increments “up” and “down” from 90°) in healthy young adults. A coefficient of variation was used to assess the reliability at each angle. The authors concluded transducer angle dependent changes of muscle thickness to be negligible (<1%) (Dankel et al., 2018). Similar results were found by Ishida et al. (2017) who measured the influence of 3°, 6° and 9° deviations in unidirectional transducer tilt on measurements of rectus femoris muscle thickness in healthy young men. It was concluded that differences in muscle thickness at these angles were negligible. The average ICC for muscle thickness values was 0.99 and the SEM was 0.04 cm (Ishida et al., 2017). Differences between ICC values cited by Ishida et al. (2017) and those cited in the current study may be a result of their smaller, all male sample (14 young men). In both studies, a small digital level was affixed to the transducer to measure the angle of the transducer against the skin. As stated by the

authors, this method may not have accounted for deviations of the transducer in other planes.

In the literature, the transducer angle during ultrasound image acquisition is often vaguely reported. However, previous studies have concluded that there is a need to standardize the transducer angle for the purposes of retrieving muscle architectural information from ultrasound scans (Bénard et al., 2009; Correa-de-Araujo et al., 2017; Dankel et al., 2018; Ishida et al., 2017; König et al., 2014; Prado & Heymsfield, 2014). König et al. (2014) proposed a cast device to standardize a perpendicular placement of the transducer against the skin. The cast was affixed to the imaging region at a 90° angle to the skin using elastic straps. Inter-rater reliability was reported for the muscle thickness, fascicle length, and pennation angle of the gastrocnemius muscle using an ICC (2,1) and SEM (König et al., 2014). The ICC value for muscle thickness was lower than the one yielded in this study when the transducer was held at 90° (ICC = 0.82). The ICC value reported for pennation angle was similar (ICC = 0.80 – 0.90) and the ICC for fascicle length was higher (ICC = 0.77) than the ICC values cited in this study when either muscle was imaged at 90°. SEM values for the pennation angle and fascicle length differed between their study and ours. This may be because they used a different SEM equation ($SEM = SD \sqrt{(1-ICC)}$), while the equation used in this thesis provided a more conservative estimate of measurement error. Additionally, we suspect that differences may be due to the application to different muscles. Nonetheless, there are several potential issues with using their device. First, this device may be difficult to implement in a clinical setting. Second, the cast holds the transducer against the skin for the duration of

the image acquisition. It is common practice to remove the transducer from the skin in between images. The added pressure of the transducer head against the tissue due to lack of removal between scans may compress tissue and alter muscle architectural appearance (Orphanidou et al., 1994). Lastly, the elastic straps used to secure the transducer may cause the muscle belly to become distorted. Nevertheless, König et al. (2014) concluded that, using the cast, reliability of measurements was improved compared to control images taken without the device.

Results from the current study clearly indicate that, when a perpendicular position was estimated, the mean measured angle is dependent on the muscle being imaged and is not consistently perpendicular to the skin. The mean angle when estimating a perpendicular position was 86° for the vastus lateralis and 90° for the rectus femoris. Although, imagers were sometimes inaccurate by up to 12° . Rectus femoris fascicle lengths demonstrated poor agreement for images taken by rater 1 at all angles except for 85° , while images taken by rater 2 demonstrated fair to good agreement. Similarly, Bénard et al. (2009) observed the influence of a range of transducer positions on the muscle thickness, pennation angle, and fascicle length of the medial gastrocnemius muscle architecture. Bénard et al. (2009) concluded that five degree deviations from perpendicular transducer orientations were associated with low error (4%), while deviations larger than five degrees produced up to 25% error in fascicle length measurements. In the current thesis, it is important to highlight the differences in sample sizes at each angle after removal of poor-quality images and erroneous fascicle lengths

occurred. In some cases, samples sizes were likely too small to yield acceptable reliability coefficients or SEMs.

The extrapolation method used in this study resulted in 16% of the rectus femoris fascicle length data to be clearly erroneous (the lengths exceeded the length of the rectus femoris muscle length of the respective individual). We stress that, although reliability was improved by removing erroneous images, remaining fascicle lengths are still likely inaccurate because the mean of the fascicle lengths for the rectus femoris was almost 3 times larger than fascicle lengths previously reported in literature (9.75 ± 2.3 cm) (Moreau et al., 2009). Previous studies that have used the extrapolation method have not cited this issue. Notably, in previous literature, the rectus femoris was often observed while the muscle was in a shortened position with the knee joint near to full extension ($10^\circ - 20^\circ$). This would result in larger pennation angles that may yield more plausible fascicle lengths, as fascicle length decreases and pennation angle increases with change in joint angle (Fukunaga et al., 1997). Thus, it is possible that the limb position used in the current study may be largely responsible for the error in measurements as the muscle was in a resting position. This may not have been the case for the vastus lateralis due to the muscles larger resting pennation angles. Although, in a study by Strasser et al. (2013) pennation angles of the rectus femoris were removed from analysis because they were determined to be parallel to the aponeurosis.

3.2 Transducer Attachment

The 3D transducer attachment in this study was designed to measure the angle of the transducer during imaging. The wedge attaches to the protractor for stabilization against

the thigh and ensure that only the transducer is moving. The wedge is curved to fit the shape of the thigh and can be adjusted to accommodate different thigh geometries. Images acquired at measured angles were more reliable than the images acquired at estimated angles. This is likely due to a combination of the variations that occur when a perpendicular angle is being estimated and the more consistent pressure applied from the transducer to the thigh when the aid is in use.

3.3 Intra-Rater Reliability

This study demonstrated excellent intra-rater reliability for measuring muscle architecture for all outcomes except rectus femoris fascicle lengths. Several previous studies have reported the intra-rater reliability of measuring the muscle architecture of the vastus lateralis (Bleakney & Maffulli, 2002; Brancaccio et al., 2008; Chleboun et al., 2007; Fukunaga et al., 1997; Ishida et al., 2017; Moreau et al., 2009; Seiberl et al., 2010; Welsch et al., 1998), while, few studies have investigated the intra-rater reliability of measuring the muscle architecture of the rectus femoris (Moreau et al., 2009). Of these studies, few have reported both relative and absolute estimates of reliability; that is, ICC and SEM (Riddle & Stratford, 2013). Using a random measures ICC, rather than a different type of ICC (such as a mixed measures ICC), provides the literature with a conservative reliability coefficient which can be applied to other researchers with similar knowledge and experience (Koo & Li, 2016). The SEM value is important in order to understand the absolute reliability of a sample (Riddle & Stratford, 2013). The SEM is required to assist future research to both interpret the results within this study and compare to the results in similar studies. Several studies have reported coefficients of

variance (CV) in lieu of SEM or ICC (Bleakney & Maffulli, 2002; Brancaccio et al., 2008; Fukunaga et al., 1997). Coefficients of variance provide a ratio of variance between a standard deviation (SD) and a mean value and therefore represent the relative dispersion of data (Brown, 1998). The SEM is superior to the CV in determining the absolute reliability when performing muscle architecture measurements as it provides an absolute value in the same units as the measurement (Riddle & Stratford, 2013). SEMs can therefore be used to produce confidence intervals and determine minimal detectable changes.

Chleboun and colleagues (2007) measured the fascicle lengths of the vastus lateralis in healthy young individuals. Mixed measured, consistency ICC (3, k) and SEM analyses were used to determine the intra-rater reliability of their measurements. The ICC values reported were higher than the values reported for our study (ICC = 0.9). However, because they used a mixed measures ICC for consistency, their values are less conservative and can be expected to be higher. The SEM equation was not reported but the value was stated to be 0.1 cm (Chleboun et al., 2007). Their findings may have differed from ours as a result of both their smaller sample size (7 individuals) and their fewer of measurements (2 per image) (Chleboun et al., 2007).

Moreau et al. (2009) analyzed muscle thickness, fascicle length, and pennation angle within the rectus femoris and the vastus lateralis in healthy youth. ICC values reported by Moreau et al. (2009) were only slightly greater than the ICC values cited in the current study for rectus femoris muscle thickness and fascicle length (ICC = 0.98 and 0.98, respectively), and for vastus lateralis muscle thickness (ICC = 0.89). ICC results

were the same for rectus femoris pennation angle (ICC = 0.95) and similar for vastus lateralis fascicle length and pennation angle (ICC = 0.88 and 0.96, respectively). The ICC used by Moreau et al. (2009) was a mixed effects ICC for consistency (ICC 3, k). This ICC provides a less conservative measurement of reliability that is only applicable to the rater within the study and is not generalizable to other raters. As such, if the same ICC analysis was used, the greater reliability found by Moreau et al. (2009) may have been similar, and the findings which were similar, may have been lesser than the reliability yielded in our study.

The extrapolation method estimated the fascicle length based on the traced fascicles and the distance to the superficial aponeurosis border. Our reliability for the fascicle lengths is lower than previous findings; in that previous work, the fascicle lengths produced excellent agreement for the rectus femoris (ICC in this study = 0.87, compared to previous study ICC = 0.96 – 0.98) (Moreau et al., 2009). Nevertheless, many of the fascicle lengths, especially for the rectus femoris, were implausible and inaccurate. Therefore, this method of estimating fascicle length is not an accurate method of measuring fascicle length of the rectus femoris and should not be included in future studies.

3.4 Inter-Rater Reliability

Our results show that the reliability of muscle architecture measurements from ultrasound images is dependent on the muscle and on the rater that acquired the ultrasound images. The vastus lateralis demonstrated similar muscle architecture values and, thus, good to excellent reliability between raters when the transducer angle was standardized (ICC =

0.88 – 0.94 for muscle thickness, 0.99 – 1.00 for fat thickness, ICC = 0.79 – 0.85 for pennation angle, and ICC = 0.61 – 0.76 for fascicle length). Excellent reliability was demonstrated at all transducer angles for the muscle and fat thickness measurements of the vastus lateralis (ICC = 0.90 – 1.00). This demonstrates that measures of muscle and fat thicknesses acquired from ultrasound are reliable between raters independent of transducer angle. The rectus femoris yielded good to excellent agreement between raters for all outcomes at all angles except for 85° where poor agreement was observed between fascicle length measurements. Images taken at the same measured angles by different raters may produce comparable values. Differences could be the result of inconsistent transducer pressure between raters.

Strasser et al. (2003) tested the inter-rater reliability of the muscle thickness, and pennation angle of the rectus femoris and the vastus lateralis in elderly individuals. However, pennation angles were excluded from analysis as they were considered to be almost parallel to the aponeurosis (Strasser et al., 2013). Our ICC values were only slightly lower for muscle thickness (ICC = 0.97 rectus femoris; ICC = 0.96 vastus lateralis), and were much higher for vastus lateralis pennation angle (ICC = 0.53) (Strasser et al., 2013). Our fat thickness ICC is greater than the ICC yielded by Welsch et al. (1998) which was reported as 0.84. This improvement may reflect the benefits of using a transducer attachment.

3.5 Limitations

This study had limitations. First, the pressure of the transducer head against the skin was not quantified. Without quantifying the pressure of the transducer head against the skin, it

was difficult to ensure that the same amount of pressure was being applied throughout imaging and differences in pressure between imagers was likely. Differences in the pressure of the transducer against the skin could have interfered with imaging by adding compression to the tissues. Second, due to 2D imaging, there was no way to determine the exact plane of the fascicles within the muscle. Scout-scanning in a longitudinal plane was performed to estimate the best placement prior to saving images. Third, the system used in this study did not have an extended field of view. No full fascicles were visible in the field of view of our system. As a result, we were limited to utilizing an extrapolation method to measure the fascicle length. This produced inaccurate results, at least for the rectus femoris. Moreover, the participants were imaged in a seated position with their knee joint at 60° of flexion. Due to the lateral location of the vastus lateralis muscle and the relatively large volume of the muscle, the seat cushion may have distorted or added compression to the muscle which may have affected the images. Lastly, the participants in this study were recruited locally within McMaster University. All participants were recreationally active graduate students around the same age with largely sedentary jobs. Results from this study may not be generalizable to other populations.

3.6 Future directions

Future directions should investigate the integration of this device in studies with special populations, such as participants with knee osteoarthritis. As the results of this study vary with measurement outcome (muscle thickness, fat thickness, pennation angle and fascicle length) other measures, like cross-sectional area and echogenicity, should be observed using this protocol.

Future research should compare the use of a device by ultrasound operators with novice imaging experience and trained ultrasound technicians to see if images taken using the transducer attachment device can produce the same reliability as a trained sonographer. Creating a methodology where individuals without professional imaging training are able to perform imaging assessments that are comparable to a trained individual could make muscle architecture assessments more convenient to clinicians who do not have access to professional ultrasound technicians on site.

Repeating imaging methods described in this study would provide the literature with further information of the error that is associated between transducer angles and the amount of standard error that can be expected while using the device. This will allow us to understand the range of values that singular observations may reside within. Also, this will allow studies which intend to observe additional measurements to be able to site the additive error that may exist within their data points.

The application of this device may be helpful in studies which aim to look at muscle architecture. The device may provide reliable muscle architecture measurements in order to monitor muscle losses and gains over time. It may be difficult to ensure identical placements against the skin in a longitudinal study. This work may minimize the error of variable placements in these studies.

3.7 Conclusions

Without careful standardization, perpendicular positioning of the ultrasound transducer may not be exactly 90° to the skin's surface. When compared to a measured 90° angle,

images taken at estimated perpendicular angles demonstrated large error and poorer absolute and relative inter-rater reliability for the pennation angle and fascicle length measurements of the vastus lateralis. This was improved using a device. Deviations greater than 5° may influence measurements of pennation angle and fascicle length of the vastus lateralis and the rectus femoris. Intra-rater reliability of the rectus femoris and the vastus lateralis was excellent for all measurements (muscle and fat thickness, pennation angle and fascicle length). As well, good to excellent inter-rater reliability was achieved for all measurements except for the fascicle lengths derived from images taken at 85° transducer angles.

References

- Alegre, L. M., Ferri-Morales, A., Rodriguez-Casares, R., & Aguado, X. (2014). Effects of isometric training on the knee extensor moment - angle relationship and vastus lateralis muscle architecture. *European Journal of Applied Physiology*, 114(11), 2437–2446. <https://doi.org/10.1007/s00421-014-2967-x>
- Bénard, M. R., Becher, J. G., Harlaar, J., Huijing, P. A., & Jaspers, R. T. (2009). Anatomical information is needed in ultrasound imaging of muscle to avoid potentially substantial errors in measurement of muscle geometry. *Muscle and Nerve*, 39(5), 652–665. <https://doi.org/10.1002/mus.21287>
- Blazevich, A. J., Gill, N. D., & Zhou, S. (2006). Intra- and intermuscular variation in human quadriceps femoris architecture assessed in vivo. *Journal of Anatomy*, 209(3), 289–310. <https://doi.org/10.1111/j.1469-7580.2006.00619.x>
- Bleakney, R., & Maffulli, N. (2002). Ultrasound changes to intramuscular architecture of the quadriceps following intramedullary nailing. *Journal of Sports Medicine and Physical Fitness*, 42(1), 120–125.
- Brancaccio, P., Limongelli, F. M., D'Aponte, A., Narici, M., & Maffulli, N. (2008). Changes in skeletal muscle architecture following a cycloergometer test to exhaustion in athletes. *Journal of Science and Medicine in Sport*, 11(6), 538–541. <https://doi.org/10.1016/j.jsams.2007.05.011>
- Bredella, M. A. (2017). Sex Differences in Body Composition. In F. Mauvais-Jarvis (Ed.), *Sex and Gender Factors Affecting Metabolic Homeostasis, Diabetes and Obesity* (pp. 9–27). Cham: Springer International Publishing. https://doi.org/10.1007/978-3-319-70178-3_2
- Brown, C. E. (1998). Coefficient of Variation. In *Applied Multivariate Statistics in Geohydrology and Related Sciences* (pp. 155–157). Berlin, Heidelberg: Springer Berlin Heidelberg. https://doi.org/10.1007/978-3-642-80328-4_13
- Chleboun, G. S., Busic, A. B., Graham, K. K., & Stuckey, H. A. (2007). Fascicle Length Change of the Human Tibialis Anterior and Vastus Lateralis During Walking. *Journal of Orthopaedic & Sports Physical Therapy*, 37(7), 372–379. <https://doi.org/10.2519/jospt.2007.2440>
- Correa-de-Araujo, R., Harris-Love, M. O., Miljkovic, I., Fragala, M. S., Anthony, B. W., & Manini, T. M. (2017). The Need for Standardized Assessment of Muscle Quality in Skeletal Muscle Function Deficit and Other Aging-Related Muscle Dysfunctions: A Symposium Report. *Frontiers in Physiology*, 8, 1–19. <https://doi.org/10.3389/fphys.2017.00087>
- Dankel, S. J., Abe, T., Bell, Z. W., Jessee, M. B., Buckner, S. L., Mattocks, K. T., Mouser, J. G., Loenneke, J. P. (2018). The impact of ultrasound probe tilt on muscle thickness and echo-intensity: A cross-sectional study. *Journal of Clinical Densitometry*, (1), 1–9. <https://doi.org/10.1016/J.JOCD.2018.10.003>
- Fukunaga, T., Ichinose, Y., Masamitsu, I., Kawakami, Y., & Fukashiro, S. (1997).

- Determination of fascicle length and pennation in a contracting human muscle in vivo. *The American Physiology Society*, 378–381.
- Gans, C., & de Vree, F. (1987). Functional bases of fibre length and angulation in muscle. *Journal of Morphology*, 192, 63–85.
- Ishida, H., Suehiro, T., Suzuki, K., Yoneda, T., & Watanabe, S. (2017). Influence of the ultrasound transducer tilt on muscle thickness and echo intensity of the rectus femoris muscle of healthy subjects. *Journal of Physical Therapy Science*, 29(12), 2190–2193. <https://doi.org/10.1589/jpts.29.190>
- Klimstra, M., Dowling, J., Durkin, J. L., & MacDonald, M. (2007). The effect of ultrasound probe orientation on muscle architecture measurement. *Journal of Electromyography and Kinesiology*, 17(4), 504–514. <https://doi.org/10.1016/j.jelekin.2006.04.011>
- König, N., Cassel, M., Intziagianni, K., & Mayer, F. (2014). Inter-rater reliability and measurement error of sonographic muscle architecture assessments. *Journal of Ultrasound in Medicine*, 33(5), 769–777. <https://doi.org/10.7863/ultra.33.5.769>
- Koo, T. K., & Li, M. Y. (2016). A Guideline of Selecting and Reporting Intraclass Correlation Coefficients for Reliability Research. *Journal of Chiropractic Medicine*, 15(2), 155–163. <https://doi.org/10.1016/j.jcm.2016.02.012>
- Kwah, L. K., Pinto, R. Z., Diong, J., & Herbert, R. D. (2013). Reliability and validity of ultrasound measurements of muscle fascicle length and pennation in humans: a systematic review. *Journal of Applied Physiology*, 114(6), 761–769. <https://doi.org/10.1152/jappphysiol.01430.2011>
- Moreau, N. G., Teefey, S. A., & Damiano, D. L. (2009). In vivo muscle architecture and size of the rectus femoris and vastus lateralis in children and adolescents with cerebral palsy. *Developmental Medicine and Child Neurology*, 51(10), 800–806. <https://doi.org/10.1111/j.1469-8749.2009.03307.x>
- Narici, M. (1999). Human skeletal muscle architecture studied in vivo by non-invasive imaging techniques: functional significance and applications. *J Electromyogr Kinesiol*, 9(2), 97–103. [https://doi.org/10.1016/S1050-6411\(98\)00041-8](https://doi.org/10.1016/S1050-6411(98)00041-8)
- Narouze, S. N. (2011). Atlas of ultrasound-guided procedures in interventional pain management. *Atlas of Ultrasound-Guided Procedures in Interventional Pain Management*, 1–372. <https://doi.org/10.1007/978-1-4419-1681-5>
- Orphanidou, C., McCargar, L., Birmingham, C. L., Mathieson, J., & Goldner, E. (1994). Accuracy of Subcutaneous Fat Measurement: Comparison of Skinfold Calipers, Ultrasound, and Computed Tomography. *Journal of the American Dietetic Association*, 94(8), 855.
- Prado, C. M. M., & Heymsfield, S. B. (2014). Lean Tissue Imaging: A New Era for Nutritional Assessment and Intervention. *Journal of Parenteral and Enteral Nutrition*, 38(8), 940–953. <https://doi.org/10.1177/0148607114550189>
- Riddle, D. L., & Stratford, P. W. (2013). How Confident Can I Be About the Outcome

Measurement on My Patient? In *Is This Change Real? Interpreting Patient Outcomes in Physical Therapy* (pp. 43–58).

- Seiberl, W., Hahn, D., Kreuzpointner, F., Schwirtz, A., & Gastmann, U. (2010). Force enhancement of quadriceps femoris in vivo and its dependence on stretch-induced muscle architectural changes. *Journal of Applied Biomechanics*, 26(3), 256–264. <https://doi.org/10.1123/jab.26.3.256>
- Strasser, E. M., Draskovits, T., Praschak, M., Quittan, M., & Graf, A. (2013). Association between ultrasound measurements of muscle thickness, pennation angle, echogenicity and skeletal muscle strength in the elderly. *Age*, 35(6), 2377–2388. <https://doi.org/10.1007/s11357-013-9517-z>
- Thom, J. M., Morse, C. I., Birch, K. M., & Narici, M. V. (2007). Influence of muscle architecture on the torque and power-velocity characteristics of young and elderly men. *European Journal of Applied Physiology*, 100(5), 613–619. <https://doi.org/10.1007/s00421-007-0481-0>
- van den Hoorn, W., Coppeters, M. W., van Dieën, J. H., & Hodges, P. W. (2016). Development and Validation of a Method to Measure Lumbosacral Motion Using Ultrasound Imaging. *Ultrasound in Medicine and Biology*, 42(5), 1221–1229. <https://doi.org/10.1016/j.ultrasmedbio.2016.01.001>
- Welsch, M. A., Williams, P. A., Pollock, M. L., Graves, J. E., Foster, D. N., & Fulton, M. N. (1998). Quantification of full-range-of-motion unilateral and bilateral knee flexion and extension torque ratios. *Archives of Physical Medicine and Rehabilitation*, 79(8), 971–978. [https://doi.org/10.1016/S0003-9993\(98\)90097-1](https://doi.org/10.1016/S0003-9993(98)90097-1)

APPENDIX A – 3D-Printed Attachment

3D Scan of the Ultrasound Transducer

The transducer was held using a container so that the transducer would be in an upright position and the scanning gun could be brought around the perimeter without obstruction. The container was wrapped with black construction paper and placed upon a black mat to limit reflection. A non-reflective black mat was held between the imager and a light that couldn't be turned off to limit error caused by reflection. The scan was done using an Artec Eva portable scanner and Artec Studio 12 software at 15 frames per second. The imager held the scanner at a 0.4-0.9 m distance (specified by the software). A visual feedback allowed the imager to ensure that they were within the allowed distance, the signal would become red if the scanner was out of range. The scan was completed using geometric and texture mode. The imager walked around the entire boundary of the probe slowly. Several scans were taken to ensure that all angles of the probe were imaged.

3D Processing of the Ultrasound Transducer Scan

Images were merged together using Artec Studio 12. Scans with a resolution error above 0.7 AU were deleted based on system recommendations to improve the quality of the model. Other noise from the mat and surrounding objects were removed using the cut-off plane selection tool and smaller noise was removed with the lasso eraser tool. The good scans were aligned (5 scans). Similar points were manually identified on each scan and were used as reference points for alignment. A global registration was performed and outlier removal of 2 standard deviations were applied based on system recommendations. The model was exported the model as an stl file.

3D Modeling of the Ultrasound Transducer Attachment

The 3D model was imported into MeshMixer Autodesk software to allow adjustment and manipulation of the model. When a model was adjusted to accurately fit the transducer, the model was split in half width-wise using the Plane Cut tool. A gauge needle was downloaded and imported from thingiverse.com. The gauge needle was customized using MeshMixer to extend to the length of the protractor and the unneeded portions were removed from the model. The needle was aligned to the midpoint of the thin half of the transducer attachment corresponding to the circle indicator side of the transducer. The needle and the transducer attachment were combined into a single object using a Boolean Union tool. A hole was created through the needle and the transducer model to allow for attachment of a small screw. The model was made solid and exported as an “*.obj” file. The two sides of the probe were printed and fitted to the transducer to check for any need for changes, if changes were needed the model was rescaled accordingly. A magnet holder was downloaded from thingiverse.com and adjusted using MeshMixer. 8 magnet holders were printed. Lastly, a protractor and a wedge were downloaded from thingiverse.com and adjusted using MeshMixer.

3D Printing and Assembly of the Ultrasound Transducer Attachment

Model components were imported into the MakerBot software and oriented to a position that would allow optimal printing. All model components were exported from MakerBot print software as a *.x3g file using these specifications. Model components were printed using the MakerBot Replicator™ 2 Desktop 3D printer (MakerBot Industries, NY, USA) using a biodegradable polylactic acid (PLA) filament from MakerBot. Printing properties

are summarized in Table 13. Neodymium magnets were glued into the magnet holders to keep the attachment together. Two strip magnets were glued to the straight edged of the wedge and a line of small magnets were glued to the bottom of the protractor. A piece of black foam was glued to the curved edge of the wedge for participant comfort.

Table 15: 3D printing extruder properties.

Extruder type	mkii
Print mode	Balanced
Support	ON
Extruder temperature	230° C
Extruder travel speed	120 mm/s
Layer height	0.2 mm
Shells	2
Raft	ON
infill	20% density, hexagonal

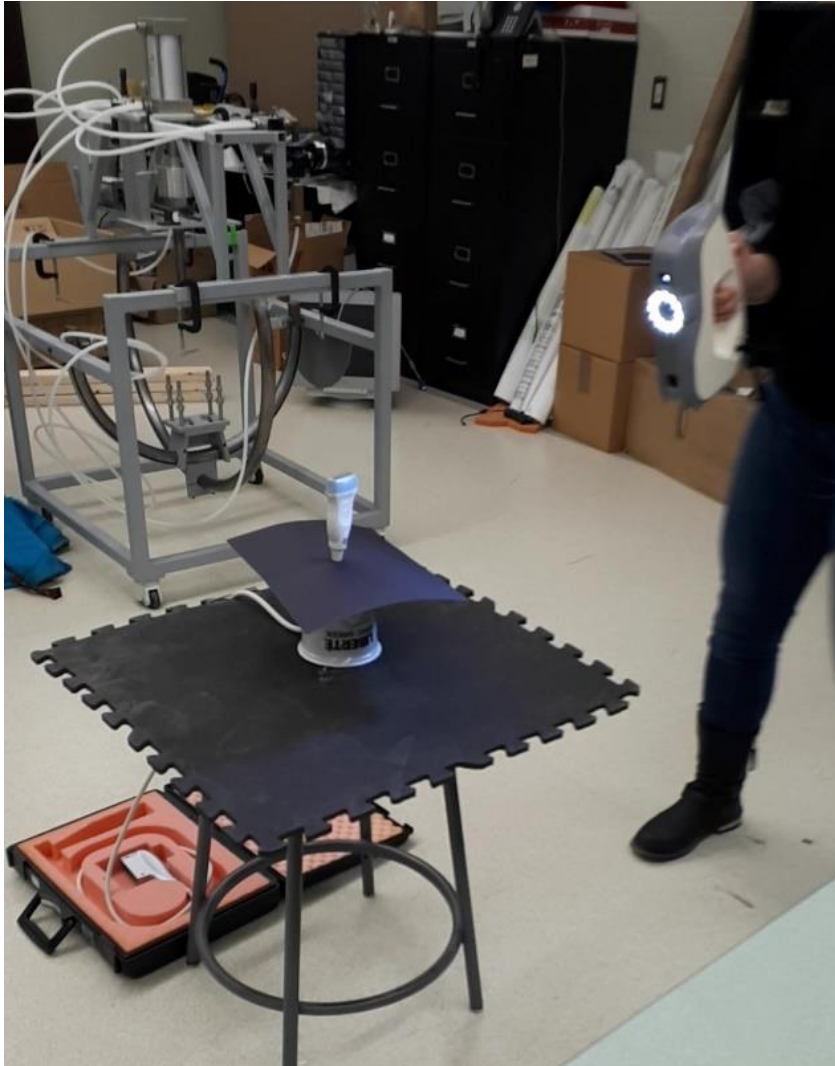


Figure 20: 3D scan of the ultrasound transducer.

APPENDIX B – Online Screening Questionnaire

Section 1 of 5

Muscle Architecture Properties of the Quadriceps

Form description

Email address *
Valid email address
This form is collecting email addresses. [Change settings](#)

Age
Short answer text

Sex *

Female

Male

Section 2 of 5

Knee Osteoarthritis Criteria

Description (optional)

Do you have knee pain? *

Yes

No

Do you have less than 30 minutes of morning stiffness in your knee? *

Yes

No

Do you experience creaking, cracking, or grating within your knee? *

Yes

No

Do you have any bony growths around the knee? *

Yes

No

Is your knee tender to the touch? *

Yes

No

Is your knee warm to the touch? *

Yes

No

Which knee is more painful/bothersome? *

Right

Left

Not Applicable

Section 3 of 5

Get Active Questionnaire

Description (optional)

Have you experienced ANY of the following within the past six months? *

A diagnosis of/treatment for heart disease or stroke, or pain/discomfort/pressure in your chest during activities of daily living?

A diagnosis of/treatment for high blood pressure (BP), or a resting BP of 160/90 mmHg or higher?

Dizziness or lightheadedness during physical activity?

Shortness of breath at rest?

Loss of consciousness/fainting for any reason?

Concussion?

None of the above

Do you currently have pain or swelling in any part of your body (such as from an injury, acute flare-up of arthritis, or back pain) that affects your ability to be physically active? *

Yes

No

Has a health care provider told you that you should avoid or modify certain types of physical activity? *

Yes

No

Do you have any other medical or physical condition (such as diabetes, cancer, osteoporosis, asthma, spinal cord injury) that may affect your ability to be physically active? *

Yes

No

During a typical week, on how many days do you do moderate- to vigorous-intensity aerobic physical activity (such as brisk walking, cycling or jogging)? *

Days/week

0 1 2 3 4 5 6 7

On days that you do at least moderate-intensity aerobic physical activity (e.g., brisk walking), for how many minutes do you do this activity? *

Minutes/day

Short answer text

After section 3 [Continue to next section](#)

Section 4 of 5

Additional Questions

Description (optional)

Do you consider yourself to be a competitive cyclist? *

Yes

No

Have you had previous knee surgery? *

Yes

No

Do you have chronic breathing problems? *

For example COPD

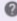

Yes

No

Do you have emphysema? *

Yes

No



Have you had a stroke? *

Yes

No

Do you have any other neurological conditions? *

Yes

No

Have you had a hip, knee, or ankle injury in the last year? *



Yes

No

Do you have any skin allergies? *

Yes

No



Do you have kidney disease? *

Yes

No

Do you have an unstable heart condition? *

Yes

No

Do you have type 1 or type 2 diabetes? *

Yes

No

After section 4 [Continue to next section](#)

Section 5 of 5

Personal Information

First and Last Name *

Short answer text

Date of Birth *

MM/DD/YYYY

Short answer text

Phone Number and Extension *

Short answer text

Email Address *

Short answer text

Preferred method of contact *

Phone

Email

APPENDIX C – Consent Form



Letter of Information and Consent

Muscle Architecture Properties of the Quadriceps: Reliability Testing and Association with Severity of Knee Osteoarthritis

- Principal Investigator: Dr. Monica Maly (PT, PhD), Kinesiology
Associate Professor (Part-time), Rehabilitation Science,
McMaster University
519-888-4567 x 37916
- Co-investigators: Peter Keir (PhD), Kinesiology
McMaster University
905-525-9140 x 23543
- Audrey Hicks (PhD), Kinesiology
McMaster University
905-525-9140 x 24643
- Janet Pritchard (PhD), Kinesiology
McMaster University
905-525-9140 x 20029
- Co-ordinator: Emily Wiebenga (BSc), Rehabilitation Sciences
McMaster University
905-525-9140 x 20748
- Student Investigator: Brittany Bulbrook (MSc Candidate), Kinesiology
McMaster University
905-525-9140 x 20748

Funding Source:

This study is funded by the Natural Sciences and Engineering Research Council.

Introduction

You are invited to participate in a study that examines the effects of muscle properties on its function in healthy adults and women with knee osteoarthritis.

Before agreeing to participate, it is important that you read and understand the proposed study procedures. The information provided describes the purpose, procedures, benefits, discomforts, risks and precautions associated with this study. It also describes your right to refuse to participate or withdraw from the study at any time. In deciding whether you wish to participate, you should understand enough about the risks and benefits to be able to make an informed decision. This is part of the informed consent process. Make sure all of your questions have been answered to your satisfaction before signing this document.

Background and Purpose

Osteoarthritis is a very common disease in Canada, with the knee affected most often. Women are more affected by the disease than men. Knee osteoarthritis is associated with reduced mobility and weakened knee muscles. The muscles in your body are made up of smaller muscle fibres. Ultrasound is a quick, non-invasive way to examine the arrangement of muscle fibres. The arrangement of these muscle fibres in a muscle influences how much force and power is produced by that muscle. We believe that knee osteoarthritis alters the arrangement of muscle fibres within a muscle, making it weaker. **The purpose of this study is to investigate the intra-rater reliability of measurements of muscle architecture, and determine the association of muscle architectural features with severity of knee osteoarthritis. A secondary purpose is to investigate the relationships of the arrangement of muscle fibres with muscle strength and range of motion at the knee joint in women with knee osteoarthritis.**

To participate in this study, you either need to be a woman, between 60 and 75 years of age, with chronic knee problems that are consistent with knee osteoarthritis, or a man or woman aged 18 - 35 years of age. Thirty-four participants aged 60-75 and 30 participants between 18 and 35 will be recruited to this study. We cannot include anyone who has the following:

- Chronic breathing problems, such as COPD or
- Emphysema
- Stroke

- Other Neurological Conditions
- Recent Leg Injuries
- Known Skin Allergy
- Kidney Disease
- Unstable Heart Disease
- Type I and II Diabetes

Procedure

If you meet the above criteria and are interested in participating, we welcome you to join our study! As a participant in this study, you will come to the McMaster Occupational Biomechanics Laboratory at McMaster University. This visit will take approximately 2 hours to complete. If required, parking for this laboratory visit will be provided free of charge. You will be asked to provide us with your phone number or email address so that we can contact you to answer any questions that may arise.

Measurements of the Study

1. Body size measurements (height, weight, thigh length, thigh circumference)
2. Mobility walking test
3. Strength and power assessment of the knee
4. Questionnaires
5. Ultrasound of the thigh
6. Muscle activation patterns

This visit will take approximately 2 hours to complete.

When you arrive for the study, your height, weight, thigh circumference and thigh length will be measured and recorded.

Muscle Activation Patterns

We will attach electrodes to the skin using tape over two of your thigh muscles. These electrodes monitor muscle activity during knee strength measurements.

Knee strength and power assessment

We will then seat you in a machine designed to measure knee strength. We will adjust the seat to your measurements and you will be securely strapped into the chair of the machine. Once you are seated, we will ask you to do a brief warm-up

to get comfortable with performing knee muscle exercises. We will then ask you to kick your knee 10 times in a row. This will allow us to record your maximum strength and find the knee angle in which you produce the most force. We will then ask you to contract your muscles as strongly as possible when your knee is not moving. We will ask you to repeat these six times at 2 different angles. You should not feel any pain or discomfort during these strength measurements; however, you may feel muscle soreness afterwards from working these muscles hard. Ice is available at your request.

***You will be provided with rest throughout the visit. Please do not hesitate to request more rest. ***

Ultrasound

Before and during the knee strength test, we will ultrasound your two of your thigh muscles. A small amount of ultrasound gel will be placed on the probe and the probe will be placed over the skin to image your thigh muscles. You should not feel any pain or discomfort. If the images from the strength and power tests appear blurry, we will ask you to perform a few repetitions again for clearer images. You may decline this request.

Risks and Benefits

There are minimal risks associated with your participation in this study. You may experience fatigue, soreness, and worsening of any existing knee pain as a result of your participation. Muscle soreness should recover after 24-48 hours. There is a risk, in some cases, that your skin may experience a reaction to the medical tape used to keep the recording electrodes in place. If you experience any serious discomfort following the study, please contact the principal investigator, Dr. Monica Maly at 519-888-4567 ext. 37916.

There are benefits to your participation. Your participation will help improve our understanding of how muscle architecture is related to knee osteoarthritis severity.

Confidentiality

All information obtained during the study will be held in strict confidence. You will be identified in the study by a code only. No names or identifying information will be used in any publication or presentation. No identifying information will be

available outside of the investigation. The information we collect will be secured in a locked filing cabinet in the Ivor Wynne Centre room A107 at McMaster University. This research space is also locked. Following completion of the study, the identifying information we collect will be destroyed. Representatives of the Hamilton Integrated Research Ethics Board (HiREB) may require access to your study-related records or may follow up with you to monitor the conduct of the research.

Participation

Your participation in this study is voluntary. If you decide to participate, you can decide to stop at any time, even after signing the consent form or part-way through the study. If you drop out of the study, your data will only be used with your explicit consent. You can withdraw from the study at any time, for any reason, without any negative consequences. You will receive a \$20 stipend upon completion of the study.

Questions

If you have any general questions, please call the principal investigator, Dr. Monica Maly, at 519-888-4567 ext. 37916. This study has been reviewed by the Hamilton Integrated Research Ethics Board (HiREB). If you have any questions about your rights as a research participant or the conduct of the study, you may contact the Office of the Chair of the HiREB at (905) 521-2100 ext. 42013. This person is not involved with the research project in any way and calling him will not affect your participation in this study. This letter is yours to keep for future reference.

**Muscle Architecture Properties of the Quadriceps: Reliability Testing and
Association with Severity of Knee Osteoarthritis**

Consent

I have read the Letter of Information, have had the nature of the study explained to me and I agree to participate. All questions have been answered to my satisfaction. I will receive a signed copy of this form.

Participant Name (please print) Participant Signature Date

I confirm that I have explained the nature and purpose of this study to the participant named above. I have answered all questions.

Person Obtaining Consent Signature Date

Principal Investigator Signature Date

APPENDIX D – Comorbidity Questionnaire

Mobilize Laboratory	
Quadriceps Muscle Architecture Properties and Knee Osteoarthritis Severity	
PARTICIPANT ID:	DATE:
<input type="text"/>	<input type="text"/>
	(MMM/DD/YYYY)

Self-Administered Comorbidity Measure

Instructions

- The following is a list of common problems. Please indicate if you currently have the problem in the first column. If you do not have the problem, skip to the next problem.
- If you do have the problem, please indicate in the second column if you receive medications or some other type of treatment for the problem. Please provide the details of your treatment in the far right columns.
- In the third column, indicate if the problem limits your activities.
- Finally, indicate all medical conditions that are not listed under “other medical problems” at the end of the page.

Problem	Do you have the problem?		Do you receive treatment for it? (provide details)		Does it limit your activities?		Treatment details	
	No (0)	Yes → (1)	No (0)	Yes (1)	No (0)	Yes (1)	List medication(s)	List frequency and dosage
Heart disease	N	Y	N	Y	N	Y		
High blood pressure	N	Y	N	Y	N	Y		
Lung disease	N	Y	N	Y	N	Y		
Diabetes	N	Y	N	Y	N	Y		
Ulcer or stomach disease	N	Y	N	Y	N	Y		
Kidney disease	N	Y	N	Y	N	Y		

Mobilize Laboratory Quadriceps Muscle Architecture Properties and Knee Osteoarthritis Severity	
PARTICIPANT ID: <input type="text"/>	DATE: <input type="text"/> <small>(MMM/DD/YYYY)</small>

Liver disease	N	Y	N	Y	N	Y		
Anemia or other blood disease	N	Y	N	Y	N	Y		
Cancer	N	Y	N	Y	N	Y		
Depression	N	Y	N	Y	N	Y		
Osteoarthritis, degenerative arthritis	N	Y	N	Y	N	Y		
Back pain	N	Y	N	Y	N	Y		
Rheumatoid arthritis	N	Y	N	Y	N	Y		
Other medical problems (please write in)								
	N	Y	N	Y	N	Y		
	N	Y	N	Y	N	Y		
	N	Y	N	Y	N	Y		
	N	Y	N	Y	N	Y		

Mobilize Laboratory**Quadriceps Muscle Architecture Properties and Knee Osteoarthritis Severity**

PARTICIPANT ID:

DATE:

(MMM/DD/YYYY)

COMMON MEDICATIONS

Please complete this section if you take medications that are not listed above

Medications for pain:	(check box)	List frequency and dosage
Ibuprofen	<input type="checkbox"/>	
Advil	<input type="checkbox"/>	
Aspirin	<input type="checkbox"/>	
Acetaminophen	<input type="checkbox"/>	
Tylenol	<input type="checkbox"/>	
Statins (eg. Crestor)	<input type="checkbox"/>	
Medications for heart conditions:		
Blood Thinners (eg. Warfarin)	<input type="checkbox"/>	
ACE Inhibitors (eg. Ramipril)	<input type="checkbox"/>	
ARBs (eg. Candesartan)	<input type="checkbox"/>	
Beta Blockers (eg. Metoprolol)	<input type="checkbox"/>	
Calcium Channel Blockers (eg. Amlodipine)	<input type="checkbox"/>	
Cholesterol-lowering agents (eg. Lipitor)	<input type="checkbox"/>	
Water Pills	<input type="checkbox"/>	
Vasodilators (eg. Nitroglycerin)	<input type="checkbox"/>	
Medications for diabetes:		
Metformin	<input type="checkbox"/>	
Glyburide	<input type="checkbox"/>	
Other: (list below)		
	<input type="checkbox"/>	
	<input type="checkbox"/>	

APPENDIX E – Basic Collection Sheet

Mobilize	
Quadriceps Muscle Architecture and Knee Osteoarthritis Severity	
PARTICIPANT ID:	DATE:
<input type="text"/>	<input type="text"/>
	(MM/DD/YYYY)

Basic Measurements

Participant should be barefoot, wearing shorts.

Age (years)			
Mass (kg)			
Height (m)			
Body Mass Index (kg/m ²)			
Thigh Length (cm)	RF (ASIS-Patella)	VL (ASIS-Patella)	VL (GT-LC)
	<input type="text"/>	<input type="text"/>	<input type="text"/>
Thigh Circumference (cm)	RF imaging region		VL imaging region
	<input type="text"/>		<input type="text"/>
Dominant Leg (R/L)			
Involved Leg (R/L)			

APPENDIX F – Six Minute Walk Test

Mobilize Laboratory	
Quadriceps Muscle Architecture Properties and Knee Osteoarthritis Severity	
PARTICIPANT ID: <input type="text"/>	DATE: <input type="text"/>
(MMM/DD/YYYY)	

Six Minute Walk Test

Instructions

"The object of this test is to walk as far as possible for 6 minutes. You will walk in a circle in this hallway for 6 minutes. Six minutes is a long time to walk, so you will be exerting yourself. You will probably get out of breath or become exhausted. You are permitted to slow down, to stop, and to rest as necessary. You may lean against the wall while resting, but resume walking as soon as you are able."

"Remember that the object is to walk AS FAR AS POSSIBLE for 6 minutes, but don't run or jog. Start now, or whenever you are ready."

5 minute remaining: "You are doing well. You have 5 minutes to go."

4 minutes remaining: "Keep up the good work. You have 4 minutes to go."

3 minutes remaining: "You are doing well. You are halfway done."

2 minutes remaining: "Keep up the good work. You have only 2 minutes left."

1 minute remaining: "You are doing well. You have only 1 minute to go."

15 seconds remaining: "In a moment I'm going to tell you to stop. When I do, just stop right where you are."

**If the patient stops walking during the test and needs a rest, do not stop the timer.

Scoring

Distance in METERS covered in **6 minutes**:

BORG score upon completing:

APPENDIX G – Raw Data: Analyses Including All Images

Raw mean muscle architecture outcomes (including all images) for all participants are displayed in Figures 21 and 22. For both muscles, there is variation between raters, especially for pennation angle, and fascicle length.

For the rectus femoris, medial transducer angles (95° and 100°) produce the largest pennation angle. The scale for fascicle lengths for both raters exceeds the longest muscle length for rectus femoris (49.3 cm). When mean values are graphed with SE bars, large SE bars suggest larger error associated with fascicle length measurements.

For images of the vastus lateralis, fat thickness and muscle thickness may not be statistically different between transducer angles. As the transducer is tilted medially, SE bars are increased for pennation angle, and fascicle length and muscle thickness.

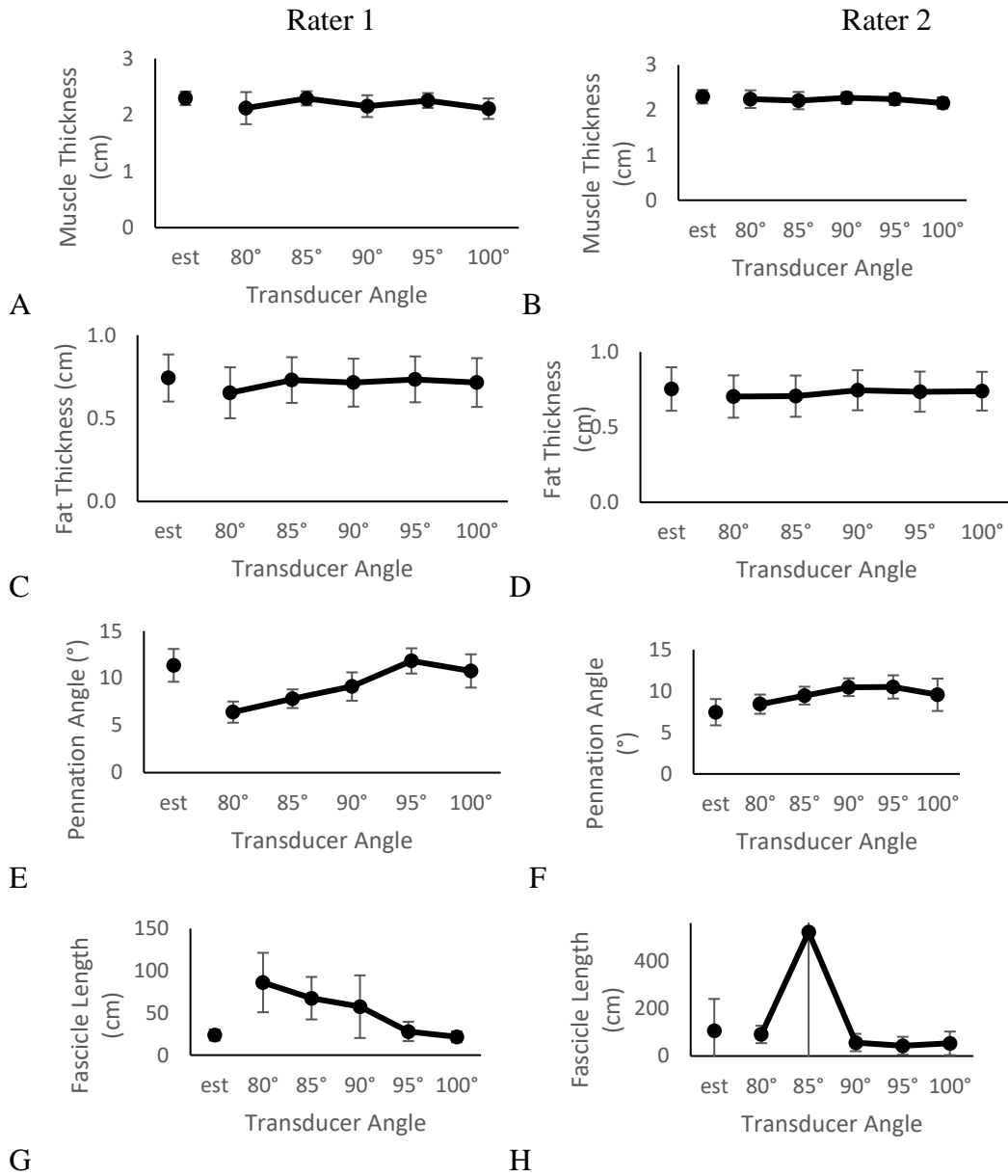


Figure 21: Mean muscle architecture measurements with standard error bars for images of the rectus femoris: muscle thickness (A, B), fat thickness (C, D), pennation angle (E, F), and fascicle length (G, H). Data from rater 1s images are displayed in the left column (A, C, E, G) and data from rater 2s images are shown in the right column (B, D, F, H). The lone markers represent the average value of the measurement from the images taken with the transducer at an estimated (EST) perpendicular angle.

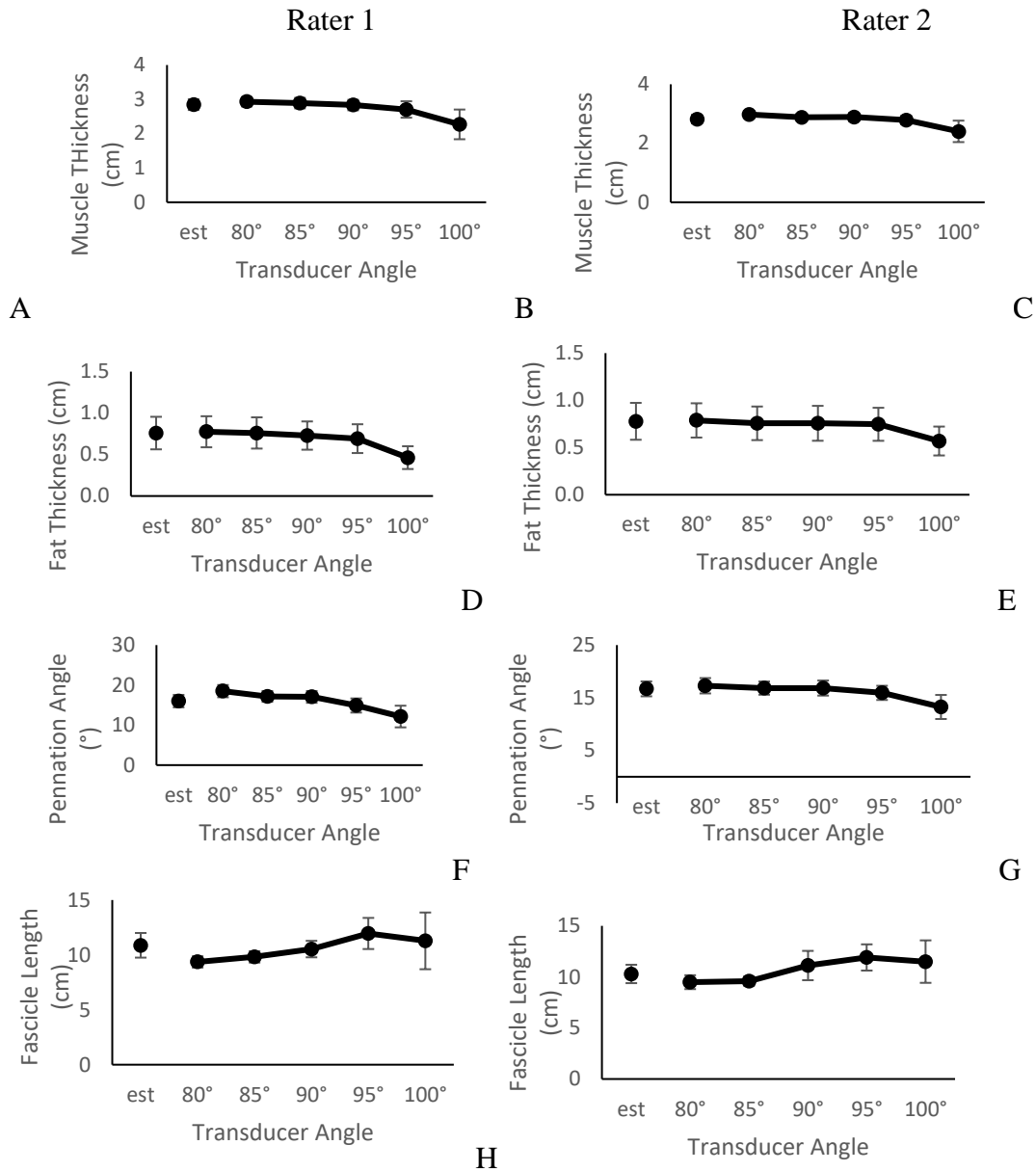


Figure 22: Mean muscle architecture measurements with standard error bars for images of the vastus lateralis: muscle thickness (A, B), fat thickness (C, D), pennation angle (E, F), and fascicle length (G, H). Data from rater 1s images are displayed in the left column (A, C, E, G) and data from rater 2s images are shown in the right column (B, D, F, H). The lone markers represent the average value of the measurement from the images taken with the transducer at an estimated (EST) perpendicular angle.

Table 14 displays SEMs for rectus femoris images taken by rater 1 and rater 2. SEMs for fascicle length exceed the length of the longest rectus femoris muscle in this sample. For

the rectus femoris, lateral transducer angles show greater error than medial transducer angles, except for pennation angle measurements taken at a 100° transducer angle by rater 2. For the vastus lateralis, a 100° transducer angle demonstrated the highest standard error for all muscle architecture outcomes.

Table 15 shows ICCs between muscle architecture measurements of the rectus femoris taken at an estimated perpendicular transducer and measured 80°, 85°, 95°, and 100° transducer angles and a measured 90° transducer angle. Agreement was rater-specific. Medial transducer angles were associated with relatively better ICCs.

SEMs for images of the vastus lateralis taken by rater 1 and rater 2 are shown in Table 16. The 100° transducer angles produce the largest standard error measurements for both raters and all outcomes.

Table 17 displays agreement between measured perpendicular images of the vastus lateralis taken by rater 1 and rater 2 at estimated transducer angles and measured 80°, 85°, 95°, and 100° transducer angles. The 85° transducer angles produce the best agreement relative to other transducer angles. Mostly poor agreement was produced by 100° transducer angles.

Table 16: Rectus femoris standard error measurements (SEMs) comparing measurements from images taken with the transducer at an estimated perpendicular angle and a measured 80°, 85°, 95°, and 100° transducer orientation to a measured 90° transducer angle. SEMs for images taken by each rater for each outcome at each transducer angle is displayed. Bolded cells show the highest error for each outcome.

	Rater	Est vs. 90°	80° vs. 90°	85° vs. 90°	95° vs. 90°	100° vs. 90°
Muscle Thickness (cm)	1	0.33	0.61	0.35	0.36	0.39
	2	0.16	0.29	0.38	0.10	0.12
Fat Thickness (cm)	1	0.14	0.28	0.13	0.13	0.16
	2	0.09	0.16	0.16	0.07	0.05
Pennation Angle (°)	1	3.94	3.68	1.92	2.26	2.84
	2	3.47	2.82	2.35	2.00	3.49
Fascicle Length (cm)	1	73.43	63.50	75.83	72.81	73.65
	2	219.27	78.12	1719.57	48.80	71.19

Table 17: Rectus femoris intraclass correlation coefficients (ICCs) comparing measurements from images taken with the transducer at an estimated perpendicular angle and a measured 80°, 85°, 95°, and 100° transducer orientation to a measured 90° transducer angle. ICCs for images taken by each rater for each outcome at each transducer angle is displayed. Dark green cells represent excellent agreements, light green cells represent good agreement, yellow cells represent fair agreement and red cells represent poor agreement.

	Rater	Est vs. 90°	80° vs. 90°	85° vs. 90°	95° vs. 90°	100° vs. 90°
Muscle Thickness	1	0.61	0.35	0.58	0.57	0.62
	2	0.91	0.74	0.48	0.96	0.92
Fat Thickness	1	0.93	0.70	0.94	0.94	0.91
	2	0.97	0.90	0.90	0.98	0.99
Pennation Angle	1	0.37	0.02	0.80	0.71	0.74
	2	0.26	0.26	0.53	0.79	0.54
Fascicle Length	1	0.05	0.74	0.43	0.18	0.04
	2	0.53	0.57	0.00	0.87	0.80

Table 18: Vastus lateralis standard error measurements (SEMs) comparing measurements from images taken with the transducer at an estimated perpendicular angle and a measured 80°, 85°, 95°, and 100° transducer orientation to a measured 90° transducer angle. SEMs for images taken by each rater for each outcome at each transducer angle is displayed. Bolded cells show the highest error for each outcome.

	Rater	Est vs. 90°	80° vs. 90°	85° vs. 90°	95° vs. 90°	100° vs. 90°
Muscle Thickness (cm)	1	0.15	0.21	0.12	0.45	0.81
	2	0.22	0.25	0.20	0.15	0.75
Fat Thickness (cm)	1	0.09	0.07	0.06	0.27	0.42
	2	0.09	0.05	0.06	0.08	0.40
Pennation Angle (°)	1	2.78	3.68	2.46	3.39	5.92
	2	3.77	3.51	3.23	3.10	5.20
Fascicle Length (cm)	1	2.19	1.16	1.24	2.61	5.36
	2	3.12	3.00	2.58	1.74	4.98

Table 19: Vastus lateralis intraclass correlation coefficients (ICCs) comparing measurements from images taken with the transducer at an estimated perpendicular angle and a measured 80°, 85°, 95°, and 100° transducer orientation to a measured 90° transducer angle. ICCs for images taken by each rater for each outcome at each transducer angle is displayed. Dark green cells represent excellent agreements, light green cells represent good agreement, yellow cells represent fair agreement and red cells represent poor agreement.

	Rater	Est vs. 90°	80° vs. 90°	85° vs. 90°	95° vs. 90°	100° vs. 90°
Muscle Thickness	1	0.93	0.84	0.95	0.52	0.29
	2	0.83	0.66	0.82	0.91	0.07
Fat Thickness	1	0.98	0.99	0.99	0.82	0.08
	2	0.99	0.99	0.99	0.99	0.44
Pennation Angle	1	0.72	0.36	0.76	0.58	0.08
	2	0.18	0.40	0.42	0.53	0.07
Fascicle Length	1	0.50	0.66	0.66	0.46	0.00
	2	0.23	0.14	0.37	0.88	0.01

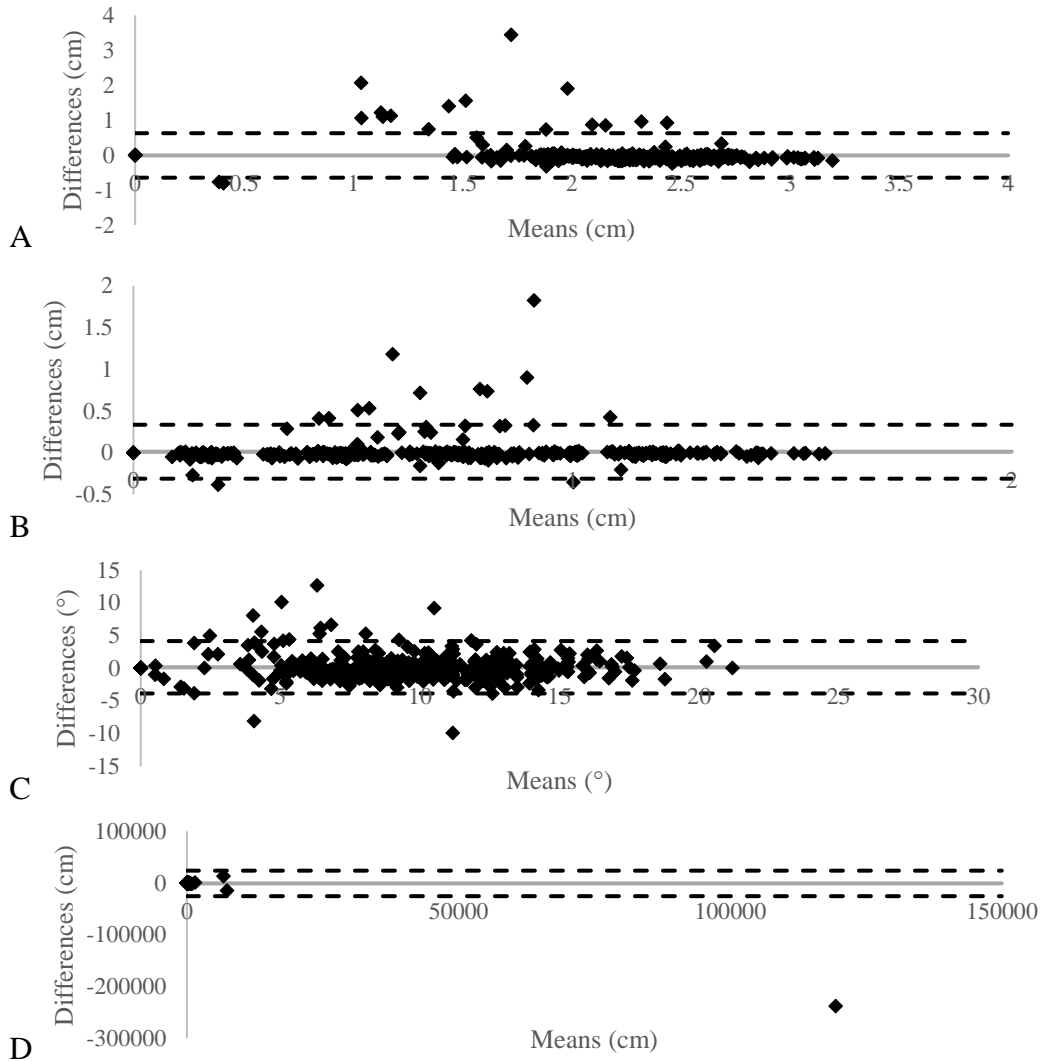


Figure 23: Bland-Altman plots comparing rectus femoris muscle thickness (A), fat thickness (B), pennation angle (C), and fascicle length (D) raw measurements from first and second measurements performed by rater 1 to assess intra-rater reliability. Data for all images of all participants taken by both raters at each transducer angle is displayed measurements. The means are plotted along the X-axis and the differences between the measures are plotted on the Y-axis. The mean is displayed with a dashed grey line. The upper and lower agreements represent 1.96 standard deviations and are displayed as black lines. The data points represent the differences between 1st and 2nd measurements.

Table 20: Intraclass correlation coefficients (ICCs) & standard error measurements (SEMs) for intra-rater reliability for muscle architecture measurements of the rectus femoris measure 1 and measure 2. For ICCs, dark green cells represent excellent agreements, light green cells represent good agreement, yellow cells represent fair agreement and red cells represent poor agreement. These analyses contain both rater 1 and rater 2 data.

	Muscle Thickness (cm) n = 360	Fat Thickness (cm) n = 360	Pennation Angle (°) n = 360	Fascicle Length (cm) n = 259
SEM	0.23	0.12	1.45	8901.72
ICC	0.89	0.95	0.94	0.005

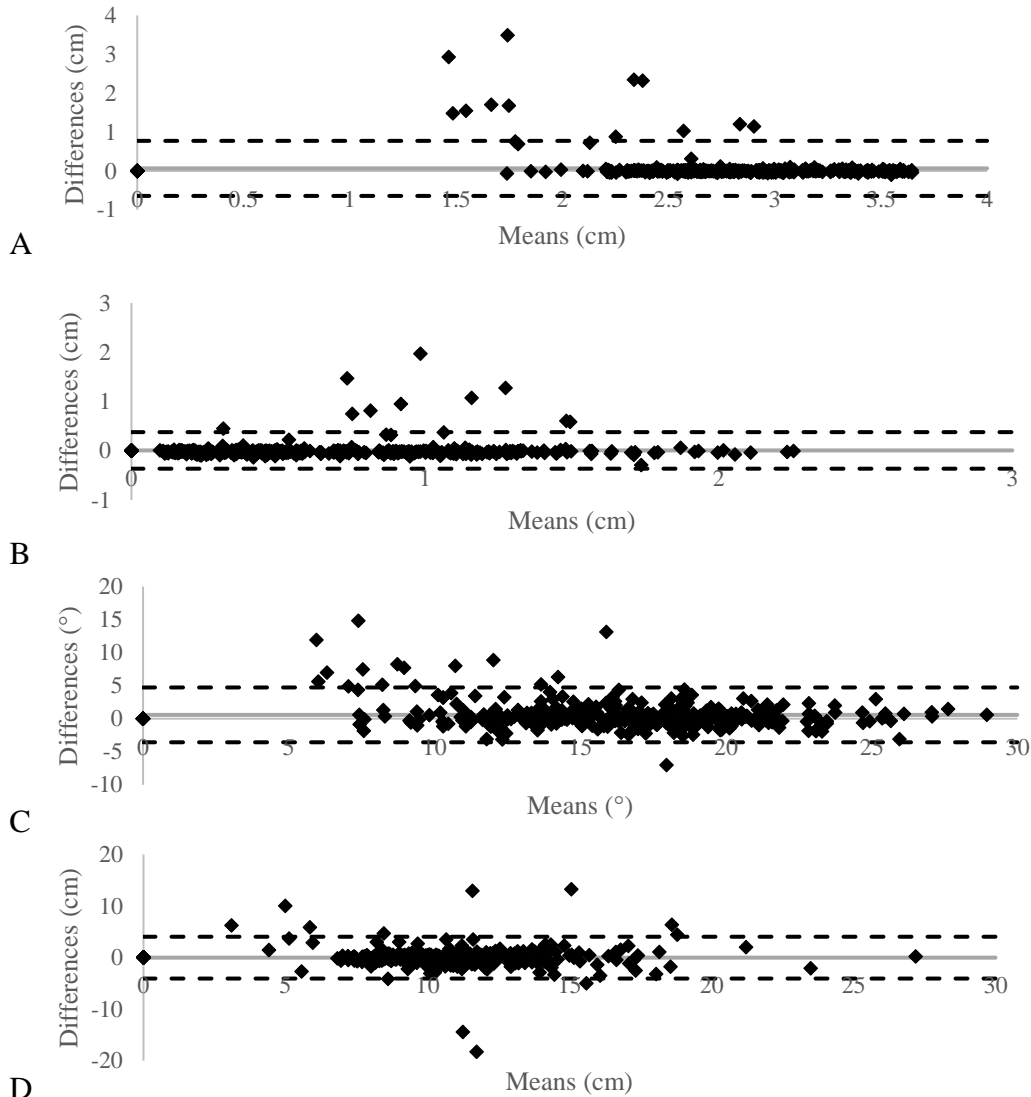


Figure 24: Bland-Altman plots comparing vastus lateralis muscle thickness (A), fat thickness (B), pennation angle (C), and fascicle length (D) raw measurements from first and second measurements performed by rater 1 to assess intra-rater reliability. Data for all images of all participants taken by both raters at each transducer angle is displayed measurements. The means are plotted along the X-axis and the differences between the measures are plotted on the Y-axis. The mean is displayed with a dashed grey line. The upper and lower agreements represent 1.96 standard deviations and are displayed as black lines. The data points represent the differences between 1st and 2nd measurements.

Table 21: Intraclass correlation coefficients (ICCs) & standard error measurements (SEMs) for intra-rater reliability for muscle architecture measurements of the vastus lateralis measure 1 and measure 2. For ICCs, dark green cells represent excellent agreements, light green cells represent good agreement, yellow cells represent fair agreement and red cells represent poor agreement. These analyses contain both rater 1 and rater 2 data.

	Muscle Thickness (cm) n = 360	Fat Thickness (cm) n = 360	Pennation Angle (°) n = 360	Fascicle Length (cm) n = 360
SEM	0.26	0.13	1.5	1.46
ICC	0.92	0.96	0.95	0.91

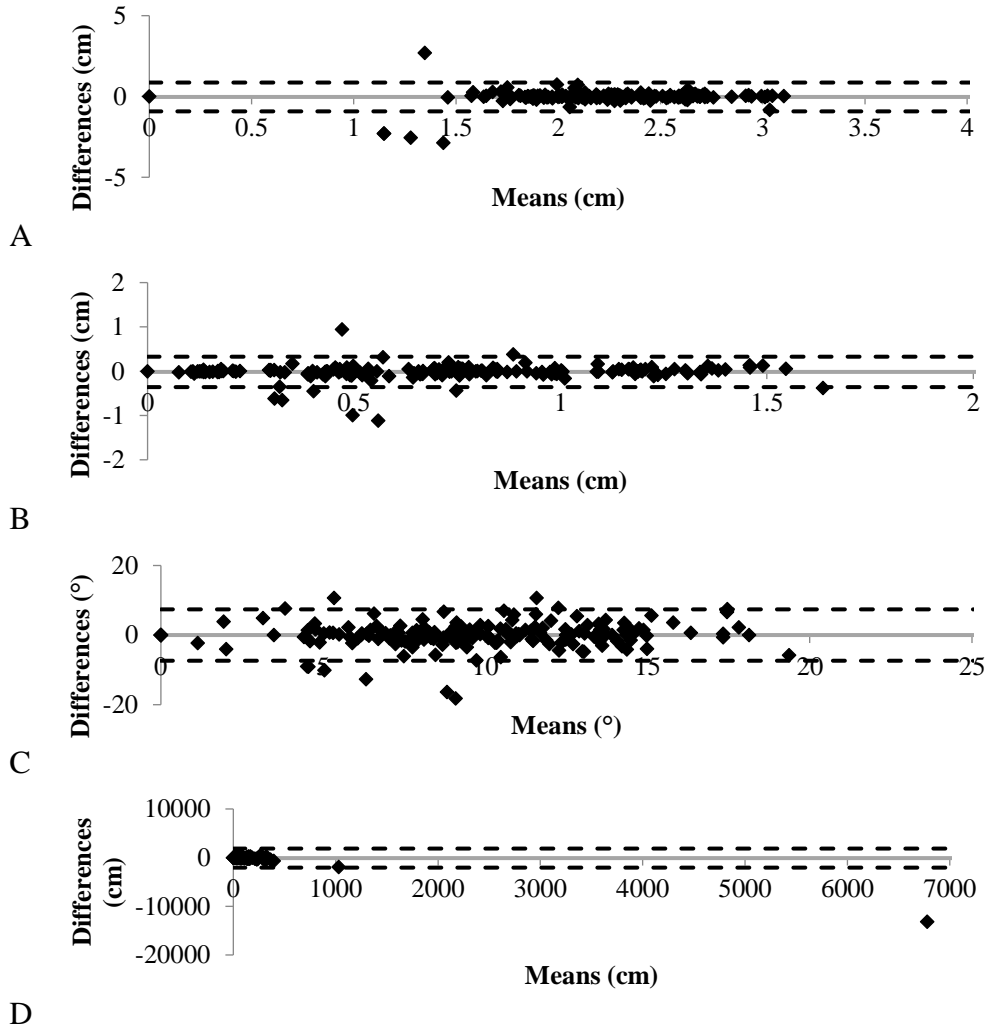


Figure 25: Bland-Altman plots comparing rectus femoris muscle thickness (A), fat thickness (B), pennation angle (C), and fascicle length (D) measurements from images taken by rater 1 and rater 2. Data for all images of all participants at each transducer angle is displayed with poor-quality images and fascicle lengths which exceeded muscle length removed (174 data points for the muscle and fat thicknesses, 165 data points for the pennation angles, and 111 data points for the fascicle lengths). The means are plotted along the X-axis and the differences between the measures are plotted on the Y-axis. The mean is displayed with a grey dashed line. The upper and lower agreements represent 1.96 standard deviations and are displayed as two black lines. The data points represent the differences between measurements from images taken by the first and second researcher

Table 22: Standard error measurements (SEMs) & intraclass correlation coefficients (ICCs) comparing rectus femoris measurements for images taken by rater 1 vs rater 2. For SEM, bold cells represent which transducer angle produced the largest error for each outcome. Dark green cells represent excellent agreements, light green cells represent good agreement, yellow cells represent fair agreement and red cells represent poor agreement.

		Est ₁ vs. Est ₂	80° ₁ vs. 80° ₂	85° ₁ vs. 85° ₂	90° ₁ vs. 90° ₂	95° ₁ vs. 95° ₂	100° ₁ vs. 100° ₂
Muscle Thickness	SEM (cm)	0.17	0.46	0.35	0.38	0.10	0.32
	ICC	0.90	0.71	0.57	0.47	0.96	0.63
Fat Thickness	SEM (cm)	0.07	0.17	0.14	0.15	0.05	0.11
	ICC	0.99	0.90	0.93	0.92	0.99	0.96
Pennation Angle	SEM (°)	3.09	2.84	2.31	2.30	2.04	3.04
	ICC	0.72	0.34	0.53	0.76	0.81	0.80
Fascicle Length	SEM (cm)	258.34	79.32	1699.56	92.57	59.76	90.92
	ICC	0.08	0.56	0.04	0.33	0.58	0.26

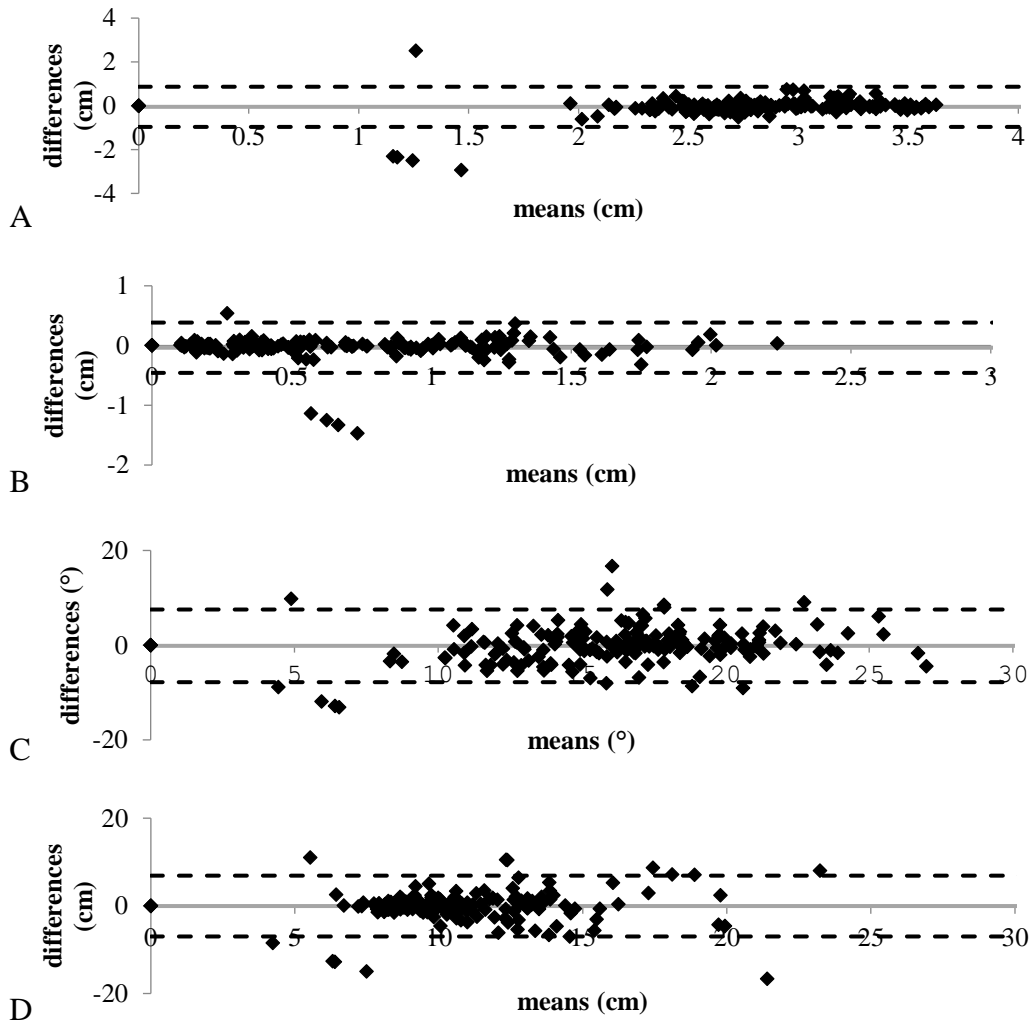


Figure 26: Bland-Altman plots comparing vastus lateralis muscle thickness (A), fat thickness (B), pennation angle (C), and fascicle length (D) measurements from images taken by rater 1 and rater 2. Data for all images of all participants at each transducer angle is displayed with poor-quality images and fascicle lengths which exceeded muscle length removed (174 data points for the muscle and fat thicknesses, 165 data points for the pennation angles, and 111 data points for the fascicle lengths). The means are plotted along the X-axis and the differences between the measures are plotted on the Y-axis. The mean is displayed with a grey dashed line. The upper and lower agreements represent 1.96 standard deviations and are displayed as two black lines. The data points represent the differences between measurements from images taken by the first and second researcher

Table 23: Standard error measurements (SEMs) & intraclass correlation coefficients (ICCs) comparing rectus femoris measurements for images taken by rater 1 vs rater 2. For SEM, bold cells represent which transducer angle produced the largest error for each outcome. Dark green cells represent excellent agreements, light green cells represent good agreement, yellow cells represent fair agreement and red cells represent poor agreement.

		Est ₁ vs. Est ₂	80° ₁ vs. 80° ₂	85° ₁ vs. 85° ₂	90° ₁ vs. 90° ₂	95° ₁ vs. 95° ₂	100° ₁ vs. 100° ₂
Muscle	SEM (cm)	0.12	0.14	0.16	0.14	0.41	0.65
Thickness	ICC	0.96	0.91	0.90	0.94	0.64	0.80
Fat	SEM (cm)	0.07	0.04	0.05	0.08	0.20	0.29
Thickness	ICC	0.99	1.00	1.00	0.99	0.91	0.66
Pennation	SEM (°)	3.20	2.38	1.84	2.41	2.68	3.66
Angle	ICC	0.58	0.79	0.85	0.79	0.76	0.84
Fascicle	SEM (cm)	2.31	1.25	0.85	2.41	2.92	4.12
Length	ICC	0.51	0.62	0.76	0.61	0.58	0.76